

AFWAL-TR-85-4137

ADA 168102

EXPLORATION OF ADVANCED CHARACTERIZATION TECHNIQUES FOR MOLECULAR
COMPOSITES



D. L. VanderHart, F. W. Wang, R. K. Eby and B. M. Fanconi
Polymers Division
National Bureau of Standards
Gaithersburg, MD 20899

K. L. DeVries
College of Engineering
University of Utah
Salt Lake City, UT 84112

February 1986

Final Report for Period February 1984 - January 1985

Approved for Public Release; Distribution is Unlimited

Best Available Copy


MATERIALS LABORATORY
AIR FORCE WRIGHT AERONAUTICAL LABORATORIES
AIR FORCE SYSTEMS COMMAND
WRIGHT-PATTERSON AFB, OHIO 45433-6533

200402192 67

When Government drawings, specifications, or other data are used for any purpose other than in connection with a definitely related Government procurement operation, the United States Government thereby incurs no responsibility nor any obligation whatsoever; and the fact that the Government may have formulated, furnished, or in any way supplied the said drawings, specifications, or other data, is not to be regarded by implication or otherwise as in any manner licensing the holder or any other person or corporation, or conveying any rights or permission to manufacture use, or sell any patented invention that may in any way be related thereto.

This report has been reviewed by the Office of Public Affairs (ASD/PA) and is releasable to the National Technical Information Service (NTIS). At NTIS, it will be available to the general public, including foreign nationals.

This technical report has been reviewed and is approved for publication.


WALTER W. ADAMS
Project Scientist


RICHARD L. VAN DEUSEN
Chief, Polymer Branch

FOR THE COMMANDER


MERRILL L. MINGES, SES
Director
Nonmetallic Materials Division

"If your address has changed, if you wish to be removed from our mailing list, or if the addressee is no longer employed by your organization please notify AFWAL/MLBP, Wright-Patterson AFB OH 45433 to help us maintain a current mailing list."

Copies of this report should not be returned unless return is required by security considerations, contractual obligations, or notice on a specific document.

UNCLASSIFIED

SECURITY CLASSIFICATION OF THIS PAGE

REPORT DOCUMENTATION PAGE

| | | | | | |
|--|-------|--------------------------------------|--|---|----------------------------------|
| 1a. REPORT SECURITY CLASSIFICATION Unclassified | | | 1b. RESTRICTIVE MARKINGS N/A | | |
| 2a. SECURITY CLASSIFICATION AUTHORITY N/A | | | 3. DISTRIBUTION/AVAILABILITY OF REPORT Approved for public release; distribution is unlimited. | | |
| 2b. DECLASSIFICATION/DOWNGRADING SCHEDULE N/A | | | | | |
| 4. PERFORMING ORGANIZATION REPORT NUMBER(S) | | | 5. MONITORING ORGANIZATION REPORT NUMBER(S) AFWAL-TR-85-4137 | | |
| 6a. NAME OF PERFORMING ORGANIZATION National Bureau of Standards Polymers Division | | 6b. OFFICE SYMBOL (If applicable) | 7a. NAME OF MONITORING ORGANIZATION Air Force Wright Aeronautical Laboratories Materials Laboratory (AFWAL/MLBP) | | |
| 6c. ADDRESS (City, State and ZIP Code) Gaithersburg, MD 20899 | | | 7b. ADDRESS (City, State and ZIP Code) Wright-Patterson AFB, OH 45433-6533 | | |
| 8a. NAME OF FUNDING/SPONSORING ORGANIZATION Same as 7a | | 8b. OFFICE SYMBOL (If applicable) | 9. PROCUREMENT INSTRUMENT IDENTIFICATION NUMBER MIPR NO: FY1457-84-N-5019 | | |
| 8c. ADDRESS (City, State and ZIP Code) | | | 10. SOURCE OF FUNDING NOS. | | |
| | | | PROGRAM ELEMENT NO. | PROJECT NO. | TASK NO. |
| 11. TITLE (Include Security Classification) (see reverse) EXPLORATION OF ADVANCED CHARACTERIZATION | | | 61101F | ILIR | 01 |
| 12. PERSONAL AUTHOR(S) D. L. VanderHart, E. W. Wang, R. K. Eby, R. M. Fanconi and K. L. DeVries | | | 13. WORK UNIT NO. | | |
| 13a. TYPE OF REPORT Final | | | 13b. TIME COVERED FROM Feb 84 TO Jan 85 | 14. DATE OF REPORT (Yr., Mo., Day) February 1986 | 15. PAGE COUNT 173 |
| 16. SUPPLEMENTARY NOTATION | | | | | |
| 17. COSATI CODES | | | 18. SUBJECT TERMS (Continue on reverse if necessary and identify by block number) | | |
| FIELD | GROUP | SUB. GR. | | | |
| | 11 | 09 | PBT Molecular Composites ESR | | |
| | 07 | 04 | ABPBI NMR X-ray Diffraction | | |
| | | | Nylon 6 Fluorescence Spectroscopy | | |
| 19. ABSTRACT (Continue on reverse if necessary and identify by block number) | | | | | |
| <p>The techniques of solid state nuclear magnetic resonance, fluorescence spectroscopy, electron spin resonance, and x-ray diffraction were applied to characterize aspects of the solid state structures of rigid rod polymers and their blends with flexible polymers. NMR and fluorescence spectroscopies were used to investigate the degree to which the rigid rod - flexible polymers blends exist as phase separated systems. It was found that these materials form primarily phase segregated structures, a condition which limits the reinforcing potential of rigid rod polymers in molecular composites. Most specimens also exhibited NMR signals indicative of mobile, and presumably lower molecular weight, species. It is postulated that these mobile species are either water or residual acid from which the materials are processed. Information regarding the location of the mobile species in the structures exhibited by rigid rod polymers and their blends with flexible polymers is deduced from NMR.</p> <p>Electron spin resonance measurements confirmed that free radicals are generated</p> | | | | | |
| 20. DISTRIBUTION/AVAILABILITY OF ABSTRACT UNCLASSIFIED/UNLIMITED <input type="checkbox"/> SAME AS RPT. <input checked="" type="checkbox"/> DTIC USERS <input type="checkbox"/> | | | 21. ABSTRACT SECURITY CLASSIFICATION Unclassified | | |
| 22a. NAME OF RESPONSIBLE INDIVIDUAL W. W. Adams | | | 22b. TELEPHONE NUMBER (Include Area Code) (513) 255-9148 | | 22c. OFFICE SYMBOL AFWAL/MLBP |

11. TECHNIQUES FOR MOLECULAR COMPOSITES

19. during mechanically stressing rigid rod polymer fibers. The as-processed fibers contained appreciable levels of free radicals and annealing at elevated temperatures caused a decrease in the free radical concentration by a factor of three. X-ray diffraction experiments were conducted at elevated pressures in a diamond anvil cell. The observed diffraction pattern is suggestive of the formation of a more ordered structure at elevated pressures.

TABLE OF CONTENTS

| | |
|---|----|
| I. INTRODUCTION | 1 |
| II. SOLID STATE NUCLEAR MAGNETIC RESONANCE | 3 |
| A. Definitions and NMR Background | 4 |
| 1. Dipolar interactions | 4 |
| 2. Chemical shift and chemical shift anisotropy | 5 |
| 3. Magic angle spinning | 6 |
| 4. Magnetization | 6 |
| 5. Quantization axis | 7 |
| 6. Relaxation | 7 |
| 7. Multiple pulse sequences | 8 |
| 8. Spin diffusion | 8 |
| 9. Cross-polarization | 11 |
| 10. Pulse sequences | 12 |
| 11. High power proton decoupling | 12 |
| B. Experimental | 12 |
| 1. Materials | 12 |
| 2. Spectrometers | 14 |
| 3. Pulse Sequences and their rationale | 15 |
| C. Overview of the NMR Effort to Determine Level of Mixing | 18 |
| D. Results and Discussion | 21 |
| 1. Proton spectra from free induction decays | 21 |
| 2. Proton relaxation and spectra taken with multiple pulse | 25 |
| 3. Other proton relaxation times | 29 |
| 4. C-13 cross-polarization spectra | 36 |
| 5. Experiments on the intimacy of mixing in composites using spin diffusion between polymer component protons | 41 |
| i. 30% PBT/70% ABPBI composite | 41 |
| ii. 40% nylon/60% PBT composite | 42 |
| a. Proton likeness and its interpretation | 43 |
| b. Proton diffusion study with proton observation | 44 |
| c. Proton spin diffusion using C-13 CP-MAS readout | 47 |
| d. C-13 spin diffusion experiment with CP-MAS | 54 |
| 6. Experiments probing the homogeneity of the rigid polymer phase using proton spin diffusion between mobile and rigid protons | 55 |
| 7. Experiments using multiple-pulse proton irradiation to prepare magnetization gradients followed by a monitoring of proton magnetization using proton C-13 cross polarization | 66 |

| | |
|---|----|
| E. Summary of the NMR Results and Evaluation of the Applicability of the NMR Methods to the Study of Molecular Composites | 68 |
| III. ELECTRON SPIN RESONANCE STUDIES | 78 |
| IV. FLUORESCENCE SPECTROSCOPY | 82 |
| V. HIGH PRESSURE X-RAY DIFFRACTION | 87 |
| A. Introduction | 87 |
| B. Approach | 88 |
| C. Object | 89 |
| D. Experimental | 89 |
| E. Results | 90 |
| F. Conclusions & Recommendations | 91 |
| REFERENCES | 92 |

LIST OF ILLUSTRATIONS

| <u>Figure</u> | | <u>Page</u> |
|---------------|--|-------------|
| 1 | 200 MHz proton spectra for Samples A-F. | 96 |
| 2 | Comparison of proton lineshapes in the ABPBI "heart cut" film in going from an ambient to an evacuated sample. | 97 |
| 3 | Comparison of proton lineshapes for unwashed (Sample P) and washed (Sample N) PBT films coagulated from MSA solution. | 99 |
| 4 | 200 MHz proton spectra of AFTECH I PBT fibers. | 101 |
| 5 | Proton spectra of Sample A (open tube) both before and after partial relaxation during a 24ms MREV-8 multiple pulse irradiation. | 103 |
| 6 | Proton spectra of the same, unevacuated samples as in Figure 1. | 105 |
| 7 | Proton lineshape changes in Sample C (unsealed) as a function of spin-locking time (rf field strength is 83 kHz). | 107 |
| 8 | Decay curves for the spin locked magnetization (rf field strength is 83 kHz) for two composite samples (F and L) of 70% ABPBI/30% PBT. | 109 |
| 9 | $T_{1\rho}^H$ decay curves for Sample G,M,I and Q (top to bottom respectively). | 111 |
| 10 | 50 MHz ^{13}C CP spectra of macroscopically oriented Samples K (A and B) and J (C). | 113 |
| 11 | 50 MHz ^{13}C CP spectrum of an oriented bundle of PBT fibers (Sample G). | 115 |
| 12 | 50 MHz ^{13}C CP spectra of an oriented bundle of PBT fibers (Sample G). | 117 |
| 13 | 50 MHz ^{13}C CP spectra of two unoriented composite films, Samples K and I: 30% PBT/70% ABPBI (A) and 60% PBT/40% nylon (B). | 119 |
| 14 | Different 50 MHz ^{13}C CP-MAS spectra of the ABPBI film (Sample K prior to the 2X stretching). | 121 |
| 15 | 15 MHz CP-MAS spectrum of PBT fibers (Sample G). | 123 |
| 16 | 50 MHz ^{13}C CP-MAS spectra of Samples M (upper) and I (lower). | 125 |
| 17 | 50 MHz ^{13}C CP-MAS spectra and difference spectra of Sample J as a function of proton spin-locking time, prior to a 1 ms CP period. | 127 |

| | | |
|-----|--|-----|
| 18 | 200 MHz proton spectra of Sample I as a function of t in the spin diffusion pulse sequence given. | 129 |
| 19 | Growth of the nylon component magnetization from the data in Figure 18. | 131 |
| 20 | 50 MHz ^{13}C CP-MAS spectra as a function of the proton spin diffusion time. The pulse sequence is discussed in the text. | 133 |
| 21 | Plots of the relative growth of nylon magnetization and the decay of PBT magnetization as a function of the square root of the diffusion time, t , for the Spectra of Sample I in Figure 20. | 135 |
| 22 | ^{13}C CP-MAS spectra resulting from the unsuccessful attempt to observe evidence of intimate mixing in Sample I using the relatively inefficient ^{13}C spin diffusion. | 137 |
| 23 | 50 MHz ^{13}C spectra and difference spectra of Sample G for various delay times t in a $T_1\rho$ experiment following the method of Torchia et al (reference 29). | 139 |
| 24 | Idealized situations for distributing mobile protons, indicated by dots, in a polymer blend of homopolymers 1 and 2. | 141 |
| 25 | Expected growth rates for initially depleted polymer proton magnetization. | 143 |
| 26 | 200 MHz proton lineshapes for the PBT/ABPBI composite, Sample L, which was coagulated from an MSA solution above the critical concentration for phase separation. | 145 |
| 27 | 200 MHz proton lineshapes for a monitoring of proton spin diffusion in Sample L from the broader polymer protons to the mobile protons. | 147 |
| 28 | Plots of the behavior of the narrow-line intensity in Sample L according to the data of Figures 26 and 27. | 149 |
| 29 | 200 MHz proton spectra for the PBT/ABPBI composite, Sample F. | 151 |
| 30 | 200 MHz proton, spectra for composite Sample F. | 153 |
| 31 | Generation of free radicals in nylon-6 fibers as a function of strain. Reproduced from reference 8. | 155 |
| 32. | Change in molecular weight versus strain for nylon-6 fibers. Reproduced from reference 8. | 156 |
| 33a | Electron spin resonance spectrum of AFTECH 1 fibers before and after thermal treatment. | 157 |
| 33b | Electron spin resonance spectra of AFTECH 1 fiber fractured by crushing under liquid nitrogen, and subsequently warmed to room temperature. | 158 |

| | | |
|-----|---|-----|
| 34a | Electron spin resonance spectrum of AFTECH 2 fibers before and after thermal treatment and pulled to rupture subsequent to thermal treatment. | 159 |
| 34b | Electron spin resonance spectra of AFTECH 2 fibers fractured by crushing under liquid nitrogen and subsequently warmed to room temperature. | 161 |
| 35 | Effect of mechanical deformation on the ESR spectrum of AFTECH 1 fiber that had been thermally treated. | 162 |
| 36 | Solid state fluorescence (dashed curve) and excitation (solid curve) spectra of poly (2,5(6) benzothiazole), ABPBT, fibers. | 163 |
| 37 | The solution fluorescence spectrum of poly (2,5(6) benzothiazole), ABPBT, in methane sulfonic acid, excited by 412 nm radiation. | 165 |
| 38 | Solid state fluorescence spectra of poly (2,5(6) benzothiazole), ABPBT, fibers, as received (dashed curve), precipitated from MSA and exposed to concentrated HCL solution (middle spectrum) and precipitated from MSA and exposed to HCL vapor for 15 minutes (bottom spectrum). | 166 |
| 39 | The solution fluorescence spectrum of poly (p-phenylene-bisbenzothiazole), PBT, in methane sulfonic acid recorded with 435nm excitation radiation. | 167 |
| 40 | The solution fluorescence (dashed curve) and excitation spectrum (solid curve) of poly (p-phenylene-bisbenzothiazole), PBT, in methane sulfonic acid. | 168 |
| 41 | The solid state fluorescence (dashed curve) and excitation (solid curve) spectra of poly (p-phenylene-bisbenzothiazole), PBT, precipitated from MSA. | 169 |
| 42 | Solid state fluorescence (dashed curve) and excitation (solid curve) spectra of a molecular composite of poly (p-phenylene-bisbenzothiazole), PBT, and nylon. | 170 |
| 43 | Diamond anvil pressure cell. | 171 |
| 44 | Flat plate x-ray diffraction patterns obtained with dope. | 172 |
| 45 | Energy dispersive x-ray diffraction pattern obtained with dope at 12,700 atm. | 173 |

LIST OF TABLES

| <u>Table</u> | | <u>Page</u> |
|--------------|---|-------------|
| 1 | Proton Longitudinal and Multiple-Pulse Relaxation Parameters | |

I. INTRODUCTION

Molecular composites are attractive structural materials owing to the potential for improvements in fracture and impact toughness over conventional fiber reinforced composites.¹⁻³ These experimental materials are combinations of rigid chain polymers that function as the reinforcement and flexible polymer molecules that serve as the matrix materials. It is well recognized that the ability of rigid rods to reinforce a matrix is enhanced as the aspect ratio of the rods increases.⁴ By analogy, in a blend of rigid-rod and flexible polymers the properties would be expected to improve as the rod phases approach molecular diameters. What militates against achievement of molecular dispersion is that the rigid-rod polymers are usually processed from semidilute solutions. In the process of coagulation from these solutions, the solvent must be removed and in so doing, the polymer blend passes through stages of increasing concentration since the fluid in the coagulation bath is a non-solvent. Early in this process the thermodynamics of the solution dictate that the rigid-rod polymer will undergo phase separation.⁵ A large growth of the rod-phase diameter is to be avoided during this period, perhaps by relying on the generally high viscosity of the solutions. The expectation is that the dimensions normal to the chain axes of the rigid-rod phase will be

kinetically determined and thus will likely be dependent on the processing history. Therefore, it is important to be able to measure the narrower dimensions of the rigid-rod domains.

A number of exploratory materials of this sort have been developed and evaluated for mechanical properties.^{3,6} A wide range of properties have been found in these materials which may be related to variability in structure, in particular, the degree to which the rigid rod polymers are dispersed in the flexible polymer matrix.

Characterization of the degree to which the components of molecular composites are mixed has been difficult by standard methods. In the present work we examined the potential of solid state nuclear magnetic resonance (NMR) and fluorescence spectroscopies to measure this quantity. The major effort in the present work was on solid state NMR. It was not our purpose to undertake any systematic correlation of processing history with domain size. Our effort was restricted to analyzing a few samples to see if solid state NMR and fluorescence techniques could provide information on domain sizes. Although the work was only exploratory we concluded that spectra obtained by both methods were sensitive to aggregation of the rigid rod polymer component.

Two additional techniques were examined for potential to measure other aspects of both rigid rod polymers and their molecular composites. Electron spin resonance (ESR) studies were conducted on two developmental fibers of the heterocyclic polymer poly(phenylenebenzobisthiazole)(PBT). The object of the ESR study was to determine if free radicals were generated during mechanical deformation and rupture. High pressure x-ray diffraction measurements of PBT were carried out to investigate possible solid-solid phase transitions that may be relevant to processing and ulti-

mate use properties. The general conclusions reached in high pressure x-ray and ESR investigations were that data may be obtained which were unavailable by other methods, and that further work may lead to a better understanding of the processing and performance of rigid rod polymers.

II. SOLID STATE NUCLEAR MAGNETIC RESONANCE

NMR is not a direct imaging technique for measuring domain sizes of a few nm in spite of the publicity received by medical NMR imaging. The observables of NMR in solids are usually sensitive to very local structural characteristics such as magnetic dipole-dipole interactions between nuclei (range of sensitivity usually less than .4 nm), chemical shifts (a property of the electronic structure of the molecule), and the motional dynamics (principally rotations) of the molecules. To probe dimensions larger than, say, 0.5 nm requires less direct approaches than those associated with direct NMR observables.

With the perspective of the foregoing paragraph, it is easy to understand that the NMR methods are strong candidates for testing the intimacy of mixing in a polymer blend if the mixing actually occurs at the molecular level. This is the so-called miscible blend, or in the case of the materials studied here, if the kinetics of phase separation are extremely sluggish, a 'molecular' composite. On the other hand, if domain sizes are of dimensions substantially larger than molecular dimensions, then it is expected that one would have to resort to indirect approaches to estimate domain sizes. For the latter case, the property of the abundant proton spin system in a solid called 'spin diffusion' can be used to probe dimensions larger than 0.5 nm. This property of the spin system, which will be described more fully, is analogous to heat conduction. In the presence of gradients of magnetization (analogous to gradients of temperature), the

dimensions of the domains can be inferred from the rates of reequilibration. It is clear that a fundamental requirement for conducting the spin diffusion experiment is the ability to distinguish between NMR signals belonging to each of the polymer components of a blend.

Before proceeding further, it is appropriate to give some definitions and NMR background information that will be essential to the understanding of the experiments and their interpretations. For more details than given here the reader is referred to comprehensive treatises on NMR.^{7,8,9}

A. Definitions and NMR Background

1. Dipolar interaction: This is the dominant interaction in the solid state. A nucleus with a non-zero spin such as a proton or a C-13 nucleus senses the local magnetic field of nearby spins. The strength of this interaction is proportional to the inverse cube of the distance separating the spins and to the angular function $(3\cos^2\theta - 1)$ where θ is the angle between the internuclear vector direction and the static magnetic field. The first order (secular) Hamiltonian for the dipolar interaction between two nuclei depends on whether the two spins in question are like or unlike spins. Basically, the interaction between like spins includes an exchange term (not present for unlike spins) that, for example, produces a coherent exchange between the states $I_1(+)I_2(-)$ and $I_1(-)I_2(+)$ in an isolated two-spin system. The exchange term provides the basis for understanding the process of spin diffusion alluded to in the previous section, because in a typical organic solid, spins are not isolated in pairs but are coupled, one to another, in a very extended fashion. The magnitude of the dipolar interaction is typically 20-60 kHz for proton-proton interactions and 10-20 kHz for directly bonded C-13-proton

interactions. Isotropic molecular tumbling plus translational diffusion averages out the dipolar interactions in liquids so that the NMR linewidths of liquids are much smaller than those of solids.

2. Chemical shift and chemical shift anisotropy: In liquids, the isotropic chemical shift is the parameter which makes NMR so useful as an analytical tool. The electrons around a nucleus shield the nucleus to a very small extent and alter the applied magnetic field. The shielding is a function of orbital hybridization and the nature of the chemical substituents bonded to that atom. Because lines are very narrow in liquids, small shifts are easily detected. The range of shifts for protons in liquids is approximately 10 ppm. The corresponding shift range for C-13 is 200 ppm. Thus, it is clear that C-13 spectra are more sensitive to small electronic changes. In the solid where fast molecular motions are often absent, or at least anisotropic, the chemical shift broadens resonances significantly due to the tensorial nature of the interaction. In other words, since the electronic cloud around a nucleus is generally not spherically symmetric, neither is the shielding for different orientations of the magnetic field with respect to the molecular axes. Thus, a single chemical site in a spectrum of a powder sample will be broadened according to this tensorial chemical shift interaction. The tensor describing this interaction is a second rank tensor and the resulting width of the "powder" resonance due to this effect is called the chemical shift anisotropy. Values for the chemical shift anisotropies of protons are typically in the 4-8 ppm range except for H-bonded protons. Anisotropies for C-13 nuclei are typically 30-50 ppm for carbons with tetrahedral bonding and 150-250 ppm for most other kinds of carbons.⁹ Therefore, even in the absence of the strong dipolar couplings in solids,

a difficult spectral overlap problem would exist due to chemical shift anisotropy, if several chemical sites were present. Magic angle spinning addresses this problem.

3. Magic angle spinning: In principal, this method takes advantage of the fact that both the dipolar and chemical shift interactions are second rank tensors of order zero, defined with respect to the static magnetic field (B_0) direction. If spinning is fast with respect to both of the interactions, it is easy to show mathematically that when a sample spinning axis is oriented such that it makes an angle ($54^\circ 44' = \arctan \sqrt{2}$) with respect to B_0 , then both the dipolar and chemical shift interactions are averaged to zero. In practice, magic angle spinning (MAS) is usually too slow to average the strong dipolar interactions, but it does a good job on the chemical shift interactions. In fact, for the latter interaction one need not spin faster than the interaction in order to see a resonance at the isotropic chemical shift. However, if spinning is slower, then other absorptions called spinning sidebands appear, displaced from the central resonance position by the spinning frequency.

4. Magnetization: The magnetization is the population excess in a given spin state relative to another spin state. NMR signals arise from population differences between energy levels connected by the magnetic dipole operator, I_x , where the x axis is defined to be perpendicular to the static field (z) direction. The energy levels giving rise to these population excesses have energy differences in the millidegree Kelvin range. Thus, the population differences at ambient temperatures are of the order of 1 in 10^5 . As a result, the NMR signals are usually quite weak, par-

ticularly for C-13 since its isotopic abundance is only 1.1%. (Protons are 100% naturally abundant.) Computer-aided signal averaging is the usual method for enhancing signal-to-noise ratios.

5. Quantization axis: This is the axis along which magnetization is directed, or the axis whose magnetic field defines the energy level of the spin system. Normally this is the static field direction. However, the application of a strong radio frequency field, on resonance, can quantize the spins along the rf field, which is generally referred to as B_1 .

6. Relaxation: This is the process by which a non-equilibrium magnetization returns to its normal Boltzmann population. Relaxation is generally determined by the characteristics of molecular motion. T_1 is the time constant for reequilibration along B_0 . It is determined by motions whose components lie in the mid-MHz range, near the resonance frequencies of the nuclei themselves. $T_{1\rho}$ is the time constant for reequilibration of populations quantized (or 'locked') along B_1 . Since these energy levels are separated by spacings about three orders of magnitude less than those along B_0 , this relaxation is sensitive to motions about three orders of magnitude slower, i.e. the mid-kHz range. (It is important to recognize that in a solid where motions are typically slow, the presence of motions with components in the kHz range is much more likely than motions with components in the MHz range, therefore, $T_{1\rho}$ is generally much shorter than T_1 .) Typical ranges for T_1 in solids are 0.1-1000s, and for $T_{1\rho}$ 0.1-1000 ms. The relaxation time T_2 is not a relaxation time associated with energy levels. It is a description of the time constant for the persistence of magnetization in the observation plane of detection (normal to B_0). As such, in a solid it

is often inversely proportional to the dominant interaction experienced by the nucleus being observed, e.g. the dipole-dipole interaction or the chemical shift interaction. Finally, the time constant T_{1xz} is the time constant for relaxation under multiple pulse (see below). It is very similar to $T_{1\rho}$ in its sensitivity to motion, but in a system whose inhomogeneities of structure have dimensions of a few nm, T_{1xz} is quite distinct from $T_{1\rho}$ since spin diffusion is quenched in a T_{1xz} experiment, while it proceeds apace in a $T_{1\rho}$ experiment.

7. Multiple pulse sequences: These are sequences of strong, closely-spaced rf pulses which are accompanied by stroboscopic observation in a certain time 'window' in each pulse cycle. Even though the spins are following very complicated trajectories during the application of such sequences, this stroboscopic observation verifies that during such sequences, like spins are decoupled from one another with respect to their dipolar couplings. Since no dipolar couplings exist during this period, no spin diffusion occurs either, because spin diffusion is a property of dipolar-coupled spins. The chemical shift is scaled but is not zero under multiple pulse, so this provides a way to monitor chemical shifts of protons while suppressing the strong dipolar interactions. Also, as mentioned earlier, if the magnetization is 'locked' under multiple pulse so that relaxation can be monitored, the relaxation time, T_{1xz} , reflects the motions of individual spins, not complicated by spin diffusion.

8. Spin diffusion: This is the process of magnetization transport between like spins in the presence of a magnetization gradient.⁸ In this paper spin diffusion will refer mainly to proton-proton spin diffusion. The basis for the process is the existence of dipolar couplings in an organic system. Moreover, it is also assumed that the entire solid is a cou-

pled network in that there are no islands of spins isolated by barriers. The coupling of each spin to several others allows one to approximate the spread of magnetization by means of diffusion equations. It is known that spin exchange is by no means a random process so that on a microscale (a scale of molecular dimensions) it is probably inappropriate to speak of diffusion, yet because of the many-body nature of the spin-spin interactions, the diffusion equations are a good approximation. In order to use the concept of spin diffusion to obtain domain size information it is necessary to estimate the diffusion constants appropriate to any given system. Quite a bit of work has been done on the n-alkane system both experimentally and theoretically leading to a calculated diffusion constant of $6.2 \times 10^{-12} \text{ cm}^2/\text{s}$.¹⁰ In systems of lower proton density such as the PBT system it might reasonably be expected that the diffusion constant, D , will scale as the proton concentration to the $(-1/3)$ power. Thus, a diffusion constant of $4 \times 10^{-12} \text{ cm}^2/\text{s}$ would seem appropriate for PBT. The presence of molecular motion tends to reduce the dipolar couplings and also D . However, in the limit of very small residual dipolar couplings resulting from molecular motion, the residual dipolar linewidth may lead to an underestimate of D since other relaxation mechanisms can contribute to spin-exchange if motions are not too much faster than the dipolar interaction strength for a rigid lattice.

Spin diffusion proceeds most efficiently when the spins are quantized along B_0 . By comparison, the diffusion constant describing diffusion when the magnetization is quantized along a large, resonant B_1 field is half as big. Spin diffusion is quenched altogether during the application of multiple pulse sequences.

The observation of spin diffusion effects requires that magnetization gradients be established within the system. The production of such gradients requires some kind of inhomogeneity to be present in the system. For example, in a phase-separated polymer blend, one phase may be more mobile than the other. Thus, relaxation should be more efficient in one phase than the other. Consequently, as relaxation proceeds, gradients would tend to appear. Spin diffusion would then tend to resist the establishment of strong gradients in a mixed system. With diffusion constants in the range quoted above, we can estimate the distances over which proton magnetization might propagate in times characteristic of T_1 or $T_{1\rho}$. A formula which can be used to estimate a mean squared displacement,¹¹ x , is

$$x^2 = 2Dt \quad (1)$$

where t is the diffusion time. This formula follows from the solution to the diffusion equation for an instantaneous δ -function distribution of proton magnetization. For $t = 1\text{ms}$, x values are in the range 0.9-1.1 nm; for $t = 1\text{s}$, x values are in the range of 28-35 nm. So in a phase separated system whose smallest domain dimensions might be 3-8 nm, typical equilibration times will be in the range of 2 to 20 ms. It should be noted that the process of spin diffusion (based on spin exchange) conserves total magnetization. The observation of spin diffusion is best carried out when other sources of magnetization change are negligible. Other sources involve the various relaxation mechanisms. It is apparent that for a given temperature and chemical system, the best case is to let spin diffusion develop while the magnetization is quantized along B_0 . In

this case, only the relatively inefficient T_1 processes interfere. If T_1 is much longer than the equilibration times, all changes in the magnetization levels within different regions can be attributed to spin diffusion rather than relaxation.

9. Cross-polarization: This is the process (abbreviated CP) in which unlike spins which are dipolar-coupled to one another can transfer magnetization from the spin system of higher order to that of lower order. In this paper the method is the so-called spin-lock¹² CP in which strong resonant rf fields are applied to the proton and C-13 spin systems. The magnetization is initially ordered along the proton rf field and then part of this order is transferred to the C-13 nuclei in a level crossing experiment. The net result is that when the so-called Hartmann-Hahn condition is fulfilled¹³, the carbons respond as if they were protons. In this process, the total order is redistributed by spin diffusion among the carbons and the real protons. In this way, the carbons gain a polarization approximately four times larger than their corresponding Boltzmann polarization. Two important advantages arise out of the use of the CP method: first, signal enhancement and second, the carbons (with their greater resolution in the solid state) can be used to monitor the local proton magnetization. The disadvantage of the method is that cross-polarized C-13 signal strengths can be distorted. The reasons for these variations are manifold,¹⁴ but some of the more common ones are unequal $T_{1\rho}^H$'s in a sample, differences in CP efficiencies between protonated and unprotonated carbons (the necessary dipolar couplings are weaker for the latter), and nearly isotropic motion in some regions of a sample (giving very weak dipolar couplings). In a polymer system below the glass transition temperature, the principal source of intensity distortion is the dif-

ference in efficiencies between protonated and unprotonated carbons. It usually takes about 200-500 μ s to generate full intensity for a protonated C-13 signal and about 1-3 ms for an unprotonated C-13 signal.¹⁵

10. Pulse sequences: This term describes the choice of timing intervals, rf phase, rf pulse lengths, and observation window in a given experiment. Pulse sequences are the core of the versatility of the NMR methodology. Since NMR signals are detected in a phase-coherent way, the magnetization can also be manipulated correspondingly. Multiple pulse sequences and cross-polarization sequences have already been alluded to. These and other echo sequences will be described in more detail in the experimental section.

11. High Power Proton Decoupling. This term refers to the application of very strong, usually resonant rf fields (B_1) applied to the protons in order to eliminate dipolar coupling between protons and another kind of nucleus, e.g., C-13. The B_1 fields must usually be several times the average local proton dipolar fields in order to be effective. The observation of C-13 signals in solids is most often carried out in the presence of such proton decoupling in order to measure the chemical shifts of the C-13 nuclei without interference from the large proton - C-13 dipolar interaction.

B. Experimental

1. Materials

All materials were supplied by the Air Force Materials Laboratory. As noted before, the nature of this investigation was to explore the NMR methods and not investigate the materials in a systematic way. The samples in the order in which they were received were as follows:

Sample A: PBT film, Celanese #31023-41-5, heat-treated and oriented.

Sample B: PBT sheared film-D4 unoriented. This film is deuterated on the phenylene ring. No heat treatment was indicated.

Sample C: ABPBI film, "heart cut", unoriented.

Sample D: ABPBT fiber #021683 as spun and oriented.

Sample E: 30%PBT/70%ABPBT molecular composite film, unoriented.

Sample F: 30%PBT/70%ABPBI molecular composite film.

Sample G: Heat treated PBT fiber, Celanese (AFTECH I).

Sample H: Heat treated PBT fiber, DuPont (AFTECH II).

Sample I: 40%Nylon(Zytel 42-DuPont)/60%PBT film (from W.-F. Hwang), coagulated out of methane sulfonic acid (MSA) at room temperature, washed in water with pH monitoring, compression molded at 255° C.

Sample J: 30%PBT/70%ABPBI stretched 2x during coagulation out of MSA into water.

Sample K: ABPBI film stretched 2x during coagulation out of MSA into water.

Sample L: 30%PBT/70%ABPBI coagulated from MSA at a concentration where the PBT is expected to have phase separated prior to coagulation. This sample will be referred to as the phase separated composite. The appearance of this sample was very inhomogeneous in color, varying from light to dark brown and the homogeneity of composition was not investigated.

Sample M: Nylon Zytel 101 (DuPont via W.-F. Hwang); molded into a plate about 6 mm thick.

Sample N: PBT film coagulated into water from MSA, washed thoroughly in water, and dried.

Sample P: PBT film coagulated into water from MSA (but not washed) and dried.

Sample Q: Nylon 66 pellets from our laboratory; from Chemstrand.

2. Spectrometers

With the exception of a few C-13 MAS spectra, all data were taken on a Bruker CXP-200 spectrometer¹⁶ operating at a static field of 4.7T (200.05 MHz for protons, 50.305 MHz for C-13). The probe used for proton observation was a low-Q probe employing damping resistors. The recovery time of the probe following pulse excitation was 2 μ s. The rf field strength for most of the proton experiments was 125 kHz (2 μ s 90° pulse); $T_{1\rho}^H$ experiments were usually carried out at a reduced level of 83 kHz. The multiple pulse experiments were carried out at an rf field of 166 kHz (a 1.5 microsecond 90° pulse). The samples for the proton observation were 5 mm OD.

The C-13 spectra were taken either in an 8 mm non-spinning cross-polarization probe or in a MAS probe purchased from Doty Scientific¹⁶ of Columbia, S.C. In these cross-polarization experiments, the rf field strengths were matched at approximately 72 kHz. Spinning rates for MAS were limited mainly by inability to get a well-balanced sample into the rotor. Spinning rates were typically in the range of 2.5-3.5 kHz. In order to obtain sideband-free spectra, a non-commercial spectrometer operating at 15.08 MHz for C-13 and 60.0 MHz for protons was used for a few MAS experiments. Rf field strengths were matched at 58 kHz, spinning frequencies were 2.2 kHz, and the rotor OD was 8 mm.

3. Pulse Sequences and Their Rationale

Spin $1/2$ nuclei, such as C-13's or protons, precess in the presence of an applied magnetic field, and they do so around the axis defined by that field and at a rate given by γB where γ is the gyromagnetic ratio and B is the magnetic field strength. In the usual NMR experiment, precession occurs about the static field, B_0 , and will in addition, occur about a strong rf field, B_1 , applied near resonance. For a sample equilibrated in the presence of B_0 , macroscopic magnetization only exists along B_0 ; however, NMR detectors can only detect precessing magnetization which requires a magnetization transverse to B_0 . In the simplest case where the magnetization is to be measured along B_0 , it is necessary to cause some projection of the magnetization normal to B_0 so that precession can be observed. This is accomplished by the application of a short, resonant, rf pulse which directs the magnetization away from B_0 into the so-called observation plane. Using the convention that the z direction is defined to be the direction B_0 , a rotating frame coordinate system is defined which rotates about this z axis at the frequency of the applied rf. In this rotating frame, mutually perpendicular x and y axes are defined (the z axis still lies along B_0) along directions normal to B_0 . Along these axes the applied rf field is stationary. This rotating frame is the basis for the nomenclature 90°_i , P_i ($i=\pm x, \pm y$) where a number (e.g. 90°) refers to an rf pulse which causes magnetization to precess through an angle of that number of degrees (e.g. 90°). The subscript refers to the direction in the rotating frame defined by the phase of the rf; thus a 90°_x pulse is applied with an rf phase 90° different from a 90°_y pulse and 180° different from a 90°_{-x} pulse. Finally, a P_i pulse is a pulse whose phase only is specified.

Observation of z magnetization is usually accomplished with a single 90° pulse; the transient response is called a free induction decay (FID). If sufficient time for population equilibration is allowed (at least 5 times T_1), then the Fourier transform of this transient response is the equilibrium spectrum (the ' M_0 ' spectrum).

The pulse sequences used herein are often combinations of subsequences and most of the subsequences used in this paper, along with their rationale, follow:

1. $[90^\circ_x - \tau - 180^\circ_y - \tau]$; the sequence is referred to as a "Hahn echo" sequence.¹⁷ Magnetization, initially along B_0 , is placed in the observation plane and allowed to precess freely for a time τ . Then a 180° pulse is applied with a 90° phase shift and another free precession period of duration τ follows. At the end of this time an echo forms because all contributions to the precession behavior due to interactions, (e.g. static field inhomogeneity, resonance offset, chemical shift, and heteronuclear dipolar couplings) which depend linearly on I_z , are exactly cancelled. Only homonuclear dipolar interactions and true relaxation effects are not cancelled. This sequence can be used to select magnetization from a mobile proton species while suppressing signals from a broad, dipolar-coupled resonance.

2. $[90^\circ_x - \tau - 90^\circ_y - \tau]$; This is a so-called dipolar echo. Instead of a 180° pulse, as in the Hahn echo, a 90° pulse is applied. This pulse refocusses homonuclear dipole-dipole interactions between two isolated spins. However, since spins are usually coupled to more than one other spin, τ should be of the same order or less than the FID time of the dipolar-coupled line in order to avoid excessive echo attenuation. This sequence can be used to enhance magnetization from a material with weaker

dipolar couplings when a second material with stronger dipolar couplings is present. One drawback of this sequence is that the dipolar echo also refocusses, to a large extent, those interactions refocussed by the Hahn echo.

3. MREV-8 version of the multiple pulse cycle:^{19,20} $[\tau-P_x-\tau-P_y-2\tau-P_y-\tau-P_x-2\tau-P_x-\tau-P_y-2\tau-P_y-\tau-P_x-\tau]$. Successive application of this cycle, where all P_i are 90° pulses, suppresses the homonuclear dipolar interaction provided the pulses are short (typically $2\mu\text{s}$ or less) and τ is comparably short (usually less than $4\mu\text{s}$). Magnetization is usually prepared in a particular direction prior to applying the multiple pulse cycles. As a result, magnetization may be either 'locked' along or precess around the chemical shift axis which lies along the (101) direction in the interaction frame called the toggling frame. Observation of precession leads to a chemical shift spectrum under multiple pulse (since dipolar interactions are eliminated). Observation of the locked magnetization allows measurement of T_{1xz} the relaxation time under multiple pulse.²¹ Observation of the magnetization is stroboscopic, occurring once per cycle, usually in one of the 2τ windows. The importance of the multiple pulse technique for this discussion is that spin diffusion is suppressed during the multiple pulse trains.

4. $[90_x-P_y]$ This sequence is called a spin-locking sequence. Initial z magnetization is rotated into the y direction by a 90°_x pulse. The P_y pulse then "locks" this magnetization since both B_1 and the magnetization become colinear. The time constant for decay of locked magnetization is defined to be $T_{1\rho}$.

5. Spin-lock cross-polarization sequence.¹² This sequence is used for transferring magnetization from one kind of nucleus (e.g. protons) to another kind (e.g. C-13). Typically the sequence begins by spin locking the protons. Then either coincident with the beginning of the P_x pulse or after some delay, a resonant carbon rf field of arbitrary phase is turned on. During the period when both rf fields are present, C-13 magnetization, arising from proton (dipolar)-coupled carbons, grows along the B_1 direction of the C-13 rf. Growth (or transfer) is most efficient when the precession frequencies about both the proton and C-13 rf fields are equal; this is the so-called Hartmann-Hahn condition.¹³ C-13 signals are generally observed immediately after turning off the C-13 rf and with P_x on (high power proton decoupling).

The actual sequences employed in these studies will be referred to explicitly if they differ from those discussed above. But these subsequences form the basis of the other sequences.

C. Overview of the NMR Effort to Determine Level of Mixing

Aside from the limited supply of well characterized sets of samples, our approach to this problem was, we believe, without prejudice in the following sense: we allowed for the possibility that the polymer blends would be mixed at a molecular level (because of kinetic considerations) even though, as mentioned in the introduction, the expectation was that the polymers should tend to phase separate during coagulation.

If a polymer blend is really a "molecular composite," i. e. mixed on a molecular level, then any long-range lateral order which the homopolymers might possess should be disrupted. Moreover, molecular

mobilities should change relative to the homopolymer. In fact, the blend should possess characteristics quite different from those of the homopolymer.

From the NMR point of view, a molecular composite could possess the following characteristics relative to its homopolymer components:

- a) Relaxation times would not be the superposition of the homopolymer relaxation times. In fact, any relaxation parameter measured in the presence of spin diffusion should give homogeneous relaxation.
- b) Proton linewidths (broadline) would not be superpositions of the component homopolymer linewidths.
- c) Order, as perceived, for example, in the ^{13}C MAS spectra would be altered and probably produce broadening of previously sharper resonances.
- d) Any method for generating proton magnetization gradients between the polymer components should lead to a quick disappearance (over ~ 1 ms) of the gradients as soon as spin diffusion is allowed to take place.

We anticipated from the outset that it would be difficult for the PBT/ABPBI blend to separate spectrally individual resonances, owing to the chemical similarity of the components. Therefore, particularly for this system, we were interested in the possibility that certain of the criteria (particularly a and b above) for intimate mixing might be applied. Thus, it was clear that the homopolymers PBT and ABPBI had to be characterized.

In studying the homopolymers, it became obvious that most of the homopolymers were not pure in the sense that they contained mobile protonated species (obvious candidates here are water and residual acid). The mobile protonated species and their variable content made the application of criteria a and b quite meaningless because individual characteristics of the blends component polymers were therefore not easily determined.

We explored the possibility that if the mobile protonated species were even weakly dipolar-coupled to the polymer then they could be used qualitatively to probe, via spin diffusion, the homogeneity of structure of the composite, or even of the homopolymer. Several experiments were carried out in which magnetization was transferred between mobile and less mobile (polymer) protons. These experiments should also, in the case of the homopolymers, have a bearing on whether impurities are trapped in interstitial regions or distributed throughout the polymer.

The characterization of relaxation in these samples via multiple pulse techniques, i.e. measuring T_{1xz} 's, was also examined since the T_{1xz} measurements allow protons to relax without spin diffusion. Thus, if the mobile species are confined to the outside of domains, then perhaps the relaxation of the polymer domains can still be determined.

The nylon/PBT composite offered many more options for investigating the intimacy of mixing because differences in aliphatic and aromatic carbon resonances can be distinguished both with and without MAS. Moreover, even 'broadline' proton spectra could be reasonably decomposed into contributions from either species although recognition of the component spectra is more definitive in the ^{13}C spectra. Thus, spin-diffusion experiments could be carried out fairly well. Considerable effort was ex-

pendent in what was regarded as being the most definitive experiment, namely, (a) create a magnetization gradient under multiple pulse using T_{1xz} differences (no spin diffusion), (b) then let spin diffusion take place for a variable time, and (c) finally cross-polarize to the ^{13}C nuclei to "read out" the status of the proton magnetization. The "read out" phase was therefore not subject to doubt as to which polymer component the magnetization was to be attributed to. What follows is a description of the particular results on the homopolymers and the composites and their interpretation.

D. Results and Discussion

1. Proton Spectra from Free Induction Decays

Equilibrium (M_0) proton spectra for several of the original samples are displayed in Figure 1. The four spectra (Figure 1C-1F) in particular showed a significant (30-65%) fraction of the total proton intensity in a narrower line whose width ranges from 2-3.6 kHz. This narrow line component did not always show a symmetric band shape. The apparent dominance of the narrower line in the spectrum (Figure 1F) of PBT- D_4 is attributable to the absence of protons on the phenylene ring. In contrast, the two oriented materials (Figure 1A and 1B), each of which has its preferred axis oriented along B_0 , possess a much smaller fraction of narrow component. In the heat-treated PBT film (Figure 1B), the outer resonances, separated by 27 kHz, are associated with the two phenylene proton pairs in the ortho-meta positions; the central line of similar width is attributable to the two remaining protons on the benzobisthiazole moiety. Since the benzobisthiazole protons are separated from one another by approximately 0.50 nm, (while the phenylene proton pairs are only 0.25 nm apart) their 16 times smaller splitting (for B_0 parallel to the

chain axis) is masked by proton-proton dipolar interactions involving other protons. There is a small fraction (1.2%) of narrow component (~ 1 kHz in width) superimposed on the central polymer resonance.

The features of the ABPBT fiber spectrum (Figure 1A) are similar to those of PBT. The smaller splitting of the resonance due to the ring protons can be qualitatively understood in that the three protons of the monomer consist of one pair at adjacent sites on the benzene ring while the third is more isolated on the same ring. Again the pair gives rise to the wider spectral feature, but since the polymerization linkages are not collinear as they are in PBT, the proton pair in an oriented (along B_0) ABPBT chain does not have its H-H vector lying along B_0 as it does in PBT. Therefore, the dipolar interaction is smaller (23.1 kHz). The central resonance feature is primarily due to the third proton but the peaked shape of this resonance indicates some minor portion of a more mobile proton species. None of the samples in Figure 1 was sealed in vacuum; all were exposed to ambient humidity which ranged from 35-50%.

Although we were first unaware of it, ABPBI is very hygroscopic. ABPBI will take up as much as two molecules of water per monomer unit.²² So we decided to compare the spectrum of Sample C, the "heart cut" ABPBI both before and after vacuum drying. Figure 2 shows the proton spectra before (solid lines) and after (dashed lines) drying for 30 minutes in vacuum and sealing. Although the samples were the same and the probe was properly tuned for each sample, the total intensity after drying fell to 79% of the original. Concurrent with this was a general broadening of the spectrum, including the originally broader polymer resonances; in addition, a small impurity resonance became visible. Thus, we conclude that evacuating the sample removed some 21% of the total protons (probably in the form of

volatile water) and that the polymer resonances broadened. The reason for the latter could be two-fold. First, the amino proton could be in rather rapid proton exchange with the available water protons which in turn may be rapidly (on the timescale of dipolar interactions which is approximately 10^{-5} s) moving through the lattice. Removal of the water would then cause these amino protons to remain fixed, thus increasing the dipolar broadening of all non-exchanging polymer proton resonances. From Figure 2, however, the strength of the broadening coupled with the relative isolation of the amino proton from the ring protons, suggest that in the hydrated form, the ABPBI is also more mobile so that molecular motion averages part of the dipolar interaction. When water is removed, the chains become more rigid. It is concluded from these observations that water was intimately mixed into the ABPBI which was equilibrated with ambient relative humidity. Sample F, the composite of PBT and ABPBI, was also evacuated and sealed. The narrow fraction fell from about 46% to 12% of the total intensity.

It is not obvious from the narrower resonance features in many of the above samples just what the mobile proton species are. In Figure 3, spectra are plotted of Samples N and P, both PBT samples were coagulated from MSA. The first was washed, the second was not washed although it was coagulated in water. Both samples were sealed in vacuum. Both spectra show a narrower resonance constituting about 14% of the total intensity. The upper spectrum of the unwashed material shows a shift in the position of the narrow resonance with respect to its washed counterpart. As discussed in the section on relaxation, the broadening and shift is understood as arising from the replacement of some of the mobile species in Sample P with a second mobile species whose resonance is narrower and shifted 5-6 ppm

upfield (See the difference spectrum in Figure 3). While washing certainly alters some of the impurity material, evacuation for a period of half an hour is insufficient to volatilize and expel these impurities; therefore they are either not volatile or are trapped in the polymer matrix.

Figure 4 shows the proton spectra of several preparations of the heat treated AFTECH I fibers. The upper spectrum is of an oriented sample, sealed in vacuum, the center spectrum is of a chopped fiber, sealed in vacuum, and the lower spectrum is of chopped fibers exposed to air. Two things are to be noted. First, the full width at half height (FWHH) of the unoriented material is about 24 kHz as compared to 20 kHz in those PBT samples containing the strong narrower component. Secondly, the fibers show no detectable water when exposed to ambient relative humidity for several months. Thus, it appears that the structure of the heat treated fiber is such that water is excluded. Moreover, the increase in linewidth can correspond either to densification of the structure and/or slight reduction in the amplitudes of some hindered motions characteristic of unannealed samples.

While the hygroscopic nature of ABPBI is recognized, the nature and homogeneity of the distribution of mobile proton species, particularly in the unannealed PBT samples, is less well known. This will be addressed under Section F of the results.

The proton lineshape for Sample I, the nylon/PBT composite will be discussed later in the section dealing with experiments on the intimacy of mixing.

2. Proton Relaxation and Spectra Taken with Multiple Pulse

As mentioned earlier, the multiple pulse technique is a method for quenching spin diffusion thereby measuring properties, i.e. spectra or relaxation times,²¹ characteristic of the individual sites in an inhomogeneous system. Table I gives the time constants, $T_{1xz}(i)$, and the corresponding proton percentages associated with each $T_{1xz}(i)$ for the unevacuated original set of samples (A-F) received. The total time, t_c , for the MREV-8 multiple pulse sequence is also given. Two cycle times were used for each determination and the results for the two cycle times agree reasonably well. Most of the decay curves were fitted to a sum of three exponentials although those of the two oriented samples, A and D, were fitted sufficiently well by two exponentials. In Samples A and D, the two time constants differ by more than an order of magnitude. The assignment of the shorter time constant to mobile protons and the longer one to polymer protons cannot be true, however, since the mobile protons in these samples represent only a few percent and not the observed 23-28%, of the total proton content. A more likely explanation is that the PBT and ABPBT fibers consist of fibrils whose lateral dimensions are small (<7 nm) and whose sizeable fraction of surface chains might be mobile enough to generate shorter relaxation times. Or, it may be possible that interactions with the minor mobile proton species could shorten the relaxation times.

The samples B, C, E, and F all include components with time constants of the order of 1 ms and these components have sizeable percentages (40-69%). Sample C, the ABPBI "heart cut" film has the highest percentage of short T_{1xz} . Since this sample, as discussed in the previous section, has picked up substantial amounts of water which probably penetrates the bulk of the ABPBI, causing enhanced polymer motion, it is reasonable that

TABLE I.

Proton Longitudinal and Multiple-Pulse Relaxation Parameters

| Sample | Material | $T_{1xz}(1)$ | $T_{1xz}(2)$ | $T_{1xz}(3)$ | $\%(1)^b$ | $\%(2)^b$ | $\%(3)^b$ | t_c^c | $T_1^H(s)$ |
|--------|---------------------------|--------------|--------------|--------------|-----------|-----------|-----------|---------|-------------------|
| A | PBT film | 9.1 | 124 | | 26 | 74 | - | 30 | 2.0 |
| | | 8.2 | 121 | | 28 | 72 | - | 48 | |
| B | PBT-d4 film | 1.4 | 8.0 | 93 | 45 | 21 | 33 | 30 | 0.04 ^d |
| | | 1.7 | 9.5 | 110 | 51 | 15 | 33 | 48 | |
| C | ABPBI film 'heart/cut' | 0.93 | 5.5 | 29 | 66 | 27 | 7 | 30 | 0.014 |
| | | 0.72 | 4.3 | 35 | 68 | 26 | 6 | 48 | |
| D | ABPBT fiber | 9.4 | 182 | | 27 | 73 | | 30 | 0.29 |
| | | 7.5 | 161 | | 23 | 77 | | 48 | |
| E | 30% PBT/70% ABPBT | 1.2 | 8.8 | 93 | 41 | 29 | 30 | 30 | 0.22 |
| | | 1.4 | 8.8 | 96 | 40 | 29 | 31 | 48 | |
| F | 30% PBT/70% ABPBT | 1.1 | 7.7 | 35 | 56 | 25 | 19 | 30 | 0.36 |
| | | 0.91 | 7.0 | 33 | 58 | 28 | 14 | 48 | |

a) Values are based on the separation of decays into two or three exponential components. Times are in ms.

b) Percentages are those percentages of the total magnetization contributing to the T_{1xz} decay of that component.

c) t_c is the total cycle time for the MREV-8 multiple pulse cycle (in μs).

d) T_1^H of the narrow-line resonance is shorter than that of the broad resonance; the latter is given.

the percentage of short-time-constant protons be larger than estimated from the lineshape. Moreover, the rather short intermediate time constants and the small amount (only 6-7%) of the material with a "long" time constant suggest that the mobile fraction is well mixed. In fact, measurements of $T_{1\rho}^H$ on Sample C indicate that the long component is probably a second component within the narrow component.

Sample B, the PBT-D₄ film, shows two shorter time constants, the sum of which is approximately equal to the narrow fraction (60-70%). The longer time constant is similar to the long time constant in Sample A, which indicates that the mobile species are probably external to the PBT domains. The long time constant fraction is due to the PBT protons on the polymer chains in the interior of the domains.

Samples E and F are both composites with 30% PBT. Sample E contains ABPBT and Sample F contains ABPBI. That Sample F should have a higher percentage of mobile component (56%) than Sample E (40%), according to the T_{1xz} analysis in Table I, is reasonable if we again invoke the idea that ABPBI is more hygroscopic than ABPBT. In Sample F, the shorter two T_{1xz} values are similar to those in the ABPBI film, and the relative proportions are similar but not exactly comparable. It is tempting to evaluate whether Sample F is a "molecular" composite from the long T_{1xz} (33 ms), whose percentage roughly coincides with the long time-constant percentage expected based on the results of sample A. However, the T_{1xz} value is considerably shorter than for pure PBT (121ms) in Sample A; moreover, Sample A was heat treated. The 33 ms T_{1xz} would only indicate phase separation if the lack of annealing accounted for the T_{1xz} differences. Indeed, $T_{1\rho}^H$ measurements of the PBT samples (Samples N and P) cast from MSA yielded relaxation times in the 20-30 ms range, although

these latter values were ostensibly influenced by spin diffusion from mobile protons. So the interpretation of the longer T_{1xz} in Sample F is perhaps an indication of phase separation, but not unambiguously so. Sample E, on the other hand, has a long time constant close to those for the homopolymer (Samples A and D). Apparently, Sample E contains some well ordered domains and we might expect on this basis that the material is phase separated. However, if we assumed that the mobile fraction was accounted for in the short-time-constant fraction while the intermediate- and long-time-constant fractions corresponded to the polymer protons, then the equality of these latter fractions for Sample E is not expected based on the relaxation behavior of the homopolymers (Samples A and D). In the homopolymers, the ratio of the long to short fraction is about 3:1. Thus, in a very crude sense the T_{1xz} data for Sample E suggest that some phase separation is occurring judging by the order implied in the long T_{1xz} . However, a fraction about twice as large as expected based on the homopolymers, seems to be mobile enough to relax quite efficiently. This could be taken as evidence for phase separation into domains smaller than for the homopolymer, although one must remember that Sample E was probably not heat treated while Sample A (and probably Sample D) was. In other words, the differences in the T_{1xz} behavior of Samples A, D, and E might reflect heat treatment differences rather than constraints to domain growth in the composite relative to the homopolymers.

One way to assign various T_{1xz} components to different proton populations is to follow the lineshape as a function of T_{1xz} . Only a few experiments of this sort were done but certainly more could be done. Figure 5 shows what happens to the lineshape in Sample A as one goes from the normal M_0 lineshape to the lineshape following 24 ms of T_{1xz} relaxation.

While the lineshapes are very similar, the sharp component is missing thereby indicating that the mobile component is included in the short T_{1xz} component. (The early disappearance of the mobile component in a $T_{1\rho}^H$ experiment was also a common observation.)

Spectra were also taken using multiple pulse. These spectra are narrowed considerably (down to 0.8-1.3 kHz) as a result of the removal of the proton-proton dipolar interaction. What remains to broaden these resonances is the chemical shift anisotropy (~ 5 ppm) and possibly magnetic susceptibility broadening (1-3 ppm). Figure 6 shows the multiple pulse spectra of samples A-F. Very little resolution of individual resonances is apparent. There is no obvious distinction between a broad and a narrow component. The reason for this is that the mobile protons are experiencing a finite dipolar coupling, but these protons are moving more rapidly than the pulse-cycle time through the lattice. Thus, since the multiple-pulse sequence is designed to eliminate static dipolar interactions, the sequence evidently does not do much to eliminate those weaker residual dipolar interactions resulting from motional averaging. Therefore, on a relative basis, the "narrow" line in the M_0 spectrum takes on a width in the multiple pulse spectrum comparable to the originally broad, but now narrowed, M_0 component whose dipolar interactions are truly eliminated. So the multiple pulse spectra, particularly for samples whose mobile proton content is high, are not very useful for analysis. Multiple-pulse spectra were not obtained on the other samples.

3. Other Proton Relaxation times

In many respects, the proton relaxation times are very important in determining the quality of the interpretation of various experiments. For example, the $T_{1\rho}^H$ values, if they are of the same order as typical

cross-polarization times (i.e. 0.5-2 ms), will cause potentially serious distortions in ^{13}C CP spectra. Also, the proton T_1^H 's generally determine the length of time during which equilibration of magnetization in a spin diffusion experiment can be observed. If, for example, domain sizes are approximately 10 nm, then spin diffusion should be followed for 10-30 ms, during which time T_1^H contributions to magnetization change should be negligible (less than 2% of M_0). This means one would like T_1^H 's to be generally greater than 1s.

Table I includes T_1^H values for Samples A-F. The T_1^H 's are generally shorter than 1s, except for the PBT film (2s). In fact, the "heart cut" ABPBI and the PBT-D4 show very short T_1^H 's. One possibility is to attribute the short relaxation times to the presence of the mobile proton species. In this connection the composite of ABPBI and PBT, Sample F, shows a T_1^H much longer than the heart cut ABPBI sample which is not consistent with the foregoing hypothesis since both samples have substantial and nearly equal fractions of mobile material. So while the mobile proton species is probably implicated in shortening $T_{1\rho}^H$ it is not simply the amount of mobile proton intensity which determines T_1^H . In any case, the T_1^H 's are short to marginal for conducting spin diffusion experiments. T_1^H values were not determined for all of the remaining samples. It was found that evacuation did not substantially change T_1^H in most cases. For example, the evacuated heart cut ABPBI still had a T_1^H less than 30 ms; the evacuated PBT sample (unwashed) had a T_1^H of 200 ms. Evacuated samples of nylon 66, nylon PBT, AFTECH I PBT fiber, and AFTECH II PBT fiber had T_1^H values of 0.7, 0.6, 3.0 and 1.0 seconds respectively. (The dif-

ference in the AFTECH fibers may be related to differences in the unpaired electron concentrations as described in the ESR section of this report.)

Rotating frame relaxation times, $T_{1\rho}^H$, were measured on a few of the samples, using rf field strengths of 83 kHz. The decay of the proton magnetization is complex and therefore rather than show each set of data we illustrate some typical behavior. For this purpose we divide the materials into two groups: those having substantial mobile proton fractions and those with very little of these protons (e.g the heat treated PBT fibers and film and the evacuated nylon and nylon/PBT composite).

A typical set of proton lineshapes following various periods of proton spin locking is shown in Figure 7 for the unevacuated heart-cut ABPBI (Sample C). One result which stands out from this data is that the narrow line consists of more than one kind of proton. The downfield portion has a very short $T_{1\rho}^H$ (~600 μ s). The upfield side of the narrow line decays non-exponentially over the times (> 4ms) when its intensity can be measured well. The $T_{1\rho}^H$ of the broad component is approximately 2 ms. Although spin diffusion goes on in a $T_{1\rho}^H$ experiment (at half of the rate compared with a T_1^H experiment), these spectra aid in qualitatively assigning the T_{1xz} components in order of increasing times (see Table 1) to the low-field narrow-line component, the broad polymer resonance, and the high-field narrow-line component, respectively.

Upon evacuation of the heart cut ABPBI, the high-field narrow portion remains (see Figure 2), and the low-field narrow portion is either broadened or nearly eliminated. However, the $T_{1\rho}^H$ of the broad feature still has a decay constant of 2 ms. Therefore, if spin diffusion from a mobile species rather than polymer motions themselves were relaxing the polymer

protons, then the mobile protons remaining after evacuation would be required to possess either stronger dipolar couplings and/or more efficient $T_{1\rho}^H$ relaxation relative to the unevacuated sample and thereby maintain the efficiency of the $T_{1\rho}^H$ relaxation of the polymer protons. On the other hand, the lineshapes of Figure 2 indicate that the mobility of the polymer is certainly affected by evacuation so that through a combination of circumstances the apparent $T_{1\rho}^H$ of the polymer proton resonances is unaffected.

The $T_{1\rho}^H$ behavior of Samples N and P, the PBT films coagulated from MSA, helped to characterize the PBT material prior to heat treatment. The magnetization decays for the broad component were nearly exponential with the $T_{1\rho}^H$ values being 20.7 (after an initial 5% decay over the first ms) and 28.3ms for Sample N (washed) and Sample P (unwashed) respectively. Both samples although evacuated and sealed had a substantial narrow component (14%) with linewidths, respectively, of 2.3 and 1.8kHz (see Figure 3). The narrow line of Sample N was quite asymmetric, and its $T_{1\rho}^H$ behavior showed that it consisted of two parts separated by approximately 5-6 ppm. The low field portion was similar in position, width, and shape to the narrow line of Sample P. The $T_{1\rho}^H$ behavior of this portion was very non-exponential, displaying an early slope corresponding to a 3ms $T_{1\rho}^H$, however, its final slope approached that of the PBT protons. (This is expected if these narrow-line protons are coupled to the PBT protons by spin diffusion). The high field portion of the narrow line of Sample N had a decay behavior that roughly paralleled the $T_{1\rho}^H$ decay of the PBT protons. Its linewidth was about 1.1 kHz. This component which was evidently introduced by extensive washing was missing entirely in Sample P. The ratio of intensities of the low field to high field portions of the narrow com-

ponent of Sample N was 2:1. So the PBT samples which are not annealed show a substantial narrow component and a $T_{1\rho}^H$ for the broad resonance which is much shorter than the T_{1xz} of Sample A and somewhat shorter (as will be seen presently) than $T_{1\rho}^H$ for the annealed PBT fibers. The role of the narrow component in reducing $T_{1\rho}^H$ values for the PBT protons via spin diffusion is not yet clear. This topic will be addressed later. What is clear is that mobile protons exist in the unannealed PBT system with short $T_{1\rho}$'s so that, if they are coupled to the PBT protons, the $T_{1\rho}$'s of the PBT protons will be shortened. T_{1xz} relaxation would clearly provide a superior method for characterization of the intrinsic mobility of the PBT protons.

The spectra of Sample F, the ABPBI/PBT composite, in vacuum, exhibit some similarities and some differences to the homopolymer systems. The narrow (3 kHz) line which constitutes 12% of the total proton magnetization exhibits two different $T_{1\rho}^H$ behaviors for the down field portion and upfield portions of the line with very similar time constants to the narrow components of the ABPBI sample. The decay of the broad polymer proton component is shown in Figure 8 to be very non-exponential; but the decay rate is substantially longer than for the ABPBI sample (the initial slope corresponds to a 3 ms $T_{1\rho}^H$, the final slope is 21 ms). We examined this data to see if the longer final slope could be due to a phase-separated PBT phase, since the final slope had a $T_{1\rho}^H$ characteristic of Sample N. This identification could not be made since the intercept at $t=0$ of the final slope corresponded to a 44% fraction of the broad component which is larger than the 22% fraction of PBT protons in the total polymer. However, if PBT is phase-separated and if domains are small enough so that spin diffusion is active in relaxing the PBT domains, then

extrapolation of the long time slope can overestimate the real fraction of PBT present. This result, taken together with the T_{1xz} fractions and percentages (unevacuated Sample F) allows for the possibility of phase-separation but, if so, into dimensions less than 10 nm so that significant spin diffusion can take place over timescales of 20 ms in the rotating frame.

The hypothesis about mixing with domains smaller than 10 nm in Sample F can be tested qualitatively by looking at the $T_{1\rho}^H$ decay for the PBT/ABPBI (Sample L) which was coagulated out of MSA at a concentration high enough to produce phase separation of a portion of the PBT. In this case, the domain sizes of the PBT regions whose solution precursors were phase separated ought to be larger than in Sample F and this would lead to the assumption that the long time constant in Sample L should have a smaller spin-diffusion contribution, and therefore a longer apparent time constant. Figure 8 gives the decay of the broad component of Sample L. The longer time slope yields a $T_{1\rho}^H$ of 10 ms indicating a long decay time half that of sample F. The trend, therefore, is opposite that expected. A difference between Samples L and the evacuated Sample F is that Sample L showed a narrower sharp resonance (~1 KHZ wide) and the whole narrow line decayed with a $T_{1\rho}^H$ of approximately 2 ms (See Figure 8). So there are clear differences in the mobile proton components in Samples F and L. It will be shown later that the interaction of the protons in the narrow portion of the line with the broader polymer protons is different in these two samples. In fact, the narrow-line protons will be seen to be more uniformly distributed in the polymer matrix in Sample L than in Sample F in spite of their narrower linewidth in Sample L. It appears that the $T_{1\rho}^H$ behavior of the broad resonances is linked to the narrow-line pro-

tons, but that these latter species are quite variable in these samples and little information about phase separation can be deduced from the long time slopes of the $T_{1\rho}^H$ decay curves. Measurement of T_{1xz} decays would probably help clarify the situation but before any interpretation can be made regarding phase separation, an identification of decay rates with the individual polymer species is required...and that is very difficult outside of C-13 CPMAS spectra.

The $T_{1\rho}^H$ behavior of the materials with a small to vanishing narrow-line component are easier to describe. Figure 9 shows decay curves for the evacuated chopped fibers of PBT (AFTECH I; Sample G), nylon 66 (Sample M), nylon 66 pellets (Sample Q), and the nylon/PBT composite (Sample I). Sample G has an initial 10% decay which can be partly identified with impurity protons and seen most easily in spectra of oriented samples (See Figures 4 and 5). The longer decay rate is 44 ms. Sample Q exhibits an exponential decay with a $T_{1\rho}^H$ of 8 ms. This sample, being in the form of pellets probably, has much lower crystallinity than Sample M whose $T_{1\rho}^H$ decay time becomes 19 ms after an initial decay whose slope corresponds to a 10 ms $T_{1\rho}^H$. Finally, the nylon/PBT composite (Sample I) shows a reasonably exponential decay with initial and final slopes corresponding to a 14 and 17 ms $T_{1\rho}^H$ respectively. In Samples I and Q the lineshape is stable as a function of spin-locking time. In Sample G the lineshape is also stable except for the early decay of the impurity protons. In Sample M the resonance width increases 10 kHz from short to long locking times, presumably because the wider crystalline resonances are slowest to decay.

For the nylon/PBT the lack of a lineshape change with t strongly suggests that the two polymers are well mixed on a scale of 10 nm. The rationale for the argument is as follows: (a) The proton lineshape, as

will be seen, is well approximated by a superposition of nylon and PBT homopolymer resonances and this suggests phase separation, at least on the scale of nearest neighbors. (b) Phase separation into large domains would be expected to yield lineshapes which depend on spin locking time and produce a $T_{1\rho}^H$ for Sample I which is a superposition of, say, 74% of the protons relaxing like those in Sample M and 26% like those in Samples G, N, or P. Contrary to this expectation, the final slopes of the $T_{1\rho}^H$ curves for Samples M,G,N and P are all longer than for Sample I. (c) No significant population of mobile protons exists to shorten $T_{1\rho}^H$. (d) The observed $T_{1\rho}^H$ for Sample I is quite consistent in magnitude with that expected for intimately mixed domains of nylon and PBT where crystallinity of the nylon phase is lower, due to mixing, than in the homopolymer (Sample M) and spin diffusion from the nylon (modelled more closely by Sample Q) relaxes the PBT protons. (e) This latter explanation would produce the observed lineshape stability as a function of spin-locking time. This conclusion about the scale of mixing is verified later by more direct spin diffusion experiments.

4. C-13 Cross-Polarization Spectra

Selected samples were observed by ^{13}C solid-state NMR methods. All spectra were taken with high power proton decoupling during observation. Signals were generated via {proton - C-13} cross-polarization (CP). In addition, some CP spectra were taken on static samples while other samples were rotated at the magic angle; the latter spectra are referred to as CP-MAS spectra. CP spectra generally involve a lot of overlap of the individual carbon resonances because of the chemical shift anisotropy. However, in an oriented sample, the CP spectra can convey information about orientation while at the same time improving possibilities for identifying

identify individual carbon resonances. Of course, CP-MAS spectra are "high resolution", particularly for crystalline regions; and this technique provides the greatest opportunity for resolving individual carbon resonances.

Figure 10 shows non-spinning CP spectra of samples J and K, which are, respectively, the stretched (2x) samples of ABPBI and a 30% PBT/70% ABPBI composite. Both samples were coagulated in water from MSA. These samples were macroscopically oriented in the sample holder. Spectra 10A and 10B correspond to Sample K while Spectrum 10C applies to the composite, Sample J. The orientation of the sample changes with Spectrum 10A having B_0 perpendicular to the macroscopic draw direction while in Spectrum 10B and 10C, B_0 is parallel to the draw direction. In comparing Spectra 10A and 10B it is obvious that substantial orientation exists in these samples since the spectra are so different. For example, it is well documented that the most shielded principal value of an aromatic carbon chemical shift tensor lies in the direction normal to the plane of the aromatic ring. The strong shoulder near 25 ppm in Spectrum A indicates this position which is quite typical for aromatic carbons. Resonances occur here when B_0 is nearly perpendicular to the plane of the aromatic rings. The virtual absence of resonance intensity anywhere near 25 ppm in Spectrum B indicates that the chain axes have a strong projection along the stretching direction. The same is true for Sample J in Spectrum 10C. In fact, spectra 10B and 10C look virtually identical. We have also compared spectra (not shown) of unstretched and 2x stretched ABPBI. These spectra are indistinguishable. Therefore, it appears that the 2x stretching did little to improve orientation, beyond that developed during coagulation.

In Figure 11, a spectrum of an oriented PBT fiber bundle is shown where B_0 is parallel to the draw direction. This spectrum is somewhat of a contrast with those of Figure 10 (B and C). The prominent peak near 230 ppm for oriented PBT in Figure 11 can be compared with a rather weak shoulder at 230 ppm for oriented ABPBI in Spectrum 10B. The increase in intensity of this shoulder in Spectrum 10C relative to 10B indicates that the PBT in the composite is oriented.

Because of the different CP efficiencies for protonated and non-protonated carbons¹⁵, protonated carbons cross-polarize faster due to their stronger proton-C-13 dipolar couplings. It generally takes 200-500 μ s to fully cross polarize a protonated carbon and about 1-3 ms for a non-protonated carbon. Thus, particularly at short CP times, the protonated carbon contribution to the spectrum is richer than for the non-protonated carbon counterparts. This is illustrated for oriented Sample G in Figure 12. From Spectrum 12A it is clear that the protonated resonances in this oriented sample are contained in the higher field component of the two dominant resonance groups. Since four of the seven distinguishable PBT carbon resonances are unprotonated carbons some caution must be exercised in properly matching the Hartmann-Hahn condition for CP, otherwise significant spectral distortion can exist even for longer CP times.

Figure 13 shows CP spectra of less oriented materials. Spectrum 13A corresponds to Sample F, an unoriented, wound, film; Spectrum B is also an "unoriented" wound film (Sample I). Spectrum 13A, as expected, looks like a "typical" aromatic carbon chemical-shift-anisotropy powder pattern, even though there are many different aromatic carbon resonances contributing. In spectrum 13B one can pick out the resonances from the tetrahedrally

bonded nylon carbons in the 10-60 ppm range. These carbons generally display a powder pattern 30-60 ppm in total width, quite in contrast to the aromatic carbons whose powder patterns are about 200 ppm wide. So, one could probably do a decent job of deconvolving the nylon from the PBT contribution to the C-13 spectra even though no information about individual resonances within each group can be obtained.

The 50.3 MHz CP-MAS ^{13}C spectra for the unstretched ABPBI film corresponding to Sample K are given in Figure 14. Spectrum 14A is taken with a 40 μs blanking of the proton decoupling pulse at the beginning of signal observation. The proton-C-13 dipolar interaction in this experiment²³, broadens protonated carbon lines and makes them disappear before signal observation begins, so Spectrum 14A represents non-protonated carbon resonances. In Spectrum 14B, a short, 100 μs CP time is used so that protonated resonances appear more strongly than the non-protonated resonances. Spectrum 14C is the CP-MAS spectrum with a 1 ms CP time. In Spectrum 14C, one sees many resonances, most of which are spinning sidebands, separated by an integer multiple of the spinning frequency (2.75 KHz) from the central resonances whose seven peaks occur at approximately 113, 117, 121.9(2), 136.0, 142.4, and 153.8 ppm with respect to liquid tetramethylsilane. From Spectra 14A and B, one can deduce that the protonated carbons resonate at 113, 117 ppm and 121.9 ppm. The last mentioned resonance position is also occupied by an unprotonated carbon.

In contrast to Figure 14, Figure 15 is a 15.08 MHz spectrum of Sample G, the AFTECH I PBT fiber. Because of the lower field, 2 kHz spinning is able to reduce most sidebands to insignificance. Isotropic chemical shifts occur at 117, 128(2), 135(2), 152, and 166 ppm. Three of these seven shifts correspond to protonated carbons and in a manner similar to

that used in Figure 14, it can be deduced that the two carbons at 128 ppm (phenylene carbons) and the carbon at 117 ppm are protonated. The assignment is not our immediate concern, but we note that the highest field position likely corresponds to the carbon on the thiazole moiety attached to the phenylene ring. This carbon is most isolated from other protons on the same chain and may be most sensitive to the Hartmann-Hahn match. This is the only carbon which should be fully resolvable in a PBT/ABPBI composite.

Figure 16 shows 50.3 MHz CP-MAS spectra of sample M, the molded nylon 66 (Nylon Zytel 101), and Sample I, the 40% Nylon/60% PBT composite. Only the amide carbon in the nylon spectrum has visible sidebands since the remaining carbons are aliphatic and have small anisotropies. Sidebands are again copious in Spectrum 16B with most of them coming from the PBT aromatic carbons. There is even some sideband-centerband overlap at 166 ppm, and 117 ppm; minor overlaps with second sidebands occur in the aliphatic region. Both of these samples have seen similar temperatures (near the nylon melting point) in their forming: yet, judging by the narrowest aliphatic components, Spectrum 16A shows highest crystallinity. In fact, a rough integration of the sharp resonance components in each spectrum shows a 35% crystalline fraction in Spectrum 16A and a 23% fraction in Spectrum 16B. Thus, there is an immediate indication that the presence of the PBT has significantly hindered the growth of the nylon crystalline phase, although crystalline domains still exist. Therefore, Figure 16 indicates that the Nylon/PBT composite has some phase separation, but PBT is intimately enough mixed into the nylon to reduce nylon crystal growth.

Unfortunately, the greater intrinsic width of the PBT resonances means that little can be said about whether the PBT resonance lines indicate less order due to the presence of nylon.

5. Experiments on the Intimacy of Mixing in Composites Using Spin Diffusion Between Polymer Component Protons

1. 30% PBT/70% ABPBI Composite

The most promising techniques for studying intimacy of mixing of the PBT/ABPBI system are those whereby CP-MAS is used as a "read-out" mode following a spin diffusion period. This statement follows from the practical result that only CP-MAS can clearly differentiate PBT and ABPBI resonances. (For highly oriented samples, maybe CP without MAS might work). As will be described later, attempts to combine multiple pulse relaxation and cross-polarization (the 'best' experiment) were not successful enough to warrant trying them in a MAS probe. So, for this composite, we chose to do a simple 'test' for intimate mixing rather than attempt to measure the intimacy of mixing directly. The 'test' is to observe CP-MAS spectra at a fixed CP time following a variable spin-locking time on the protons. If the system is truly a "molecular composite", then, since equilibration times for adjacent chains should be of the order of 1 ms, the $T_{1\rho}^H$ decays of the proton magnetization from the PBT and ABPBI, as seen via the C-13 signals, should be tightly coupled.²⁴ On the other hand, if the proton magnetization decays at different rates, then phase separation is indicated. Figure 17 shows 50.3 MHz spectra of Sample J, the 2x stretched 30% PBT/70% ABPBI film, taken with 1 ms CP time after proton spin-lock times of .004, 3, and 5 ms, where a 73 kHz rf field strength was employed. Difference spectra are also shown as are the total integrals of the signals. To facilitate lineshape comparison, the weaker

signals at longer times are normalized so that all spectra have the same total intensity. The arrow indicates the single, resolvable PBT line at 166 ppm. Note that the intensity of this line increases somewhat at longer times, indicating that the relative contribution of the PBT component is increasing at longer times. Qualitatively this is also indicated by the decrease of the 122 and 135 ppm resonances relative to the 117 ppm and 142 ppm resonances, respectively. The approximate $T_{1\rho}^H$'s of each of the components were determined to be 3-4 ms for the ABPBI and 4.7-5.3 ms for the PBT.

This rather crude experiment suggests that a "molecular composite" probably does not exist; nevertheless, the time constants are close enough so that, in view of the fact that $T_{1\rho}^H$ values for pure PBT are usually 20 ms or longer, large domains (>10 nm) of pure PBT or ABPBI are also likely excluded. This experiment was also repeated at 15 MHz using a spinning speed of 2.1 kHz and an rf field strength of 56 kHz. Similar results were obtained with the PBT and ABPBI having $T_{1\rho}^H$'s of 4 ms and 3 ms, respectively.

We did not have time to conduct this experiment on Sample L, the "phase-separated" PBT/ABPBI composite, but this experiment would be a rather important control.

ii. 40% Nylon/60% PBT Composite

This material offers several ways to inquire into the question of mixing owing to the fact that resonances from the individual components may be identified clearly via C-13 CP and CP-MAS spectra and reasonably well via spectra from proton FID's. In this section, we will describe several experiments involving either direct proton observation or indirect (via ^{13}C) proton observation.

a. Proton Lineshape and Its Interpretation

Since the number of protons per unit volume in nylon is approximately three times that of PBT, it follows that the proton linewidths are also different. In fact, the Nylon 66 pellets (sample Q) and the nylon 66 (Zytel 101 molded plate-Sample M) had linewidths of 43.8 and 46 kHz, respectively, while the unoriented PBT samples, N and P, had linewidths of 19 kHz; the chopped heat treated PBT fibers (Sample G) showed a 24 kHz linewidth.

For rigid chains in the composite, it would be reasonable to expect a broadening of 4-10 kHz in the PBT spectrum from nearest neighbor nylon chains. At the same time, a dilution of the nylon chains with the proton-poor PBT chains should produce line narrowing. If mixing is occurring at the molecular level, a visible broadening of the PBT resonances and a narrowing of the nylon resonances is expected. In addition, molecular motion, due to less efficient packing, could be more facile than for the homopolymers leading to a further narrowing of the lines. On the other hand, if the polymer components are phase separated, then the M_0 lineshape should be the superposition of component lineshapes with a 74.2% contribution from Nylon protons and a 25.8% contribution from PBT protons. The experimental lineshape (see ahead to Figure 18) can be approximated by a component whose $70 \pm 3\%$ contribution has a lineshape like that of the nylon Zytel molded plate and the remaining component having a linewidth of 20 kHz, which falls between that of Samples N (or P) and G. Thus, the lineshape is very close to being a superposition of the individual components, implying that at least on a nearest neighbor basis, the sample looks phase separated. This is a very "local" criterion, however, since the domains need not be larger than a few nanometers in order to give this

result. Nevertheless, the recognition that the observed spectrum consists of superposed homopolymer spectra establishes the basis for proceeding with the following spin diffusion experiment.

b. Proton Diffusion Study with Proton Observation

In order to conduct a spin diffusion experiment, magnetization gradients must be generated in the sample. Ideally, sharp gradients are preferred in order to simplify the analysis.²⁵ In order to establish sharp gradients, the preparation time must be short compared with those times over which spin diffusion reequilibrates the magnetization in the various domains. Clearly, the reequilibration times depend on domain sizes. For distances down to 1 nm, this means that if spin diffusion is allowed to proceed during gradient preparation, then the preparation should take no more than 0.2 ms. On the other hand, a multiple pulse preparation with the accompanying quenching of spin diffusion could extend for several ms.

We chose to take advantage of the linewidth differences between PBT and nylon in order to establish a magnetization gradient quickly. The preparation was a single dipolar echo followed by restoration of the magnetization either parallel or antiparallel to B_0 : The sequence for this preparation was $(90_x-30_{\mu s}-90_y-30_{\mu s}-90_{\pm x})$. Following this preparation there was a variable ("spin diffusion") time during which spin diffusion took place. Finally, a single-pulse observation was made with transmitter and receiver phase cycling to suppress multiple quantum coherences²⁶. In Figure 18, a set of spectra are shown as a function of the spin diffusion time. The initial magnetization at 50 μs represents 23% of the total equilibrium magnetization; however its distribution between PBT and nylon

shows that the PBT contribution is more than double that from the nylon. The biggest lineshape changes occur over the first 4-7 ms. Following that, change is still observable, but it is small.

One can analyze the contribution of the two polymer components to each lineshape in Figure 18 by subtracting that component of the lineshape whose shape is the spectrum of sample M, the molded nylon Zytel 101. Figure 19 gives a plot of the relative growth of the nylon magnetization versus the square root of the spin diffusion time. At early times, the growth of magnetization is expected to follow a square root of t dependence, and this is true for the composite, at least for the initial 50% of the recovery. After this, recovery slows down and small changes are still taking place between 30 and 50 ms. Figure 19 has two nearly parallel curves. The upper curve is a so-called corrected curve which approximately takes into account the small drift of the total proton magnetization during the diffusion time. As noted earlier, not only transport due to spin diffusion but longitudinal relaxation (T_1^H) processes contribute to the change of magnetization levels. In this case, the decay in the total proton integral over the 50 ms interval covered in Figure 18 is 11%. Each point of the corrected curve of Figure 19 is obtained from the uncorrected one by simply dividing by an amount proportional to the total proton signal integral at that point. It should also be noted that because of the alternate inversion of the magnetization along $\pm B_0$ prior to the spin diffusion period, two statements follow. First, as the spin diffusion time gets much larger than T_1^H , the observed magnetization approaches zero. Secondly, growth of the magnetization of any component (prior to

correcting for T_1^H effects) implies a growth via spin diffusion. It is also true that T_1^H effects accumulate more slowly with the magnetization alternation than if this alternation were absent.

The interpretation of domain sizes using data like that of Figure 19 requires more detailed modeling which was not attempted. However, in the spin diffusion modeling of poly(ethyleneterephthalate)(PET) fiber morphology²⁵ similar recovery curves were observed and a scaling of those results to the present case gives an overall periodicity of 7 nm where the scaling has involved the assumptions that the average diffusion constant, D , for the composite is 5×10^{-12} cm²/s (4×10^{-12} cm²/s for PBT and 6×10^{-12} cm²/s for nylon). Also assumed is an overall dimensional scaling directly proportional to the value of the abscissa at the point where the initial slope line in a curve like that of Figure 19, attains the ordinate value corresponding to equilibrium magnetization. The 7 nm determined from this experiment is interpreted as an average repeat distance along the narrowest dimension of the domains. For example, suppose that PBT were in fibrillar form, then the sum of the PBT fibril lateral dimension plus the interstitial nylon phase is 7 nm.

The recovery curve of Figure 19 is not analogous in all respects to the PET data on which the composite diffusion data analysis is based. The data of Figure 19 show that the linear portion of the recovery only accounts for about half of the total recovery to equilibrium while in the PET samples, the linear portion of the recovery curves comprised 60-80% of the recovery. The earlier departure from linearity for the composite could indicate a heterogeneous structure in one of the components. Indeed, the proton spin diffusion results seen via the C-13 spectra show

that the crystalline regions of the nylon are the last to be populated by spin diffusion. Therefore, the 7 nm dimensions probably do not take into account the nylon crystalline regions.

The experiment described in the foregoing paragraphs may also be criticized in that the initial gradients formed in the dipolar echo preparation are not uniform throughout the sample. The dipolar echo preparation produces magnetization which depends not only on whether a proton is a nylon or PBT proton but also on the geometrical distribution of the local dipoles within a given phase. In recognition of this, experiments were performed on the homopolymer systems of the chopped PBT fibers of Sample G and the nylon pellets of Sample Q. The dipolar echo indeed selects protons whose linewidths are narrower than the average. However, after about 0.4-0.6 ms, the nylon lineshape is nearly its M_0 width. In PBT, linewidth recovery takes a similar time. Thus, the first two or three points in Figure 19 are suspect because the attribution of linewidth to the two polymer components is not rigorously valid for early times. The short time slope may, therefore, not be as steep so that the periodicity may be as large as 11 nm.

c. Proton Spin Diffusion Using C-13 CP-MAS Readout

The weakness of the experiment described in the foregoing section is the uncertainty, particularly at early times, as to whether the proton signals are coming from the nylon or PBT protons. One way out of the problem is to use the C-13 signals, generated via CP, as a monitor of the proton magnetization. The easiest way to separate the two polymer signals is via MAS. However, simple as the idea sounds, other complications must be dealt with. What follows is a list of complications and what was done to overcome or account for them.

First, to generate sharp magnetization gradients, the same dipolar echo preparation scheme could not be used since MAS interferes with the refocusing of the echo. Therefore, a series of four dipolar echoes was used $[90_x-(12_{\mu s}-90_y-12_{\mu s})_4-90_{\pm x}]$. The shorter intervals between pulses reduce the interference from MAS and the use of four echoes instead of one increases the contrast between the nylon and PBT magnetization.

Second, the observation of C-13 signals (via CP) instead of proton signals means that one does not have an instantaneous measure of proton magnetization. To approximate an instantaneous measure, a short CP time (0.2 ms) was used. This time, however, is insufficient to equilibrate the C-13 nuclei with the protons. This is particularly true for the non-protonated carbons which cross-polarize more slowly than their protonated counterparts. Thus, one must take account of the distorted spectra resulting from short CP times.

Third, there is no simple check for the total proton magnetization. Although the PBT is proton-poor relative to the nylon, it has the same carbon density on a per weight basis. One can go through a simple calculation to show that under the assumption of proton spin diffusion and no proton relaxation effects, the change in the undistorted PBT C-13 intensity due to proton spin diffusion should be 4.28 times the change in nylon signal intensity. However, the relationship must be altered to take account of incomplete cross-polarization, spinning sideband intensities, and a consideration of which regions of a spectrum one is integrating over.

Figure 20 shows 50.3 MHz C-13 spectra at various diffusion times following the dipolar-echo-train preparation period. The lower spectrum is a scaled CP spectrum* (M_0) using a 0.2 ms CP time. This spectrum represents the equilibrium signal. The lines marked 'P' or 'N' correspond to

centerband position of the PBT or nylon resonances respectively; the positions marked "X" are spinning sidebands which principally belong to the PBT aromatic carbons. Diffusion times are given at the right of each spectrum. At the far right of Figure 20 are difference spectra for the aliphatic region only. These difference spectra have been obtained by subtracting a scaled M_0 spectrum from each of the displayed spectra. The scaling of M_0 was chosen such that the protonated aromatic PBT resonances at 117 and 128 ppm would null. These protonated carbons are least susceptible to Hartmann-Hahn mismatches; moreover, they cross-polarize most efficiently. Thus, these resonances should give the best indication of the PBT proton magnetization level. In other words, the difference spectra give a visual check on how far from equilibrium are the magnetization levels of the PBT and nylon protons. The difference spectra indicate that the most rapid spin diffusion changes occur over the first 3-6 ms. However, deviation from equilibrium is still detected at 50 ms.

The spectra of Figure 20 have a couple of noteworthy features. First, in the nylon spectrum the sharp (crystalline) features gradually develop at longer diffusion times, whereas the broader nylon resonances gain their near-maximum intensity at a very early stage (by approximately 1 ms). This provides experimental verification that the non-crystalline (as opposed to the crystalline) nylon regions are pretty well mixed with the PBT phase, as expected.

The second point of note is the build up, as opposed to the expected decrease, of intensity for the protonated PBT resonances over the first several hundred microseconds. (Maximum intensity is reached at a diffusion time of 0.7 ms.) The reason for this is very likely that the 1.1% fraction of protons directly bonded to a C-13 nucleus (and primarily

responsible for the CP intensity at short CP times) experience dipolar broadening (up to a maximum of 20 kHz) from this nucleus in addition to the proton-proton dipolar interactions. In the dipolar-echo preparation period, magnetization from these protons is more attenuated than from their neighbors. Thus, at very short diffusion times, one observes CP signals at the protonated carbons which are weaker than they would be if the C-13 coupled protons were in equilibrium with their non-C-13-bonded protons. This equilibration apparently takes of the order of 0.5-1 ms. (A similar rate of reequilibration was noted for the homopolymer systems when the proton linewidth was measured following a linewidth-selective dipolar echo preparation.) Indeed, a non-protonated C-13 resonance such as the resonance at 135 ppm is probably a better monitor of the proton magnetization level of the PBT protons since the protons used to cross-polarize in this case are not directly bonded to the C-13 and thus survive the dipolar-echo preparation period with magnetization more typical of the majority of protons in the PBT phase. In fact, the unprotonated PBT carbon resonance at 135 ppm in Figure 20 has maximum intensity at the shortest diffusion time.

Figure 21 shows plots of relative C-13 magnetization levels versus the square root of diffusion time. The data are based on the spectra of Figure 20. The lower growth curve represents the total aliphatic nylon intensity, corrected for a very minor aromatic sideband content. The upper curves represent the protonated aromatic PBT intensity at positions 107 and 128 ppm (filled circles) and the non-protonated PBT C-13 intensity at positions 135 and 152 ppm (open circles). Equilibrium is represented by the line whose ordinate is unity. The intensities given in these plots have been normalized by dividing by the total proton magnetization which

decreases slowly due to T_1^H effects. The total proton magnetization was assumed to be constant for the first 10 ms and the decay beyond this point was obtained from appropriately scaled linear combinations of the aliphatic nylon and centerband PBT (110-140 ppm) resonance integrals. The total proton magnetization decayed 17% between 10 and 70 ms according to this indirect measure of the total proton magnetization.

Considering the simplicity of the idea of using CP to the C-13 nuclei to monitor proton magnetization, it is now clear that the C-13 spectra, particularly at early diffusion times and particularly for protonated resonances, do not give a totally accurate representation of the proton magnetization for the reasons discussed. Thus, while it was hoped that the curve of Figure 19 could be checked, or verified, by the curves of Figure 21, in fact one ends up at a compromise position. The reasoning is as follows.

- a) Figure 19, as mentioned earlier, probably contains a steeper slope than indicated by proton lineshape deconvolution at early times because of the linewidth selection of the dipolar preparation sequence.
- b) The lower curve of Figure 21 probably contains a steeper slope at early times because of the preferential attenuation of the C-13-bonded protons in nylon following the dipolar echo preparation.
- c) The finite CP time (0.2 ms) of all curves in Figure 21 tends to average the proton magnetization over this period resulting in a less-steep initial slope than actual.

- d) The protonated PBT intensity in Figure 21 is distorted by the effects mentioned in (b) and (c) above with the result that slopes at early times are less-steep (even negative slopes at early times) due to both effects.
- e) Only the effect mentioned in (c) above is of significant influence (and then only for the very earliest times) for the non-protonated resonance of Figure 21; so this curve ought to be closest to the true slope. However, it is evident that there was some instability of the Hartmann-Hahn match during this experiment so there is more scatter in the data.
- f) Internal consistency requires that the undistorted upper and lower curves of Figure 21 be scaled mirror images of one another, so intersection of their initial slopes with the equilibrium line should occur at the same point.
- g) Direct observation of the proton signal in the MAS probe indicated that there was a few percent of a mobile proton species not present in the evacuated sample of Figure 20. (The MAS sample cannot be sealed in vacuum.) Thus, there is a small proton population, invisible in the CP experiment, which can add some confusion to the interpretation of this experiment.

From the above considerations, the results of the spin diffusion measurements shown in Figures 18-21 can be summarized as follows: There is a portion of the decay comprising 50-60% of the return to equilibrium during which the growth of nylon magnetization is approximately linear with the square root of diffusion time. The slope of the linear portion is such that extension of this slope to intersect the

'equilibrium' magnetization line gives, at the point of intersection, a value for the abscissa of $2-3.5 \text{ (ms)}^{1/2}$. Such a linear portion is translated into an overall periodicity of 6-11 nm as discussed previously. Moreover, considering the biases intrinsic to the data and to the determination of the early slope, the true periodicity is probably in the range 9-10 nm. It is also clear in all of the plots of Figures 19 and 21 that the final equilibration process takes a few tens of ms, and this final equilibration primarily involves diffusion into the nylon crystalline regions (see Fig. 20). These crystalline regions are clearly more isolated from PBT than the non-crystalline nylon regions. In combination with the proton (Figure 18) and carbon (Figure 16) lineshape data on the nylon/PBT composite, a picture emerges of a phase-separated system of PBT and nylon. The nylon phase is roughly 23% crystalline. With an overall periodicity along the thinnest dimension of 9-10 nm, and with 77% of the nylon and all of the PBT included on this periodic structure, a typical PBT domain would thus be about 5 nm in width (density of 1.5) and the non crystalline nylon phase would be approximately 4 nm across. The nylon crystalline regions, which, according to Figure 20, seem sequestered by the non-crystalline nylon component, are less clearly envisioned in this picture since spin diffusion into the crystalline regions is responsible for most of the slower approach to equilibrium at longer times. In recognition of the similarity between the volume fractions of nylon and PBT together with the 9-10 nm periodicity deduced from the linear portions of the slopes which reflect primarily non-crystalline nylon magnetization growth, one must consider that the nylon crystalline phase may not be as evenly dis-

persed throughout the composite as the non-crystalline phase. In any case, however, the narrowest crystal dimension is likely to be less than 10 nm.

d. C-13 Spin Diffusion Experiment with CP-MAS

After generating a C-13 signal via CP, it is possible to create states of non-equilibrium C-13 Zeeman magnetization by applying a 90° carbon pulse after some period of proton decoupling.²⁷ The selection of this Zeeman population is based on chemical shift differences. Since the C-13 CP-MAS spectrum is such that most of the nylon resonances are separated from the PBT resonances, a state can be prepared where the nylon C-13 polarization is very different from the PBT C-13 polarization.

At natural abundance levels of C-13, the most probable distance between nearest-neighbor nylon or PBT C-13 nuclei is 0.7-0.8 nm.²⁸ Therefore, since C-13 spin diffusion depends on the square of the C-13 to C-13 dipolar coupling^{8,28} the spin-exchange process is very slow. Nevertheless, the mere observation of some spin exchange between nylon and PBT carbons could be taken as evidence of intimate (1 nm scale) mixing.

The C-13 spin diffusion experiment was conducted on the nylon/PBT composite. The result, shown in Figure 22, was that no mixing was observed, i.e. no increase in the nylon signal was observed. The principal reason for this, see Figure 23, is that the non-crystalline T_1^C for the nylon, as measured via the method of Torchia et al²⁹ is of the order of 1 s. Therefore, since non-crystalline nylon chains are at the nylon/PBT interface the T_1^C process destroys the evidence of any spin exchanges between C-13 nuclei as the probability of a spin exchange over 1 s at natural abundance is small.²⁸ The only ways to test for intimacy of mixing using C-13 spin diffusion are to enrich with C-13 one or both chains so that spin exchange

times can be shortened to the order of 1 s, or to change the temperature so that the non-crystalline T_1^C can be lengthened substantially, to allow observation of the spin exchange.

Incidentally, in conducting the T_1^C experiments of Figure 23, it was also verified that the sharp-line features of the nylon spectrum correspond to the material with the longest T_1^C . This is expected on the basis of the lower mobility of crystalline chains. In fact, both the crystalline nylon peaks and the PBT peaks had T_1^C values of approximately 60 s.

The lower two spectra of Figure 23 are difference spectra showing the preferential loss of magnetization over the first 1 s and 5 s. It is interesting to note that this difference spectrum over 1 s yields an aliphatic resonance very similar to that in the first spectrum of Figure 20. Understandably, the dipolar echo-sequence preparation of Figure 20 shows a preference for preserving proton intensity from the most mobile regions of the nylon.

6. Experiments Probing the Homogeneity of the Rigid Polymer Phase Using Proton Spin Diffusion Between Mobile and Rigid Protons

If a polymer blend is really a "molecular" composite, then, even though there are mobile protons from a third species incorporated into the blend, the homogeneity of the distribution of the mobile species might give a clue as to the intimacy of mixing of the polymer chains. Figure 24 illustrates some simplified extremes for the incorporation of a mobile species into a two component polymer blend. In frames A-C of Figure 24, the blend is assumed to be phase separated into domains with the mobile species (represented by dots) either selectively residing in one of the domains (A), excluded from both domains and occupying boundary or void regions (B), or uniformly distributed throughout both phases (C). On the

other hand, in frames D and E of Figure 24, the assumption of a 'molecular' composite is made where either aggregation is not uniform and the mobile species occupies voids or defect regions (D) or the mobile species is uniformly distributed (E). Situations D and E could also correspond to homopolymer systems where mobile species might occupy similar sites.

In a proton spin diffusion experiment where one of the proton species is very mobile, and therefore has weak dipolar interactions with a second strongly-interacting proton species (a polymer), then the transfer of magnetization between the mobile and more rigid protons would be slow due to the weak residual dipolar couplings evidenced by the mobile species. In the limit of very slow spin exchange, magnetization would move through the polymer lattice, following such a spin exchange, more rapidly than the characteristic time between spin exchanges events. Thus, little information would be forthcoming about the homogeneity of structure of the polymer component. On the other hand, if the exchange between mobile and polymer protons were fast on the timescale of spin diffusion through the polymer, then some information about the homogeneity of the polymer structure could be deduced.

Experimentally it was found that the linewidths of the mobile species were in the 1-3 kHz range while the characteristic domain sizes might be in the range of 5-10 nm. The latter dimensions imply that typical diffusion times across such dimensions require a few tens of ms. Thus, even if only half of the linewidth for the mobile species represents residual dipolar interactions (the rest being due to magnet inhomogeneity or magnetic susceptibility effects), the spin exchange times will be of the order of 1 ms. In other words, even with the rather narrow linewidths, we would expect that the time dependence of magnetization

transfer from the mobile proton species to the polymer protons should be influenced by domain sizes in those cases represented by Figure 24 A, B and D.

On the other hand, if either of the situations in Figures 24C or E prevails, then very little spin diffusion need take place (only over monomer dimensions). In such cases, magnetization transfer studies would yield no information on domain sizes. Rather, magnetization transfer profiles would probably be exponential with the rates determined by the residual dipolar interactions.

One criterion for determining the distribution of the mobile species as being either throughout or excluded from the polymer phase is whether the magnetization transferred between the mobile and polymer protons grows exponentially or with a square-root-of-time dependence. Figure 25 illustrates these two growth profiles given by $(1 - e^{-t/t_0})$ and an arbitrary straight line, passing through the origin, representing the function \sqrt{t} . Note that the function $(1 - e^{-t/t_0})$ has a substantial range where the change with \sqrt{t} is essentially linear. Thus, since diffusion controlled behavior in a finite system is only linear at early times, this is where distinctions between \sqrt{t} and exponential behavior must be made. In general, because the initial conditions in a practical case often involve finite (but non-equilibrium) magnetization residing in both the mobile and more rigid proton systems, we cannot differentiate exponential from \sqrt{t} behavior based on the respective x-intercepts of the linear portions of curves such as those shown in Figure 25.

The real systems also have other problems, namely, that there is often not just a single proton containing species. For example, if residual MSA molecules are present, the CH_3 protons need not interact with the

polymer protons as strongly as do the acid protons. This could then lead to differential spin-diffusion behavior of the two kinds of MSA protons even though both kind of protons might be dispersed physically into the same regions.

Magnetization transfer between the mobile and rigid protons was measured in four samples; the data for only two such systems will be shown, both corresponding to the 30% PBT/70% ABPBI systems. These are Samples F and L, the latter presumably more phase-separated due to precipitation from MSA at a concentration above that required for phase separation.

Figure 26 shows the spectra as a function of the delay time τ in a $[90_x-50\mu s-180_y-50\mu s-90_{\pm x}-\tau-90_\phi(\text{observe})-3s]_n$ experiment. This is a simple Hahn echo, followed by a restoration of the echo magnetization either in the direction of, or opposite to the direction of B_0 . After the variable delay, the magnetization is observed using a 90° pulse with transmitter and receiver phase cycling which gets rid of certain interfering multiple quantum coherences.²⁶ As τ gets longer in Figure 26, the narrow portion of the resonance, which was originally saved, decreases while the broad polymer resonance grows due to magnetization transfer from mobile protons. At 50 ms equilibrium has not yet been established as can be seen by comparing that lineshape with the scaled M_0 lineshape. The last spectrum of Figure 26 is the difference spectrum, amplified four times, between the 50 ms lineshape and the M_0 lineshape. Over 50 ms the mobile proton magnetization has populated the polymer proton magnetization about 85-90% of the way to its equilibrium proportion. During the 50 ms, however, T_1^H processes were also at work changing the total integral by approximately 20% relative to the initial value.

From the foregoing experiment it might be postulated that the PBT, which contributes 22% of the polymer protons in the composite, is phase-separated and thus accounts for the long tail of the equilibration period in Figure 26. To test the hypothesis qualitatively we attempted the reverse polarization transfer experiment, namely, that polarization flow from the broad-line polymer protons to the narrow, mobile protons. The preparation sequence was a 10 ms proton spin lock (see Figure 8) which attenuates the narrow component 10 times more than the broad, but in doing so, produces a less-than-sharp magnetization gradient. If the mobile proton species is water and if it is more intimately interacting with the ABPBI than PBT because the former is more hygroscopic, then the broad component after 10 ms of spin locking is likely to be richer in PBT protons than its usual 22%. If so, it will take longer to repopulate the narrow protons in this experiment compared to the experiment of Figure 26. Figure 27 shows the results. The narrow-line magnetization indeed grows more slowly, as expected, at early times. However, after 50 ms the narrow line has recovered to 82% of its fractional intensity in the equilibrium lineshape, a fraction similar to the experiment of Figure 26 after 50 ms of spin diffusion.

Figure 28 shows narrow-line decay and growth curves obtained from the data of Figures 26 and 27, respectively. Each point is divided by the total proton magnetization at that time in order to compensate approximately for T_1^H decay. The steep decay for the experiment of Figure 26 compared with the slower growth in the experiment of Figure 27 indicates immediately that the mobile species is not homogeneously distributed (e.g. Figures 24C and E) in the polymer. Therefore, the polymer composite is not strictly a structurally homogeneous molecular composite which is consis-

tent with the expectations based on the sample preparation method. As mentioned earlier, the initial condition in the experiment of Figure 27 favors magnetization in more rigid regions and in regions more removed from the mobile protons. Again if it is assumed that the most likely candidate for the mobile species in this sample is water, not removed from the polymer via evacuation and preferentially in contact with the hygroscopic ABPBI, then the $T_{1\rho}^H$ preparation of Figure 27 is probably rich in PBT magnetization. If so, the spin diffusion experiment of Figure 27 indicates that most of the PBT, if phase separated, is not to be found in micron-size domains but rather to be found in domains whose overall periodicity in the narrowest direction and including the ABPBI phase, is 10-20 nm.

It is a bit surprising that the indicated domains are so small because the material was coagulated from a phase separated solution. However, since the macroscopic color of Sample L was not uniform, it is possible that the sample selected for this experiment did not represent the overall composition ratio.

The second sample (Sample F) of the 30% PBT/70% ABPBI, also evacuated, showed very different behavior. The history of sample preparation on this material is more obscure except that it was coagulated from a single-phase solution, so more intimate mixing of the phases is expected.

In contrast to Sample L, Sample F showed a narrow component whose linewidth is 3 kHz compared with 1.2 kHz for Sample L. The narrow line in Sample F consists of at least two components (see discussion concerning Sample F in Section D. 3.). As a fraction, the narrow line intensity in Sample F is only 12% compared with 39% in Sample L.

Figure 29 gives proton spectra as a function of spin diffusion time in a $[90_x-25\mu s-180_y-25\mu s-90_{\pm x}-\tau-90_{\phi}-(\text{observe})-3s]_n$ experiment. It is seen that the high field portion of the narrow component is most resistant to spin diffusion. This is also the narrower of the two narrow components. In Figure 29, the last spectrum is a difference spectrum of the 50ms and M_0 spectra. This difference spectrum shows the bias towards the high field side of the line although there seems to be a sizeable remnant of the low field component in the spectrum as well, judging by the asymmetry of the base of the line.

Figure 30 gives spectra as a function of time in a spin diffusion experiment where magnetization flows in the reverse direction. Just as in Figure 27, a 10 ms $T_{1\rho}^H$ preparation was used. Compared with the M_0 spectrum at the top of Figure 30 little spin diffusion seems to be happening. This can be seen more clearly via the difference spectra in the right hand column of Figure 30. These spectra, amplified two times, were generated by subtracting a variable amount of the M_0 lineshape so as to null the broad component. The principal contribution to these difference spectra arises from the downfield portion of the narrow component. This is the component most strongly coupled to the polymer by spin diffusion according to Figure 29; however, this same magnetization seems to be very weakly connected to the polymer proton magnetization surviving after 10 ms of spin-locking. Thus, there is strong evidence in this material for domains larger than 20 nm which are depleted of mobile protons. Therefore, Sample F appears less homogeneous than Sample L even though the expectation is the reverse. Our ability to distinguish between the inhomogeneous cases given in Figure 24 A,B, and D requires more assumptions. Unless one can eliminate the case of Figure 24D, the conclusion of phase separation does

not immediately follow for Sample F. Qualitatively, the significantly weaker coupling after 50 ms via spin diffusion of the polymer resonances with the downfield narrow component in the experiment of Figure 30 compared with that of Figure 29 points towards the phase separated structures illustrated by Figure 24A and B.

The origin of the very weakly coupled resonance on the upfield side of the narrow line region cannot be interpreted clearly unless these protons can be identified chemically. If they were the methyl protons originating from methanesulfonic acid residues, then the dipolar interactions of these protons with those of the polymer may indeed be much weaker than the acid protons, thereby explaining the weaker coupling.

No plot of magnetization transfer is made for this system, partly because of the difficulty of accurately analyzing each of the two narrow-line components and partly because the flow of magnetization is not sufficient to bring the lineshapes close to their equilibrium shapes even after 50 ms. The effect of T_1^H is to reduce the total lineshape integrals in the experiments of Figures 29 and 30 by $16 \pm 2\%$ over 50 ms. The T_1^H influence is larger than expected but not overwhelming. An attempt to follow spin diffusion for longer times in order to obtain information about larger dimensions would result in an unacceptably large contribution to the magnetization change due to T_1^H .

Results from the other two samples upon which magnetization transfer experiments were performed will simply be summarized:

Sample N (washed PBT film, sealed in vacuum): The narrow line is a 14% contribution to the total proton intensity, but it consists of a downfield and upfield component. The re-equilibration profiles due to spin diffu-

sion after a "Hahn-echo" preparation are similar to Sample F in that the low field part of the line is coupled much more strongly to the polymer protons than the upfield component. Results indicate multiple mobile proton species in a structure (in this case a homopolymer solid) probably like Figure 24D, i.e. the mobile species are not intimately mixed into the lattice.

Sample P (unwashed, evacuated PBT film): The narrow-line component represents a 14% contribution to the total proton intensity. The line seems homogeneous in the sense that the upfield and downfield protons are not separated. In the spin diffusion experiment with a Hahn-echo preparation, equilibration is more than 90% complete after 40 ms of spin diffusion. It proceeds as for sample L, but a little faster and more completely. The rates are too slow for uniform dispersion of the mobile species throughout the polymer lattice (Figure 24E). Rather, the situation of Figure 24D probably prevails with the PBT domains having minimum dimensions of less than 10 nm.

The conclusions from looking at rates of transfer of magnetization from the mobile-proton species to the more rigid polymer protons is that in neither the PBT homopolymer nor the 30%PBT/70% ABPBI samples studied are the mobile protons uniformly distributed in a homogeneous polymer phase. This means that in the PBT, the mobile protons likely occupy defect or void regions. This is also borne out by the $T_{1\rho}^H$ data which show initial decay rates for the narrow components which are several times those observed for the broad portions. This behavior persists over times of a few ms again indicating that the rapid decrease in mobile proton magnetization is not able to pull down the broad component resonances over

millisecond timescales as would be expected if the mobile species were dispersed into the polymer phase. On the other hand, washing the PBT fibers introduces a second mobile species which is only weakly dipolar-coupled to the polymer protons. The identity of these protons is not known. Although the linewidth and upfield position suggest CH_3 protons from residual MSA, appearance of the line only after extensive washing suggests that it is not methyl protons since the concentration of methyl protons should, if anything, fall upon washing. The absence of a distinguishable methyl resonance in Sample P calls into question whether the methane sulfonate ion is the counterion in this sample.

The PBT study is relevant to the interpretation of the magnetization transfer experiment in the PBT/ABPBI composites. The PBT study indicates that the mobile protons can interact reasonably strongly with the PBT polymer as well as with the ABPBI polymer, even though the latter polymer is more hygroscopic. Also, it is quite clear that the final mobile proton content can vary widely (12 to 39%) in the composite samples, even after evacuation. Since not enough is known about the preparation of both samples it must be acknowledged that there is no conclusive evidence in these data that the mobile proton species interacts more strongly with ABPBI molecules. Preparation history seems to have a larger influence on the mobile proton content than does the polymer chemical composition. Thus, the detection of large inhomogeneities in the distribution of the mobile species in Sample F still leaves open the question of whether this inhomogeneity is, at one extreme, an inhomogeneity of polymer composition or, at the other extreme, an inhomogeneous distribution of the mobile species in an otherwise homogeneously mixed polymer blend (a molecular composite).

A possible accounting of these experimental results on Samples F and L may be given on the basis of published results in these systems. It is known³⁰ from wide angle x-ray scattering (WAXS) that as-spun ABPBI shows a lateral d-spacing of 0.78 nm. This spacing becomes 0.74 nm after extensive washing and finally goes to 0.70 nm upon heat treatment. These spacings may conceivably indicate the sequential removal, by washing and heat treatment, of a mobile proton species from the polymer matrix. Thus, the as-spun polymer molecules are very likely to have more intimate contact with the mobile proton species and, following thorough washing and/or heat treatment, the mobile species becomes more excluded from the polymer matrix. Evidence of a similar progression is also observed in composite fibers of PBT and ABPBI.³⁰ Whether the process of exclusion of the mobile protons occurs homogeneously or heterogeneously throughout the polymer is less clear. In any case, for Samples F and L we might speculate, based on the much higher mobile proton content of Sample L, that Sample L did not receive as thorough a washing (and/or no heat treatment) as Sample F may have received. Thus, the mobile proton species would be expected to be more intimately mixed with the polymer phase (as indicated by the experimental results) in Sample L compared with Sample F. Furthermore, from the PBT results it can be seen that the mobile species is quite intimately mixed with the PBT chains in an unwashed sample. Therefore in Sample L the mobile protons would also be expected to be present even in a phase separated PBT phase, although probably at a lower concentration compared with ABPBI. If, in addition, one considers the fact that the fraction of the total PBT which separates in a phase separated solution of PBT and ABPBI depends critically on how far above the critical concentration one is³⁰ (and we do not know the actual and critical concentrations for the

solution from which Sample L was made) then it is clear that the experiments just described for Sample L would not easily sense even a 20 or 30% fraction of the PBT molecules phase separated from the other mixed PBT/ABPBI phase, particularly when both phases contain appreciable concentrations of intimately mixed mobile proton species. The ability to distinguish heterogeneity of structure using this technique would probably be enhanced greatly by heat treatment (more so than washing), since heat treatment should at least be capable of expelling the mobile proton species from the large domains of PBT which would derive from the original phase separated solution.³¹ Sample F, then, may well have derived its inferred heterogeneity of structure from washing or, more probably, a heat treatment. It is known³⁰ that heat treated composites of PBT and ABPBI possess d-spacings in WAXS typical of the individual homopolymers, even when the composites are formed from solutions whose concentration are less than the critical concentration, although higher order reflections are generally much weaker or missing.

7. Experiments Using Multiple-Pulse Proton Irradiation to Prepare Magnetization Gradients Followed by a Monitoring of Proton Magnetization Using Proton-C-13 Cross Polarization

The experiment described in the foregoing heading is probably the best conceptually for investigating domain structure since spin diffusion is quenched by the application of the multiple pulse train. Thus, since resolution of the polymer components is easier via the C-13 spectra, one would be able to measure the inherent differences in proton relaxation between the polymer phases and, by suitably inserting a spin diffusion time

between the multiple pulse period and the cross-polarization period, measure domain sizes both more accurately and with a knowledge of domain composition.

We tried these experiments on the Nylon/PBT composite, Sample I, using a static sample (no MAS). Short (0.1 ms) cross-polarization times were used to get a measure of the instantaneous proton magnetization levels. The problem which we encountered was that the protons bound to C-13 nuclei did not behave under multiple pulse trains like the bulk of the protons which are bonded to non-magnetic C-12 nuclei. The C-13 bonded protons experienced a local dipolar field from the C-13 nuclei so that the multiple pulse trains are applied up to 20 kHz away from resonance. That causes these protons to have a different trajectory under multiple pulse than their uncoupled neighbors. Consequently, cross-polarization intensities for protonated carbons are very distorted since the trajectory of the protons must be known in order to spin-lock them subsequently for cross-polarization, and there are many trajectories because of the many angular-dependent dipolar couplings. The cross-polarization intensities do not become a good monitor of the local proton magnetization for approximately 1 ms in a spin diffusion experiment since it takes the better part of a millisecond for a subset of proton spins in a homogeneous polymer to equilibrate with their surroundings. A significant amount of early time information is therefore unobservable. The difficulty of the experiment is therefore not rewarded by the clarity of the results. Whereas certain refinements could certainly be added to the experiment, the fundamental problem of the anomalous behavior of the C-13 bonded protons still remains. Application of C-13 resonant decoupling during the multiple pulse trains was also attempted. Results were better but distortions

still remained. The use of MAS would allow one to select non-protonated carbons to monitor the proton polarization. These carbon intensities would be less susceptible to the distortion discussed above, but there are other problems with using the non-protonated carbon resonances and MAS. These are (a) greater sensitivity of the CP intensities to the matching of rf power levels, (b) weaker signals because of the short CP times used, and (c) greater difficulty doing multiple pulse well due to MAS.

The results obtained for the PBT/Nylon composite are not shown since they were less definitive than the results given in Figures 20 and 21.

E. Summary of the NMR Results and Evaluation of the Applicability of the NMR Methods to the Study of Molecular Composites

Several homopolymers, PBT, ABPBI, ABPBT, and Nylon, both oriented and unoriented were studied by C-13 and proton NMR. In addition, preparations of PBT/ABPBT, PBT/ABPBI, and PBT/Nylon 66 composites were studied, with emphasis on the latter two.

Proton lineshapes indicated that most of these systems contain at least one and sometimes two mobile proton species. Amounts of these mobile species were seen to depend on whether the samples were sealed under vacuum or exposed to normal laboratory humidity, but it seldom happened that the mobile proton species could be eliminated by evacuation. After evacuation these systems would typically have 12-40% of their protons in the form of mobile protons. On the other hand, heat treatment of PBT or PBT/Nylon composites at temperatures above 250°C (depending on the material) reduced the level of mobile protons to the order of a percent or less. In ABPBI, polymer chains lost significant mobility upon removing some of the volatile proton species (presumably water) by evacuation.

Thus, in ABPBI exposed to laboratory levels of humidity (35-50% R.H), water apparently interacts intimately with the polymer chains. This is reasonable based on the hygroscopic nature of ABPBI.

The polymer proton linewidths in PBT showed sensitivity to heat treatment; linewidth (FWHH's) were typically 24 kHz and 19 kHz for samples heat treated and not heat treated, respectively. The latter samples also showed a significant fraction of mobile protons. Since there are no exchangeable protons on the PBT molecule as there are on the ABPBI molecule, the difference in linewidths must principally indicate greater polymer mobility and secondarily indicate a lower density (with smaller internuclear dipolar interactions) prior to heating. Whether heat treatment rigidifies the PBT chains by simple densification or by the elimination of an intimately mixed mobile proton species is not clear from the lineshapes alone. Locating the mobile proton species, however, seems important from the mechanical properties point of view since a mobile proton species in contact with the polymer chains at the molecular level could promote chain mobility and chain slippage. Indeed, the modulus and strength of as-spun PBT fibers is significantly lower than after heat treatment.³²

In looking at two PBT samples coagulated out of MSA solutions it was noted that the chemistry of the mobile proton species was partially altered by washing, i.e. a second mobile proton species, having a higher-field resonance position, was introduced. The identity of the second species was not determined, but its affinity for and/or its intimacy of mixing with the polymer chains was reduced relative to the lower-field mobile-proton species. Affinity and intimacy of mixing were judged principally by $T_{1\rho}^H$ measurements and measurements of magnetization transfer

rates between the mobile species and the polymer protons. For PBT, both washed and unwashed but not heat treated, the latter experiments gave support to the picture of the mobile proton species occupying defect regions. However, the polymer domains bounded by the defect regions are not large (<10 nm) in their narrowest dimension judging by the magnetization transfer (via spin diffusion) behavior. Finite lateral crystal sizes (6-8 nm) and different kinds of ordered structures in PBT have also been reported for fiber samples coagulated into a methanol/sulfolane bath.³³ The absence of an obvious methyl resonance in the unwashed PBT was noted. This would indicate that the mobile proton species is not residual methane sulfonic acid, or it may indicate that the methyl sulfonate ion is quite immobilized.

Different preparations of 30% PBT/70% ABPBI composites showed widely variable amounts of mobile protons after evacuation, and, like PBT, either one or two such mobile proton species were indicated. One of the samples which was prepared from a phase-separated solution in MSA, surprisingly showed a higher mobile proton content (and a smaller narrow domain dimension) than another composite sample prepared from a true solution. It was speculated that the higher mobile proton content was probably related to a less thorough washing and no heat treatment compared with the sample prepared from solution. Therefore, it is reasonable to expect that the regions devoid of the mobile species would be smaller before than after washing or heat treatment. In both cases, however, the mobile species did not appear to be dispersed at the molecular level, judging again by the $T_{1\rho}^H$ and magnetization transfer behavior.

The wide variability in the mobile proton content did not allow for definitive conclusions about intimacy of mixing of the polymer chains themselves. For example, the recognition that ABPBI is more hygroscopic than PBT did not necessarily mean that a 30% PBT/70% ABPBI composite contained more mobile protons than the PBT homopolymer, after evacuation. Thus, arguments identifying the inhomogeneity of distribution of the mobile proton species with inhomogeneous composition (e.g. phase separation) of the polymer domains were not convincing.

The role that the mobile protons play in complicating the NMR investigation is even more pervasive. For example, the simple test for phase separation, namely, that relaxation behavior be the superposition of the homopolymer relaxation behavior, cannot be administered because spin diffusion experiments verified that mobile proton species influence T_1^H and T_{1p}^H behavior. Superposition of T_{1xz} behavior is about the only reasonable criterion which could circumvent the complications due to variable mobile proton content. However, it is seen in ABPBI and possibly even in PBT that the mobile proton content influences polymer mobility and therefore T_{1xz} also. Even though the mobile proton species are probably not mixed at the molecular level, the amount of mobile protons may indirectly influence chain mobility by being correlated with polymer domain size which, in turn, determines surface to volume ratios, which in turn can influence molecular mobility via the distribution of free volume. So the success of using the T_{1xz} superposition criterion to probe possible phase separation depends critically on whether the mobile proton species are excluded from the polymer domains and depends possibly on domain size.

In the most ideal cases, the superposition of homopolymer C-13 relaxations (which are less susceptible to spin diffusion than proton relaxations), such as T_1^C or $T_{1\rho}^C$, could also be used to judge phase separation in a composite. Again, however, if chain dynamics are influenced by the mobile protons, then these criteria also fail. We did not undertake any systematic C-13 relaxation investigation in this study principally because these studies are of inherently low sensitivity and there was limited time.

Future efforts could certainly be devoted to investigating systematically, the identity of the mobile proton species, the change of concentration of the mobile protons with processing, and the corresponding changes in T_{1xz} , T_1^C , or $T_{1\rho}^C$ behavior of the homopolymers and polymer composites.

The spin diffusion experiments which were performed in these materials were also influenced by the mobile protons because most of the systems containing mobile protons had T_1^H values between 100 and 300 ms. With T_1^H in this range, T_1^H becomes a non-trivial perturbation on the change of magnetization in a spin diffusion experiment, and this limits the preciseness of interpretation of the experiments in terms of domain size.

Therefore, the presence of the mobile proton species is seen as a rather serious obstacle standing in the way of the characterization of these materials by NMR. The advantages of being able to probe the homogeneity of the polymer domains using spin diffusion between the mobile and polymer protons does not offset the complications introduced into the experiments designed to probe the intimacy of mixing of the polymer chains

themselves in these composites. However, the identity and the location of the mobile proton species may, in itself, be an interesting problem, and here NMR is capable of providing considerable insight.

In terms of investigating by NMR the level of mixing in the polymer composites, the nylon/PBT composite must be regarded as being the most promising system for study. The proton lineshape of the composite was very close to the superposition of the appropriately weighted homopolymer lineshapes. It therefore followed that spin diffusion rates could be measured by simply monitoring the proton lineshapes (a high sensitivity experiment); moreover, the absence of significant line broadening for the PBT or line narrowing for the nylon resonances indicated phase separation.

C-13 spectra, both non-spinning and with MAS, also resolved the nylon and PBT resonances, and with greater certainty of assignment than in the proton spectra. Proton spin diffusion behavior was monitored indirectly using C-13 MAS spectra. Although there are some difficulties associated with measurement of the proton magnetization at early times and although the important assay of the total proton magnetization is indirect, nevertheless the long-time spin diffusion behavior seen via the C-13 nuclei agreed well with that inferred from the direct proton observations. The short time behavior observed by both techniques gave early slopes which were about a factor of two different from one another. However, this factor of two variation is qualitatively understood in terms of the experimental biases in the methods, so that in this heat-treated (at 255°C) 60% PBT/40% nylon 66 it is concluded that the typical repeat distance in the direction of the minimum domain dimension (probably perpendicular to the PBT chains) is about 9-10 nm. This repeat distance includes both the nylon and PBT phases. It is also seen, because of one's ability to

distinguish crystalline from non-crystalline nylon resonances in CP-MAS spectra, that the nylon/PBT composite has some regions of nylon crystallinity. The factor of crystallinity is lower than that of a molded plate of nylon 66, indicating that the presence of the PBT in the composite significantly inhibits nylon crystal growth. Moreover, it is the crystalline regions of the spectra which are responsible for the long tail of the equilibration in the spin diffusion experiment. Just how intimately mixed is the nylon crystal phase with the PBT is more difficult to determine. Qualitative indications in the spin diffusion experiment are that the nylon crystalline phase is principally in contact with the non-crystalline nylon chains, as opposed to PBT chains (not surprising). Furthermore, the time required to equilibrate these crystalline protons is significantly longer than for the non-crystalline material, meaning that crystalline domains are probably less homogeneously dispersed among the PBT chains than the non-crystalline chains and that the smallest dimensions of the crystals do not exceed 10 nm.

It should be recognized that the evacuated nylon/ PBT sample contained only a very small amount of mobile protons, and even when exposed to normal laboratory humidity only picked up a few percent water protons. Therefore, proton spin diffusion could still be followed pretty well by C-13 NMR even though the mobile proton species were present and invisible in the C-13 spectra. Introduction of large quantities of mobile protons would certainly complicate the use of either proton and or C-13 NMR for monitoring proton spin diffusion.

Use of non-spinning C-13 NMR for studying PBT/ABPBI (or PBT/ABPBT) composites is very limited. It is easy to differentiate an oriented specimen versus an unoriented specimen, but to distinguish clearly

resonances belonging to either polymer is much more difficult. In film samples of ABPBI and an ABPBI/PBT composite, each coagulated in water out of MSA and then either drawn 2x when wet or not drawn, it was determined by non-spinning C-13 NMR that the undrawn samples were quite highly oriented, little additional orientation was produced by the 2x wet drawing, and the PBT and the ABPBI were both oriented in the composite as has been noted previously³⁰ in heat-treated ABPBI/PBT composites using WAXS.

CP-MAS techniques were shown to be capable of resolving PBT and ABPBI resonances in the sense that the lowest field PBT resonance was isolated from the ABPBI resonances. This can form the basis for a separation of polymer resonances, however, there are two drawbacks. First, the resonance has a very low sensitivity compared to other resonances; and second, the carbon giving rise to this resonance is unprotonated and therefore both difficult to cross-polarize and more sensitive to rf power level matching. Therefore, separations based on full lineshape analysis may be better. An area for future work would be to test the sensitivity of PBT and ABPBI CP-MAS lineshapes to preparation history. This possibility was not explored in this work but conceivably, the disappearance of disorder in a sample and the expelling of mobile protons could lead to lineshape changes, and, for the composite, the lineshapes could qualitatively indicate the degree of order (or phase separation) achieved.

For the 2x stretched ABPBI/PBT composite, an indirect measurement of $T_{1\rho}^H$ via the C-13 CP-MAS intensities showed that PBT chains on average had a very slightly (≈ 1 ms) longer $T_{1\rho}^H$ than did the ABPBI chains. Thus, this experiment was not very definitive with respect to the question of

phase separation. The indication was only that a strict molecular composite was unlikely; however, domains need not be more than 1-2 nm in their minimum dimension in order to give the results obtained, but domains could be larger.

The difficult experiment of combining multiple pulse relaxation with cross-polarization was attempted. The hope in this experiment is to isolate the proton relaxation behavior of individual sites and conduct spin diffusion studies with the highest-resolution monitoring of the proton magnetization levels (via C-13 proton cross-polarization). Results showed that particularly the protonated carbon intensities were badly distorted, presumably because the protons bonded to these carbons are being irradiated well off-resonance due to the C-13 proton dipolar interaction. Thus, this experiment is not promising, at least not if the first millisecond of spin diffusion is critical, which it often is in systems whose minimum domain dimensions may only be a few tens of nanometers.

The two composites, PBT/ABPBI and PBT/nylon represent very different challenges for the application of NMR to the question of intimacy of mixing. The former composite is very difficult to characterize because its resonances can only be clearly distinguished using C-13 CP-MAS techniques. Future efforts to characterize mixing in this material should probably focus on those preparations in which the mobile proton species have been reduced to an insignificant level (less than 2%) by, say, heat treatment and washing. Then, along with homopolymers whose preparation history is the same and whose mobile proton content is similarly low, one should analyze $T_{1\rho}$ behavior by applying the superposition criterion as a measure of phase separation. If the criterium is fulfilled, then one

should attempt spin diffusion studies based on the T_{1xz} preparation to determine domain sizes.²⁵ Or one should indirectly measure $T_{1\rho}^H$ behavior using CP-MAS techniques to look at the tightness of coupling of the $T_{1\rho}^H$ behavior of the individual components.

Even though characterizing mixing in the nylon/PBT system is much easier because of the ease of differentiating resonances belonging to PBT and nylon, an improved method, not discussed here, is to combine MAS with multiple pulse irradiation and conduct a spin diffusion experiment using a multiple pulse spectrum "readout". The idea is that the proton resonances of the aliphatic nylon can be distinguished from the proton PBT resonances using multiple pulse in combination with MAS.³⁴ Thus, one will be able to evaluate the early time spin diffusion behavior with more clarity and without the problems discussed in connection with the spin diffusion experiments shown in Figures 18-21 of this study. This experiment also has the advantage of the sensitivity of the protons.

In general, then, composites of aliphatic or partly aliphatic polymers with PBT will be much more amenable to characterization by NMR for intimacy of mixing than will fully aromatic composites.

As a final comment, the full deuteration of one polymer species and the subsequent demonstration of cross-polarization for carbons on that polymer from protons on the other polymer can be taken as conclusive evidence for mixing on a 0.4-0.5 nm scale. This method is not advocated at this time because of the pervasiveness of the mobile (and yet reasonably strongly interacting) protons, which may cause some cross polarization or chemical exchange with labile deuterons, and because of the difficulty and expense of synthesizing good, high molecular weight materials. As mentioned earlier, C-13 labelling of certain sites on both chains could also

be used to test for intimate mixing on a 0.5-0.6 nm scale via an indication of C-13 to C-13 spin exchange between carbons on different polymers. This experiment also provides unambiguous evidence for intimate mixing, particularly if the distance between labelled sites on a given chain is comparable or greater than typical distances separating chains. Again, however, we assume that these experiments are out of the question for the reasons just given. Nevertheless, should synthesis become easier at any time, then these experiments ought to be considered.

III. ELECTRON SPIN RESONANCE STUDIES

The generation of free radicals upon deformation and fracture of semicrystalline and glassy polymers has been established from electron spin resonance.^{35,36} Measurements of molecular weight degradation and increase in the number of polymer chain end groups have confirmed that the free radicals are generated by scission of carbon-carbon bonds along the polymer backbone.³⁶⁻³⁹ The growth of the free radical concentration with strain of nylon-6 fibers is illustrated in figure 31. Associated with the generation of free radicals is the degradation of molecular weight as shown in figure 32 where the fractional loss in viscosity-averaged molecular weight of nylon-6 fibers is also plotted as a function of strain. Comparison of these two plots shows a direct correspondence between generation of free radicals and molecular weight decrease. These observations support a model of carbon-carbon bond scission with mechanical stress.⁴⁰ The rupture of polymer backbone bonds also leads to an increased concentration of chain end groups which has been confirmed by infrared spectroscopy.^{36,38,40}

A recent report by Brown et al.⁴¹ of the observation of stress induced free radicals in fibers of poly(p-phenylene terephthalamide) (PPTA) rigid rod polymers suggests that similar phenomena may also occur in PBT. A factor complicating ESR measurements of mechanical stress induced free radicals in rigid rod polymers is that large initial concentrations of free radicals may be present as a result of processing in strong acid and the presence of varying amounts of paramagnetic transition metal ions. These initial concentrations may complicate the measurement of the relatively low numbers of free radicals produced during mechanical deformation.

Fiber specimens of PBT produced under the names AFTECH 1 and AFTECH 2 were obtained from the Wright-Patterson Materials Laboratory. The fibers were examined for free radicals as received and after thermal treatment. Mechanically induced free radicals were observed in annealed fibers that had been strained to rupture and other fibers which were crushed under liquid nitrogen. The measurements were conducted with a Varian E-3 spectrometer¹⁶ located in the laboratory of Professor K. L. DeVries at the University of Utah. Both types of AFTECH fibers as received gave appreciable ESR signals that diminished with thermal treatment as shown in figures 33 and 34. The amount of specimen available for both fiber types was insufficient for detailed analytical studies of the type and amounts of free radical species present. Nonetheless, comparative studies of the effects of thermal and mechanical stress treatments could be made as could direct comparison of the relative amounts of free radicals in the two fiber types."

The spectra shown in figures 33 and 34 indicate that free radicals are present in the samples as obtained. The instrument gain used to record the spectra of the AFTECH 2 specimen was 10% of that used to obtain the spectra of the AFTECH 1 from which it is concluded that the initial concentration of free radicals in the AFTECH 2 fibers was approximately 70 times larger than that in AFTECH 1. Free radicals have also been detected in PPTA fibers prior to either mechanical stressing or thermal treatment.⁴¹ In this case, the free radicals were attributed to paramagnetic transition metal ions and to organic species. As pointed out above, the present investigations were limited in terms of quantitative results by insufficient material, and the origins of the initial ESR signals were not addressed. Clearly, the effect of thermal treatment of the PBT fibers at temperatures of up to 205° C for 16 h was to reduce the initially observed signals by about 30%. A similar result was reported for PPTA,⁴¹ but in this case a reduction of 90% of the original signal was achieved by heating at 250° C for 15 h. The reductions are attributed to recombinations of the organic type free radicals owing to the increased molecular mobility of the polymers at high temperature. The free radical reduction is surprising considering the high temperature treatments the fibers are subjected to during processing. Nonetheless, additional thermal treatments were necessary to achieve minimal levels of free radicals prior to deformation since low free radical concentrations were expected from mechanical stressing as compared to the original signals.

The effect on the ESR signal of stressing the AFTECH 2 fibers to rupture is shown in figure 34. The concentration of free radical species present can be found through double integration of the ESR first derivative spectra which are displayed in figures 33 and 34. By this method an

approximate increase of 6% in free radical signal was obtained for the tensile fractured AFTECH 2 fibers. A similar result was found for the AFTECH 1 fibers as shown in figure 35. An intermediate spectrum obtained when the AFTECH 1 fibers were strained but not ruptured is also shown in this figure. This last mentioned spectrum is of significance since it indicates that free radicals were generated during deformation prior to rupture. The increase in this case was less than that observed subsequent to rupture as would be expected. Free radical generation with strain prior to rupture indicates that chain scission is involved in deformation as well as chain slippage and the associated rupture and reformation of van der Waals bonds between polymer molecules.

A second type of deformation used was to crush the PBT fibers under liquid nitrogen. Grinding of thermoplastics at liquid nitrogen temperatures has been used to obtain large numbers of free radicals that result from the extensive amount of fracture produced under these conditions.³⁸ The fractured PBT specimens were transferred to the ESR instrument and the spectra recorded before and after warming to room temperature. The differences between the low and room temperature spectra indicate the amounts of free radicals produced in the AFTECH 1 and AFTECH 2 fibers by grinding under liquid nitrogen. The spectra are shown in figures 33b and 34b and the differences account for a 29% increase in the case of AFTECH 1 and 27% increase in the case of AFTECH 2. The substantially larger increases observed in these experiments compared to the strain-to-rupture measurements is consistent with the reported findings for other polymers in which such comparisons were made.³⁸

The conditions under which the PBT spectra were obtained, particularly, in the stressed induced situations, differed from that reported for PPTA.⁴¹ Whereas we were able to find an increase in room temperature recorded spectra under strain-to-rupture conditions, Brown et al. were unable to observe changes in the free radical concentrations of PPTA unless the mechanical stressing was conducted at cryogenic temperatures similar to our crushing experiments.⁴¹ One possible explanation is that the PPTA molecules have more mobility at a given temperature than do the PBT molecules. This would also explain why the percentage reduction in the ESR signal obtained by thermal treatment was larger in PPTA than in PBT.

The conclusions reached in the ESR investigations were that signals could be obtained from PBT fibers, and that the signals increased with mechanical deformation in both straining and crushing experiments indicating that molecular chain scission was associated with mechanical deformation. A more complete ESR study coupled with IR and/or viscometry should reveal the magnitude of this effect and shed light on the degree to which these molecular processes limit the performance of rigid rod polymer fibers.

IV. FLUORESCENCE SPECTROSCOPY

As the electronic states of molecules are strongly dependent on the nature of the chemical bonding and molecular conformation, the electronic absorption and emission spectra are potentially useful probes of these aspects of structure. To date, little has been reported^{42,43} on the absorption spectra of the PBT type rigid rod polymers, and to our knowledge, no investigations involving fluorescence spectroscopy have been published. The dearth of data on absorption spectroscopy is not surprising owing to the strong electronic absorptions exhibited by the aromatic heterocyclic

groups and the characteristic metallic lustre exhibited in the solid state. The difficulty, particularly with respect to solid state spectroscopy, is to obtain sufficiently thin specimens for light transmission. In fact, the maximal thickness that can be tolerated for transmission studies may be less than that needed for the absorption spectrum to be characteristic of the bulk. Previous studies of the electronic absorption and reflection spectra of solid state specimens of organic dyes which possess metallic lustre characteristic of strong electronic transitions in the visible range have shown that the electronic state absorption profiles may change significantly as a function of sample thickness.^{44,45} These studies also showed that electronic state spectra are sensitive to the state of aggregation. For these reasons, fluorescence spectroscopy, which does not depend on having thin specimens, may be the preferred way of probing the electronic states for information of the structure of rigid rod polymers.

There are three basic types of fluorescence measurements that may be informative for rigid rod polymers and their composites. (1) Polarized fluorescence may be used to determine the degree of orientation of specimens in the presence and absence of mechanical stress. (2) Steady-state fluorescence of solutions or molecular composites of rigid rod polymers as a function of concentration may be used to elucidate the degree to which polymer-polymer interactions are affected by concentration. (3) Time-resolved intensities of polarized fluorescence from dilute solutions of these polymers would provide information on torsional rigidities, which may relate directly to performance as reinforcing polymers. In the present

investigation, the focus has been on steady-state fluorescence measurements which bear on the question of the degree of aggregation of rigid rod polymers used as reinforcements in molecular composites.

Steady state fluorescence measurements were conducted on an ABPBT fiber, a PBT film, and molecular composites of PBT with nylon. All samples were obtained from the Wright-Patterson Materials Laboratory and are referred to as the "as-received" materials. Fluorescence spectra were obtained with a SPEX¹⁶ fluorimeter equipped with a high pressure Xenon source and phototube with photon counting electronics. The emission spectrum of the ABPBT fiber excited with 515 nm radiation is shown in figure 36, and exhibits a broad band centered near 580 nm. The other spectrum in figure 36 is the excitation spectrum obtained as a plot of the fluorescence intensity at 585 nm as a function of the frequency of the exciting light. This curve should mirror the solid state absorption spectrum. The broad band is attributed to intermolecular interactions in the solid state structure as will become apparent in the following discussion. The emission spectrum of ABPBT dissolved in methane sulfonic acid (MSA), shown in figure 37, differs substantially from that of the solid state sample. The ABPBT concentration was lower than that required for intermolecular association. The dilute solution fluorescence spectrum is typical in that it mirrors the absorption spectrum¹⁴ with the overlap of the absorption and emission spectra occurring near 420 nm, the frequency corresponding to the transition from the zeroth vibronic level of the ground electronic state to the zeroth level of the excited state. Of course, the solution spectrum is of a protonated species (at the nitrogen) while the solid state spectrum may be either protonated or unprotonated depending on the amount of residual acid present. The effect of protonation was examined by com-

paring the emission spectrum of as-received ABPBT with that of ABPBT precipitated from MSA by the addition of water followed by successive washings with water to remove any residual acid. This procedure produced the emission spectrum shown by the dashed curve in figure 38. This spectrum has the same profile as that of the as-received specimen from which it is concluded that the 580 nm band is not due to an impurity. Exposure of the acid-free ABPBT to concentrated HCL solution and HCL vapor produced the emission spectra shown as solid curves in figure 38. In this case, the broad band at 580 nm has been greatly reduced in intensity and shifted to longer wavelengths. Thus, the broad band at 580 nm is attributed to the unprotonated ABPBT molecule in the solid state and the broad band at 618 nm to the protonated ABPBT molecule in the solid state. The frequency shift to longer wavelengths with protonation is similar to the behavior found for the absorption spectra between protonated and unprotonated solvents.⁴³

Attempts to obtain an emission spectrum from the PBT film as received were unsuccessful. For this reason, the PBT was extracted with MSA and the precipitate obtained by addition of water was examined. The PBT film was not entirely soluble in MSA, but the material extracted in solution produced the emission spectrum shown in figure 39. This spectrum is similar to that of ABPBT, figure 37, which means that the resonance effect along the polymer chain axis does not affect the emission spectra to any appreciable extent. Whereas the PBT molecule is thought to adopt a rigid rod structure in solution, the ABPBT molecule is more flexible which would decrease the tendency for electron delocalization between benzothiazole groups.

The solution fluorescence and excitation spectra of the PBT extract are plotted in figure 40. The excitation spectrum is obtained by monitoring the emission at 497 nm while the exciting wavelength is scanned through the absorption region. The fluorescence intensity is ratioed to that of the exciting light to cancel out effects of variable intensity of the excitation light. Peaks in the excitation spectrum occur at wavelengths where there is a maximum in the absorption spectrum. This excitation spectrum is quite similar to the observed absorption spectrum.⁴³ The concentration of PBT used to obtain the fluorescence spectra was lower than that at which liquid crystals are obtained.

The emission and excitation spectra of the PBT coagulants are shown in figure 41. The shape of the emission spectrum is similar to that exhibited by ABPBT although the band maximum occurs at a slightly lower wavelength. Comparison of the solid state fluorescence spectrum to that in dilute solution shows that the broad longer wavelength band of the solid state can be attributed to the effect of aggregation.

The final emission spectrum was obtained on a molecular composite of PBT and nylon. This spectrum, shown in figure 41, is similar to that of PBT in the solid state. From this observation it is concluded that the PBT molecules in the molecular composite are aggregated.

From the exploratory fluorescence studies it appears that this approach can provide information concerning the degree of aggregation in molecular composites. The solid state spectra are distinctly different from those of the polymer molecules in dilute solution. To quantify these findings in terms of size of the clusters will take additional work. Clearly, experiments should be conducted as a function of concentration in solution to determine to what degree the liquid crystal state affects

the emission spectra. In addition, the fluorescence spectra of model compounds soluble in nonprotonated solvents should be examined. Together with studies of a series of PBT-nylon composites with varying morphology and composition, a better picture of the potential of fluorescence spectroscopy to elucidate the structure of molecular composites of rigid rod polymers could be obtained.

V. HIGH PRESSURE X-RAY DIFFRACTION

A. Introduction

Polymers exhibit a rich variety of crystal phase transitions. These include crystal-crystal, order-disorder, reversible and irreversible transitions. They can be induced by changes in temperature, tensile stress, electric fields, hydrostatic pressure and the concentration of small molecules such as water. Further, by combinations of more than one of these parameters, it is possible to produce structures that might not otherwise occur.

The latter result is of special interest with respect to poly (benzobisthiazole) (PBT) which crystallizes with the crystals disordered by random displacements of the molecules along their axes. The disorder probably occurs because of the large number of energy minima occurring as the chains are slid by one another.⁴⁶ It is thought that this disorder contributes to the less than desired performance of PBT fibers in compression. Since the reduced performance could limit the use of these fibers in high performance composites, means of improving the order of the crystals are of interest.

B. Approach

The application of either pressure or a combination of temperature and pressure has the possibility of producing crystals with increased order. For example, a similar disorder with random displacements of the molecules along their axes in polytetrafluorethylene⁴⁷ can be reversed by the application of pressure which generates a well-ordered phase.^{48,49} Further, if the pressure is applied at high temperatures and the sample is then cooled to low temperatures, the pressure can be removed and the ordered material recovered at atmospheric pressure.⁵⁰ It is possible that a similar effect will occur for PBT, but will occur in a higher temperature range because of the more "rigid" nature of the PBT molecules. Because of this nature, application of either pressure or pressure and temperature of the PBT in the presence of small concentrations of a material such as polyphosphoric acid might be a more effective procedure than the application of either pressure or pressure and temperature alone. The application of pressure and temperature to previously unannealed neat fibers of PBT might also lead to significantly improved order. It is known, for example, that annealing alone yields modest improvements in the order.

For the investigation of the effects of various pressure treatments, the use of x-ray diffraction techniques are very important. Further, it is desirable to make measurements at pressure in order to follow changes. The diamond anvil cell is a very useful instrument for applying high pressure (up to ~20,000 MPa) to a sample and examining its structure by x-ray diffraction.⁵¹ The cell is shown in the diagram in Figure 43. The diagram illustrates one possible limitation of the technique--that is, the very small sample size from which it may be difficult to obtain a useable x-ray signal.

C. Object

The object of this work is to carry out exploratory measurements to determine whether satisfactory x-ray data can be obtained for PBT using the diamond anvil cell and rotating anode x-ray source. Another object is to look for evidence of structure changes at elevated pressures.

D. Experimental

The cell is used in conjunction with a Rigaku Denki RU 200 rotating anode x-ray source which can be operated at 200mA tube current and 60kV with a fine focal spot size. The cell available for the initial measurements was suited for use at ambient temperatures in conjunction with an energy dispersive detector set at a fixed diffracting angle. Thus, it could generate an x-ray pattern equivalent to a conventional diffractometer powder pattern.

In light of this capability of the cell and detector, it was decided to attempt to obtain these initial data with the unoriented PBT dope rather than the highly oriented fibers. It would be very difficult to align the later correctly with respect to the detector. The dope chosen was SRI polyphosphoric acid dope 2895-89 of 25 IV at 15.7% solids. It had "solidified" in an extrusion cylinder at Celanese and could not be extruded. After removal from the system, it had a much duller color than the original dope and was very stiff. It had been stored in a jar and had not flowed under its own weight during 1 year.

Pentane was used as the hydraulic fluid pressure fluid in order to reduce both unwanted interactions with the sample and unwanted scattering of the x-rays by the fluid. Further, in order to avoid crystallization of the fluid at elevated pressure, a 50:50 v/v mixture of n-pentane and

iso pentane was used. Because of the relatively high vapor pressure of these materials at room temperature, both they and the cell were cooled to about 0 C for the filling of the cell.

E. Results

Wide-angle powder patterns taken in the conventional manner with a flat plate camera at room temperature and one atmosphere confirmed that the dope was unoriented. These were taken in different regions of the sample and with the beam incident in three mutually perpendicular directions with respect to the sample. All the results are very similar to the one shown in Figure 44. There is a rather broad diffuse ring with a somewhat sharp one near the small angle "edge" of it. This sharper ring corresponds to about 12.40 \AA° which is close to the repeat of PBT.⁵² The pattern contains fewer sharp lines than have been reported for 11% poly (benzobisoxazole) in 100% H_2SO_4 .⁵³ Very likely this difference is just a result of being in relatively different portions of the phase diagrams for the polymer-acid systems. Such differences are exhibited by a 22% poly (p-phenylene terephthalamide) -sulfuric acid system at temperatures of 90 C (diffuse line) and 25 C (sharp lines).⁵⁴

When the dope was cut to produce the very small piece needed for the high-pressure cell, some deformation occurred and the sample was very likely oriented. Nevertheless, useful data were obtained. These are shown in figure 45 in which intensity is plotted vs d^* ($=1/d$) for an applied pressure of 1,270 MPa. At least one peak corresponding to a smaller spacing ($\sim 4.7 \text{ \AA}^\circ$) has now been introduced and there appears to be a few others which are rather weak. Thus the structure of the dope appears to have undergone some change upon the application of 12,700 atm. The pressure probably changed the location of the sample on the phase

diagram. The disappearance of the peak corresponding to about 12.4\AA at 1 atm is no doubt a consequence of the sample having been oriented during the process of preparing it for the high-pressure cell. It would be very difficult to align an oriented sample so that a given set of planes were in the proper orientation for detection by the energy dispersive detector.

F. Conclusions and Recommendations

The diamond anvil cell can be used in conjunction with a rotating anode x-ray source to produce useful diffraction data for PBT. It has been shown that the application of 1,270 MPa to PBT-polyphosphoric acid dope causes structural changes.

Thus, this work has shown that it would be fruitful now to proceed with an investigation of the structure of both the dope and the fiber as a function of pressure and temperature (composition should also be varied for the dope). This will permit us to answer the question of whether a high pressure route to a fiber with improved order can be found (as was discussed in the Approach Section).

However, these further investigations should be carried out with film rather than the energy dispersive detector. Then one would be able to obtain useful data with the oriented dope and even with the highly oriented fiber. It would be desirable also to carry these measurements out on the synchrotron in order to accelerate the data acquisition process. The use of an x-ray image intensifier would also offer advantages.

References

- 1a. G. Husman, T. Helminiak, M. Wellman, W. Adams, D. Wiff, and C. Benner, "Molecular Composites - Rodlike Polymer Reinforcing an Amorphous Polymer Matrix", AFWAL-TR-80-4034, May 1980.
- 1b. D. K. Wiff, W. F. Hwang and C. Benner, "Molecular Level Composites - (Rigid Rod/Flexible Coil) Blend" Bull. Am. Phys. Soc. 27, 290 (1982).
- 2a. S. J. Bai, D. R. Wiff, W-F. Hwang, "Molecular Level-(Rigid Rod/Flexible Coil) Blend", Bull. Am. Phy. Soc. 28, 390 (1983).
- 2b. W-F. Hwang, C. L. Benner, and D. R. Wiff, "Molecular Composites: Phase Relationships, Processing and Properties of Rod/Coil Polymer Blends", Int. Union Pure & Appl. Chem. 28 Macromolecular Symp., July 1982, Amherst, MA.
3. W-F. Hwang, D. R. Wiff, C. Verschoore, G. E. Price, T. E. Helminiak, and W. W. Adams, "Solution Processing and Properties of Molecular Composite Fibers and Film", J. Polym. Eng. & Sci. 23, 784 (1983).
4. J. L. Kardos and J. Kaisoni, Polym. Eng. Sci. 15, 182 (1975).
5. P. J. Flory, Macromolecules, 11, 1138 (1978).
6. W-F. Hwang, "Molecular Composites", Ordered Polymer Contract Research Review, Admiral Benbow Inn, Dayton, OH, September 24, 1984.
7. C. P. Slichter, "Principles of Magnetic Resonance", 2nd Edition, Springer-Verlag, Berlin, 1978.
8. A. Abragam, "The Principles of Nuclear Magnetism" (Oxford University Press, Oxford, England, 1961).
9. M. Mehring, "High Resolution NMR Spectroscopy in Solids", NMR: Basic Principles and Progress 11 (Springer-Verlag, Berlin, 1976).
10. D. C. Douglass and G. P. Jones, J. Chem. Phys. 45, 956 (1966).
11. J. Crank, "The Mathematics of Diffusion", Oxford University Press, Oxford, England, 1956.
12. A. Pines, M. G. Gibby, and J. S. Waugh, J. Chem. Phys. 59, 569 (1973).
13. S. R. Hartmann and E. L. Hahn, Phys. Rev. 128, 2042 (1962).
14. D. L. VanderHart and F. Khoury, Polymer, 25, 1589 (1984).
15. L. B. Alemany, D. M. Grant, R. J. Pugmire, T. D. Alger, and K. W. Zilm, J. Am. Chem. Soc. 105, 2133-2147, 1983.

16. Certain commercial materials and equipment are identified in this report in order to specify adequately the experimental procedure. In no case does such identification imply recommendation or endorsement by the National Bureau of Standards, nor does it imply necessarily the best available for the purpose.
17. E. Hahn, Phys. Rev., 80, 580 (1950).
18. J. G. Powles and P. Mansfield, Phys. Lett. 2, 58 (1962).
19. P. Mansfield, M. J. Orchard, D. C. Stalker, and K. H. B. Richards, Phys. Rev. B7, 90 (1973).
20. W.-K. Rhim, D. D. Elleman, and R. W. Vaughan, J. Chem. Phys. 59, 3740 (1973).
21. A. J. Vega and R. W. Vaughan, J. Chem. Phys. 68, 1958 (1978).
22. Private conversation with W. W. Adams.
23. S. J. Opella and M. H. Frey, J. Am. Chem. Soc. 101, 5854 (1979).
24. E. O. Stejskal, J. Schaefer, M. D. Sefcik, and R. A. McKay, Macromolecules 14, 275 (1981).
25. J. R. Havens and D. L. VanderHart, Macromolecules, in press.
26. A. Wokaun and R. R. Ernst, Chem. Phys. Lett. 52, 407 (1977).
27. N. M. Szeverenyi, A. Bax, and G. E. Maciel, J. Am. Chem. Soc. 105, 2579 (1983).
28. D. L. VanderHart and A. N. Garroway, J. Chem. Phys. 71, 2773 (1979).
29. D. A. Torchia, J. Magn. Reson. 30, 613 (1978).
30. W.-F. Hwang, D. R. Wiff, C. L. Benner, and T. E. Helminiak, J. Macromol. Sci.- Phys. B22, 231 (1983).
31. W.-F. Hwang, D. R. Wiff, and C. Verschoore, Poly. Eng. Sci. 23, 789 (1983).
32. E. L. Thomas, R. J. Farris and S. L. Hsu, AFWAL-TR-80-4045, Vol. III, Pt.I, August, 1982.
33. E. J. Roche, T. Takahashi, and E. L. Thomas, "Fiber Diffraction Methods", A. D. French and K. H. Gardner, Eds., ACS Symp. Ser. 141, p.303 (1980).
34. L. M. Ryan, R. E. Taylor, A. J. Paff and B. C. Gerstein, J. Chem. Phys. 72, 508 (1980).
35. H. H. Kausch, "Polymer Fracture", Springer-Verlag, New York (1978).

36. P. Fordyce, K. L. DeVries, and B. M. Fanconi, "Chain Scission and Mechanical Degradation of Polystyrene", *Polym. Eng. & Sci.* 24, 421 (1984).
37. T. M. Stoeckel, J. Blasius and B. Crist, "Chain Rupture and Tensile Deformation of Polymers", *J. Polym. Sci. Polym. Phys. Ed.* 16, 485 (1978).
38. B. M. Fanconi, K. L. DeVries and R. H. Smith, "Free Radicals and New End Groups Resulting from Chain Scission: 2. Mechanical Degradation of Polyethylene". *Polymer* 23, 1027 (1982).
39. L. N. Shen, "Viscosity-Average Molecular Weight Change During Fracture of Nylon-6 Fibers", *J. Polym. Sci. Polym. Lett. Ed.* 15, 615 (1977).
40. B. M. Fanconi, "Chain Scission and Mechanical Failure of Polyethylene", *J. Appl. Phys.* 54, 5577 (1983).
41. I. M. Brown, T. C. Sandreczki, and R. J. Morgan, "Electron Paramagnetic Resonance Studies of Kevlar 49 Fibers: Stress-induced Free Radicals", *Polymer*, 25, 759 (1984).
42. G. M. Venkatesh, D. Y. Shen and S. L. Hsu, "Spectroscopic Study of Rigid Rod Polymers. I. Structures of Model Compounds." *J. Polym. Sci. Polym. Phys. Ed.* 19, 1475 (1981).
43. D. Y. Shen, G. M. Venkatesh, D. J. Burchell, P.H.C. Shu, and S. L. Hsu, "Spectroscopic Study of Rigid Rod Polymers. II. Protonation Effect".
44. B. M. Fanconi, "The Exciton-Molecular Vibration Interaction in Molecular Crystals in the Strong Coupling Limit", PhD. Thesis, University of Washington, Seattle, WA. 1968.
45. P. Gramaccioni, "Spectral Properties of Polymethinium Dye Crystals", PhD. Thesis, University of Oregon, Eugene, OR. 1970.
46. D. Bhaumik, W. J. Welsh, H. H. Jaffe, and J. E. Mark, *Macromolecules*, 14, 951 (1981).
47. Disorder in the Crystal Structure of Phases I and II of Copolymers of Tetrafluoroethylene and Hexafluoropropylene, J. J. Weeks, R. K. Eby, and E. S. Clark, *Polymer* 22, 496 (1981).
48. The Crystal Structure of Polytetrafluoroethylene Homo and Copolymers in the High Pressure Phase, E. S. Clark and R. K. Eby, G. J. Piermarini, and S. Block, *Polymer Preprints* 24, No. 2, 423 (1983).
49. C. Nakafuku and T. Takemura, *Japan J. Appl. Phys.* 14, 599 (1975).
50. Malcolm F. Nicol, Joseph M. Wiget and C. K. Wu, *J. Polymer Sci.: Polymer Physics Edition* 18, 1087 (1980).

51. J. D. Barnett, S. Block, and G. J. Piermarini, Rev.Sci. Instrum. 44, 1(1971).
52. J. R. Winter, Air Force Technical Report AFWAL-TR-82-4097.
53. E. Won Choe and Sang Wim Kim, Machromolecules 14, 920 (1981).
54. K. H. Gardner, R. R. Matheson, P. Avakian, Y. T. Chia, and T. D. Gierke, Polymers for Fibers & Elastomers, ACS Symposium Series, Jett Arthur, Jr., Editor, 260, 91 (1984).

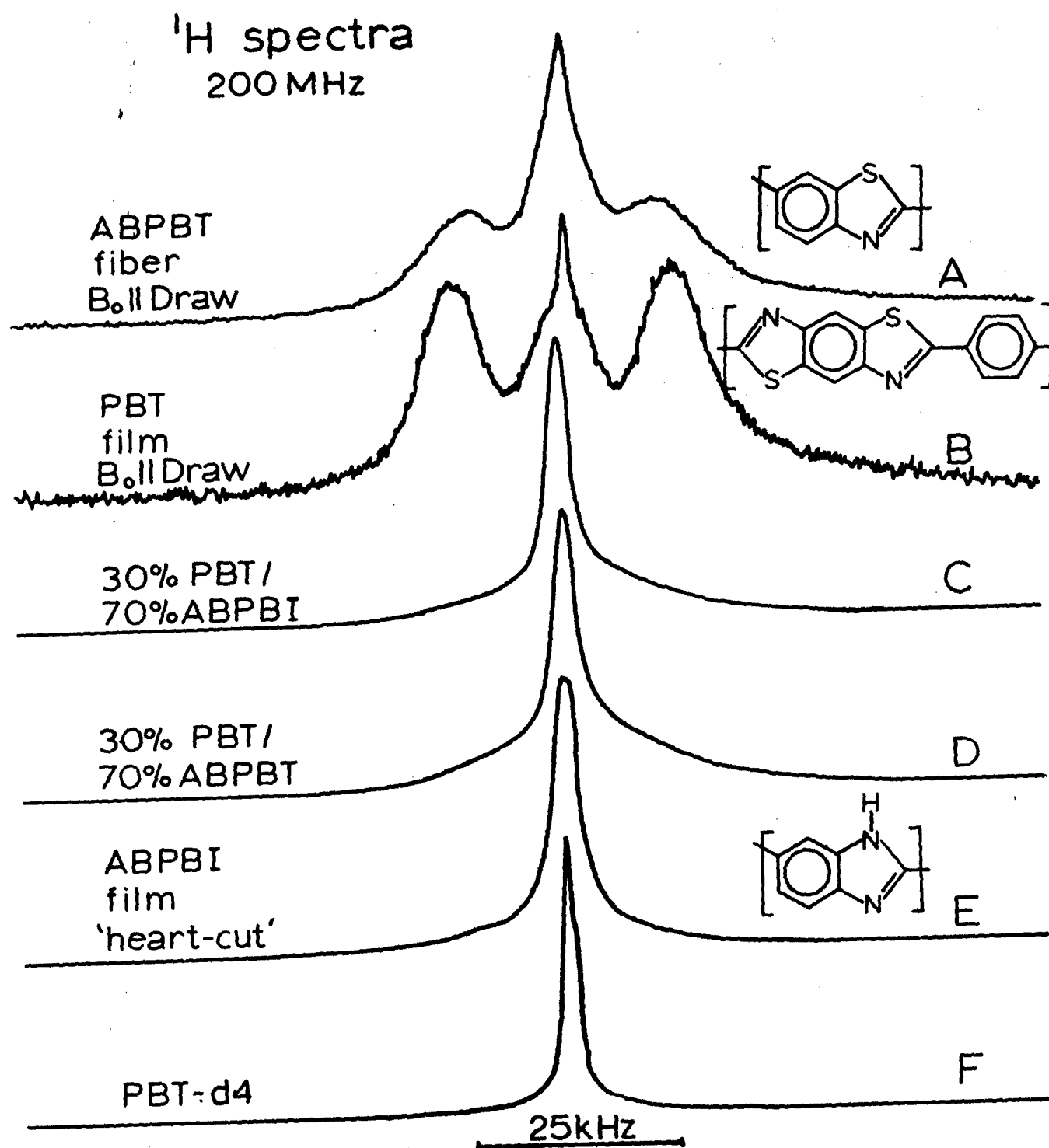


Figure 1

200 MHz proton spectra for Samples A-F. From top to bottom Spectra A-F correspond to Samples D, A, F, E, C and B respectively. Chemical structures for the three monomers involved are also given. The alignment of the frequency axis in these spectra is only approximate from one spectrum to another. All samples shown here were in unsealed tubes exposed to air.

^1H

ABPBI
film
'heart-cut'

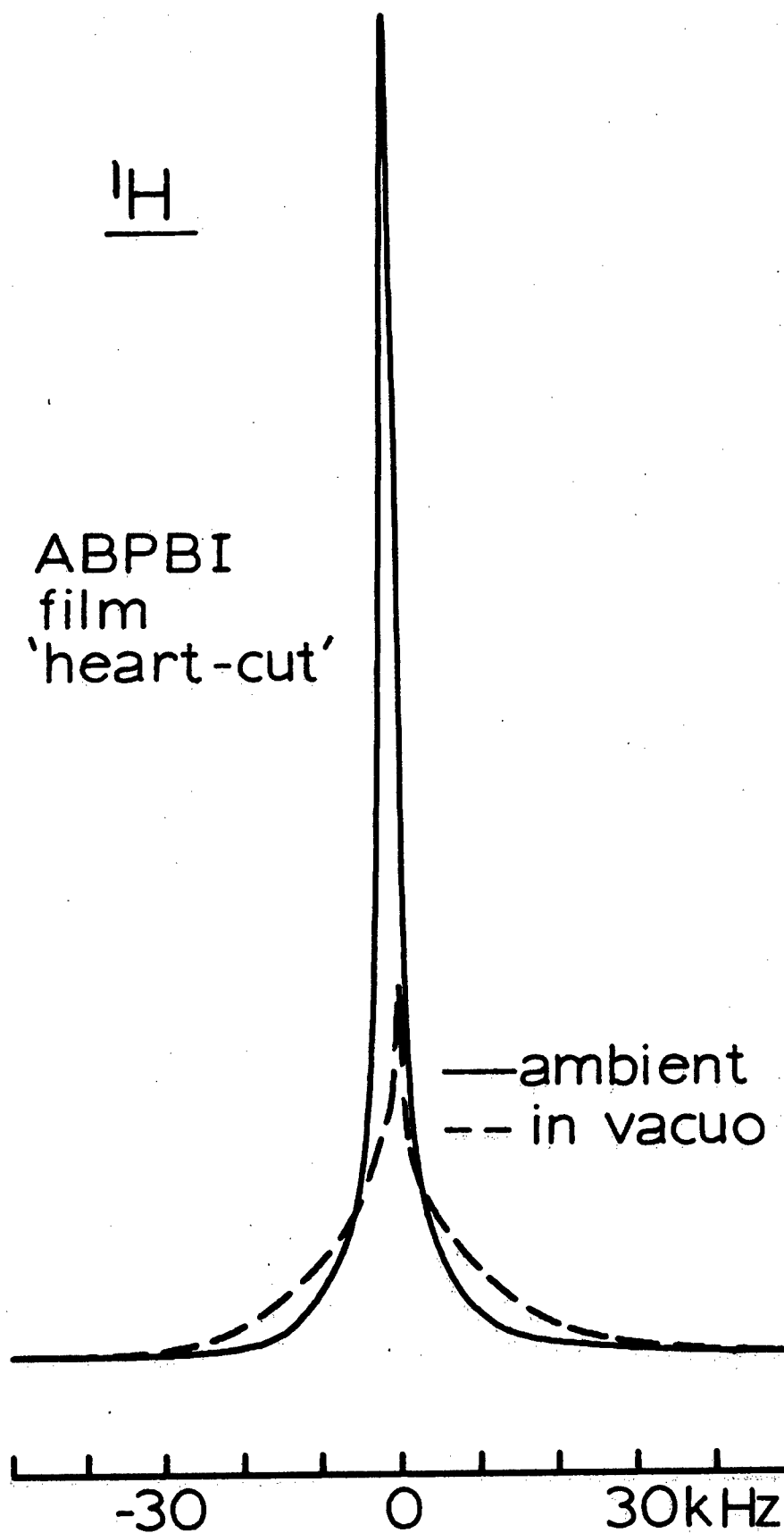


Figure 2

Comparison of proton lineshapes in the ABPBI "heart cut" film in going from an ambient to an evacuated sample. Note the large reduction in mobile proton content and the increase in linewidth for the broader polymer resonance in the evacuated sample.

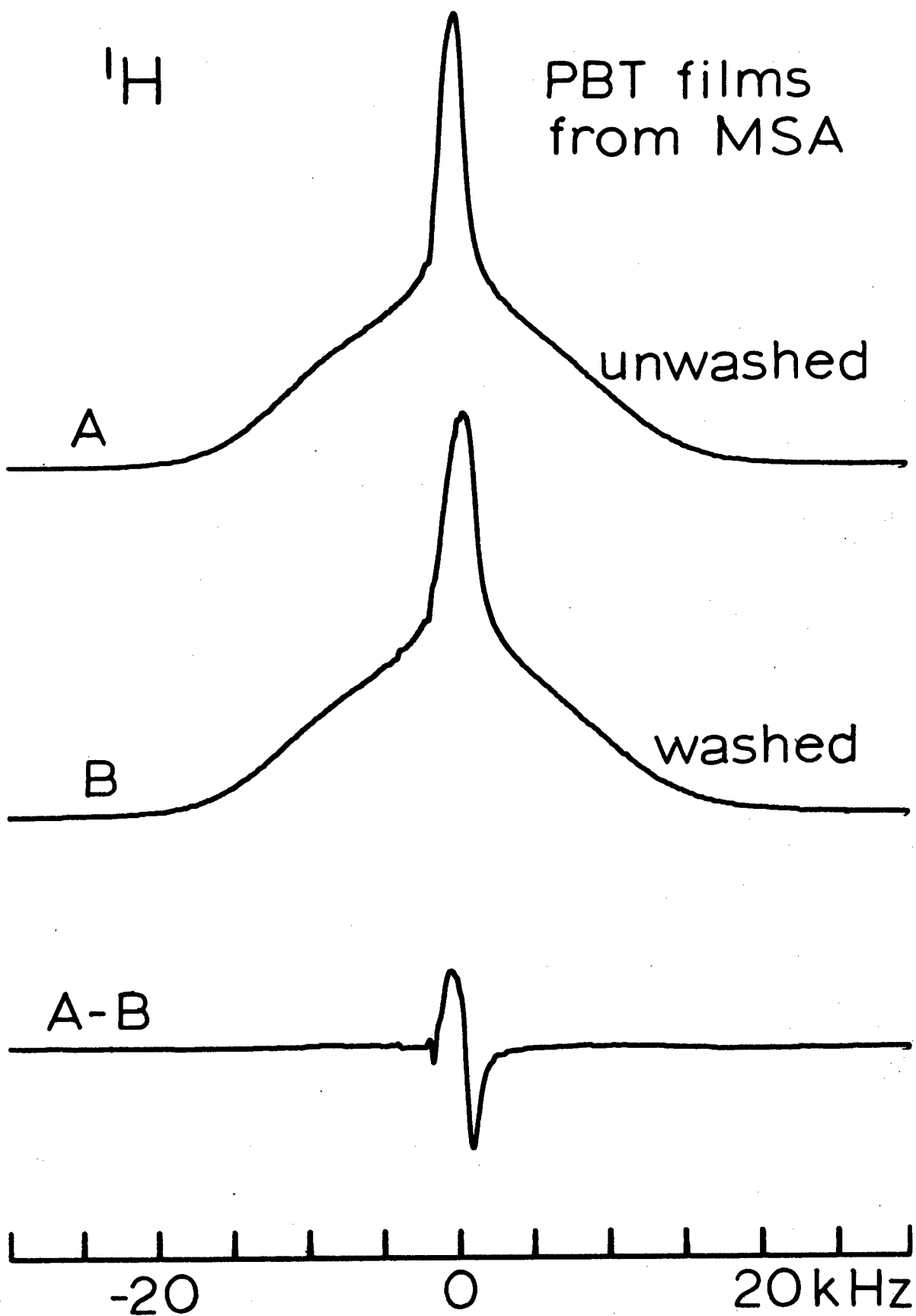


Figure 3

Comparison of proton lineshapes for unwashed (Sample P) and washed (Sample N) PBT films coagulated from MSA solution. The washed sample possesses a broader narrow resonance, which is shown by the difference spectrum (and other relaxation experiments) to be due to the presence of a second mobile proton component of about 1 kHz linewidth. The two components of the narrow line in Spectrum B are shifted 5-6 ppm from one another.

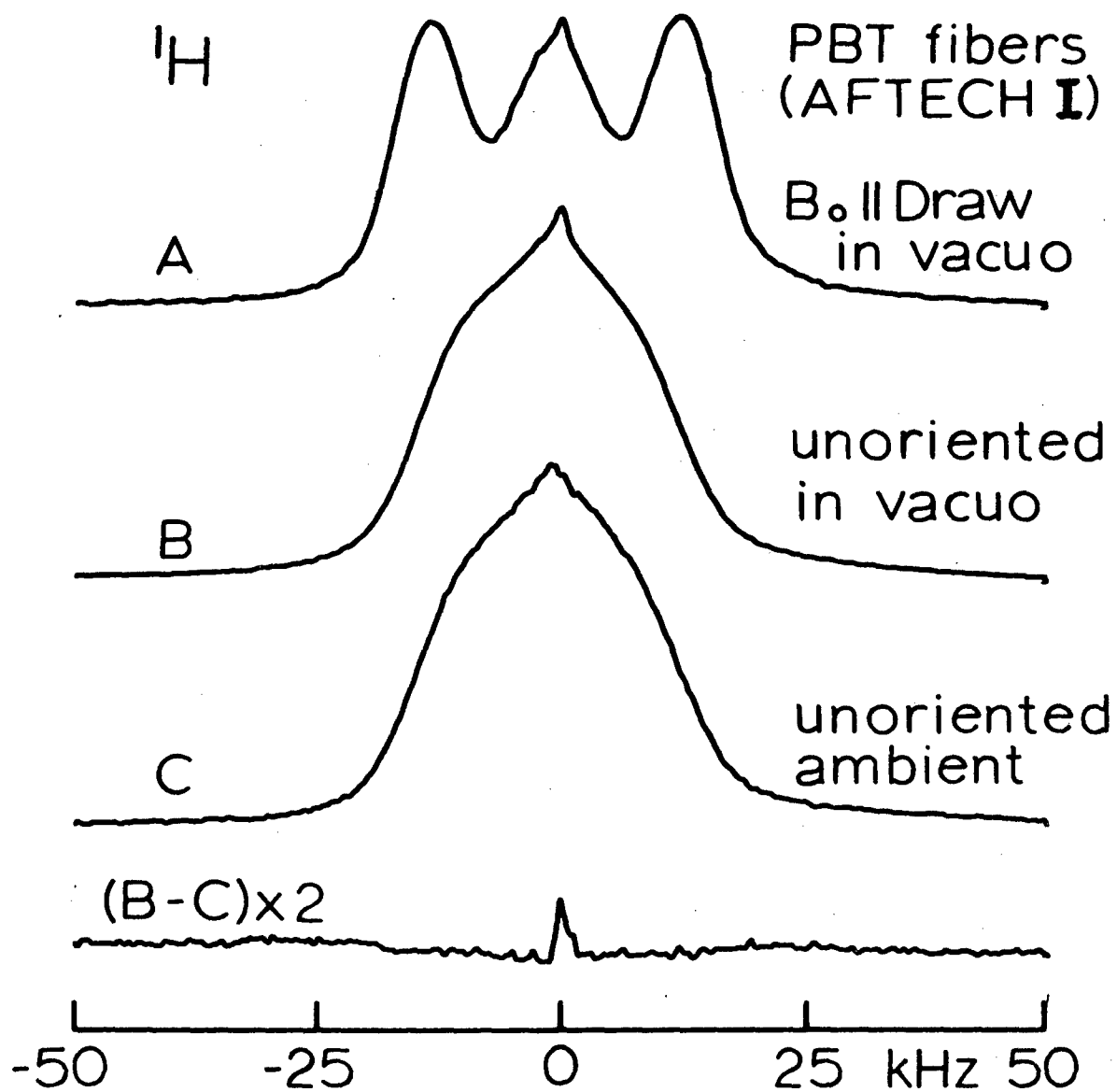


Figure 4

200 MHz proton spectra of AFTECH I PBT fibers. Spectrum A is the spectrum of an oriented bundle of fibers in an evacuated tube, Spectrum B corresponds to an unoriented evacuated sample, and Spectrum C to an unoriented fiber sample exposed to air and laboratory humidity for several months. Note that there is no significant retention of a mobile proton species such as water in the latter sample compared to Spectrum B. The small difference shown by the lower spectrum could be impurities introduced by handling since they are only 0.4% of the total intensity.

^1H

PBT film
B. II Draw

M_0

after 24ms
MREV-8

25kHz

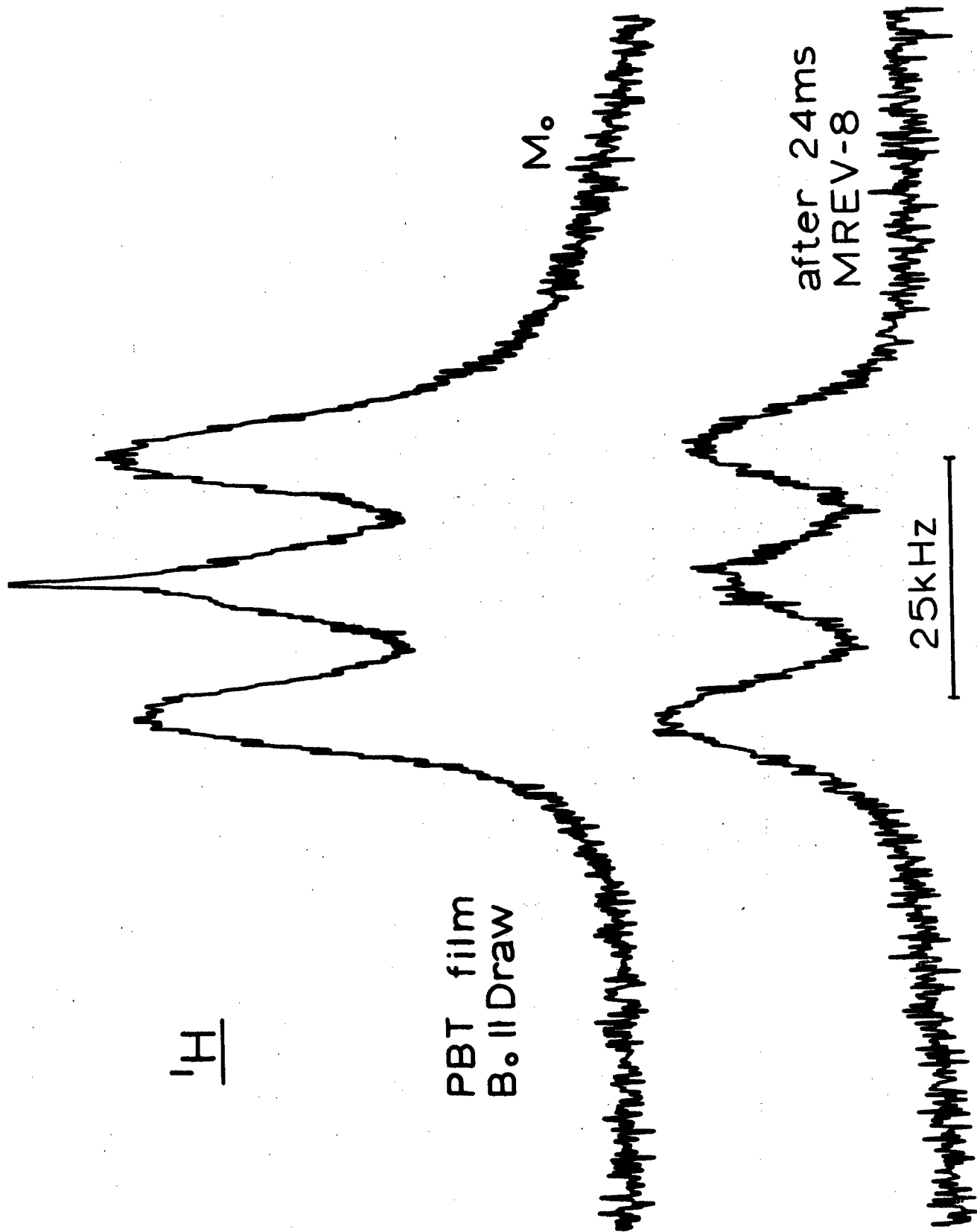


Figure 5

Proton spectra of Sample A (open tube) both before and after partial relaxation during a 24ms MREV-8 multiple pulse irradiation. The film is macroscopically oriented with its draw direction parallel to B_0 . Aside from an overall attenuation of the signal, the principal lineshape change is associated with the preferentially faster decay of the more mobile proton species resonating in the central multiplet.

^1H Multiple Pulse Spectra
(MREV-8)

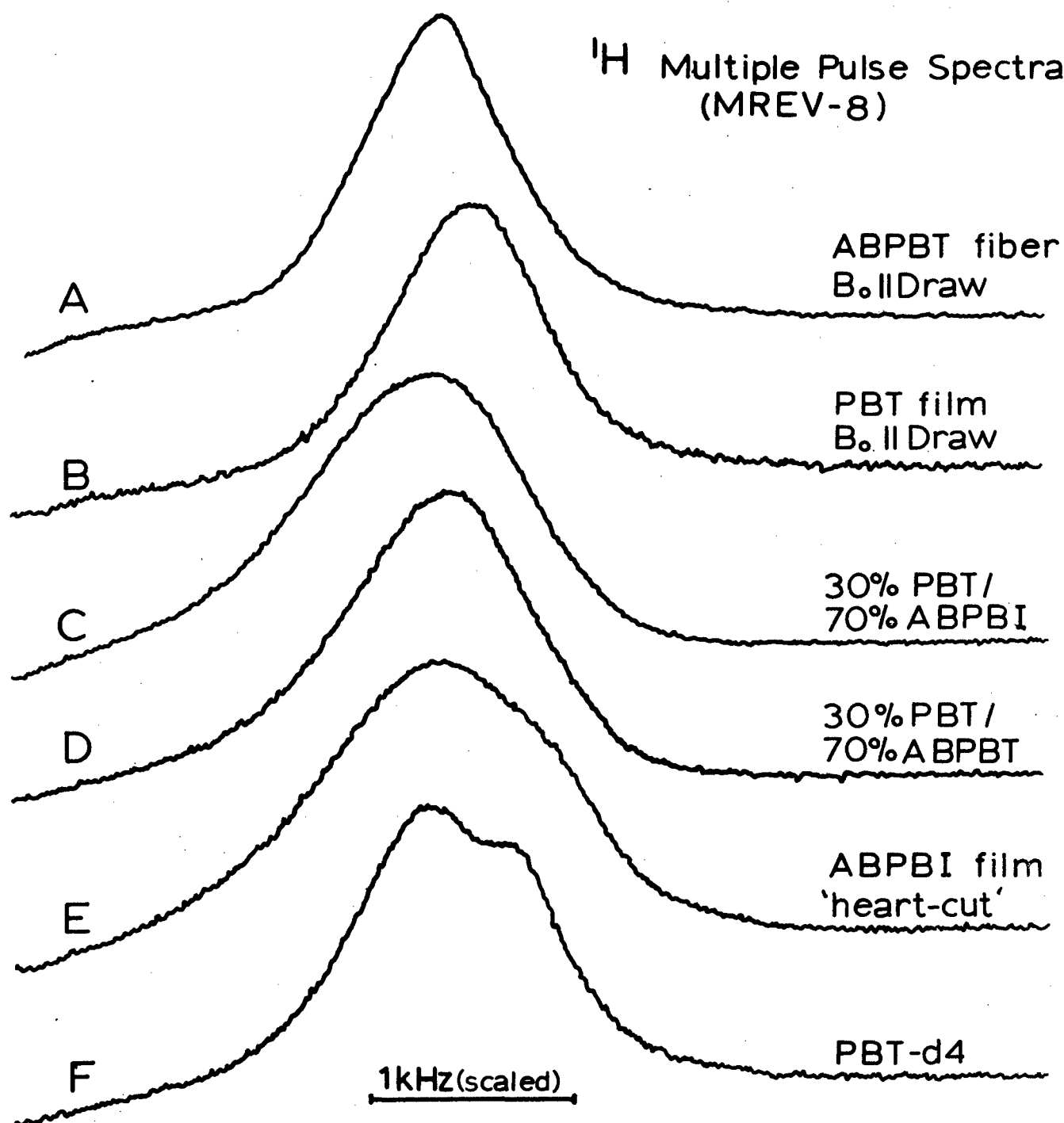


Figure 6

Proton spectra of the same, unevacuated samples as in Figure 1. These spectra are taken by stroboscopically sampling once per cycle during a train of MREV-8 pulse cycles. These spectra principally indicate chemical shift broadening and magnetic susceptibility broadening since dipolar interactions are quenched. Note that the frequency scale is greatly expanded compared with Figure 1. Note also, however, that the narrow lines, so evident in Figure 1C-1F, have acquired linewidths comparable to the polymer resonances because the residual dipolar interactions of the mobile protons are not significantly reduced by the multiple pulse irradiation.

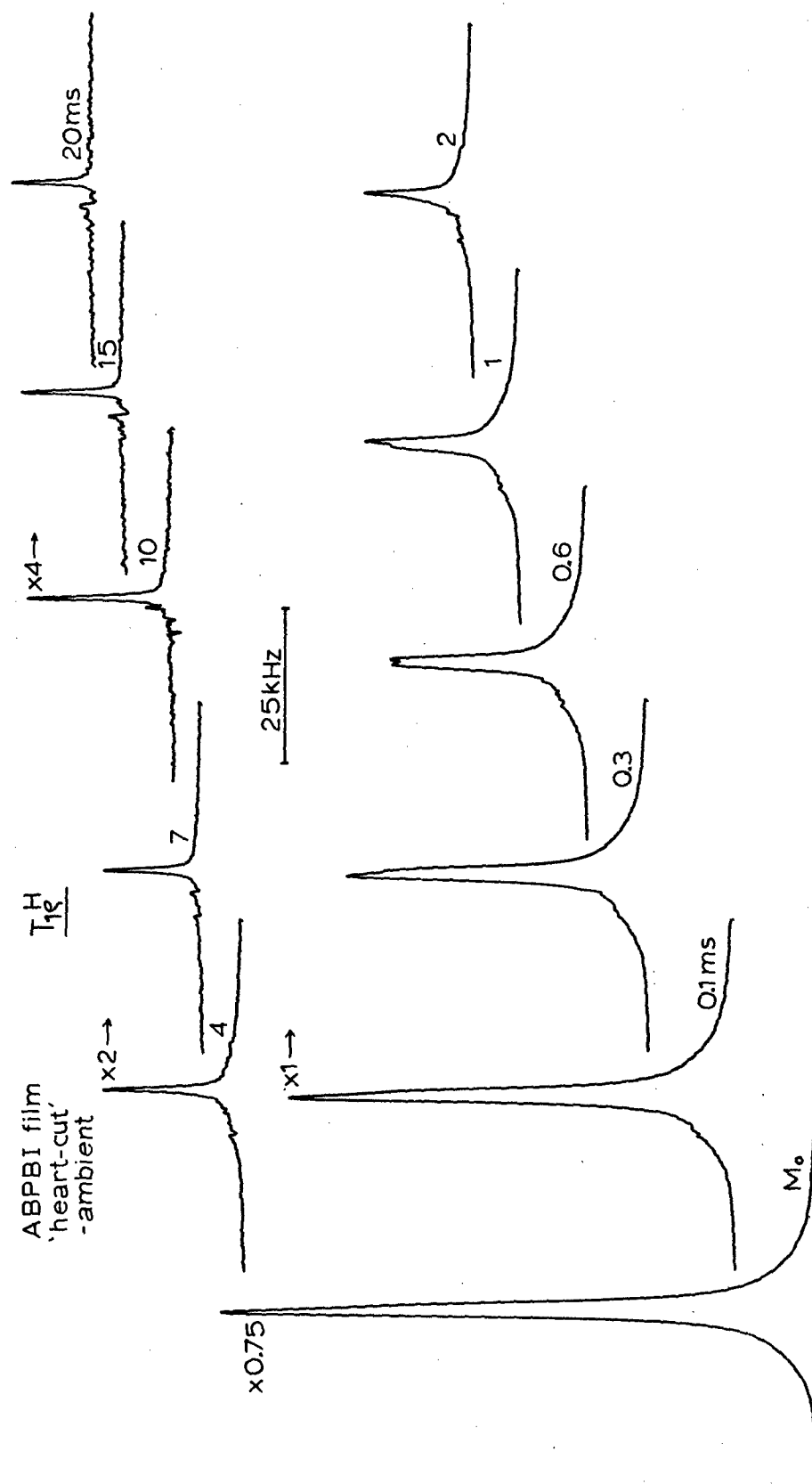


Figure 7

Proton lineshape changes in Sample C (unsealed) as a function of spin-locking time (rf field strength is 83 kHz). Times in ms are indicated at the base of each resonance; relative amplification factors are given at the top of the resonances where the factor changes. Note the exceedingly rapid decay of the downfield side of the narrow resonance, leaving a 1 kHz wide upfield region. The noisy region downfield from the narrow resonance is not significant; it is associated with low frequency noise near the rf carrier frequency.

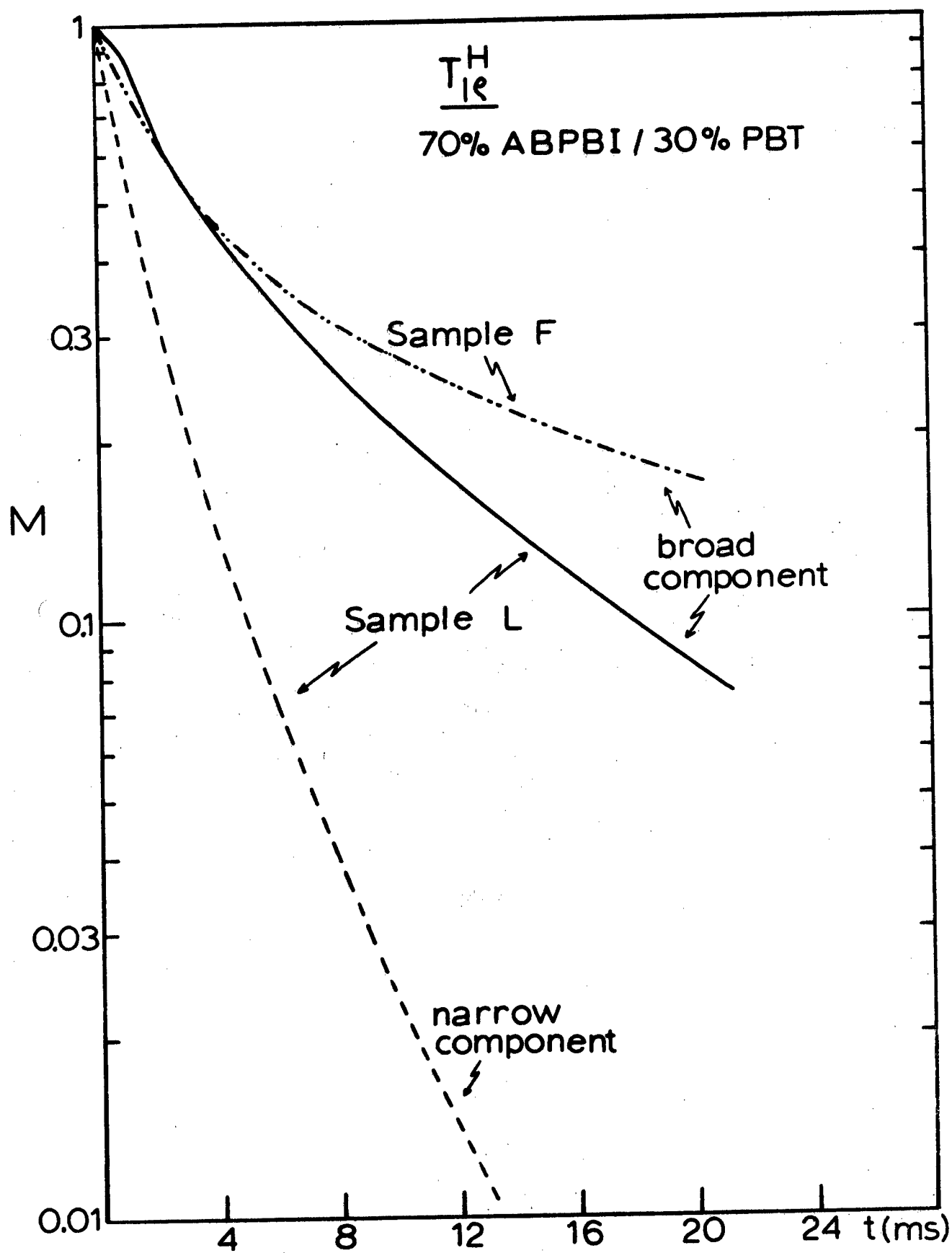


Figure 8

Decay curves for the spin locked magnetization (rf field strength is 83 kHz) for two composite samples (F and L) of 70% ABPBI/30% PBT. Both samples are in evacuated tubes. The broad component decay of both samples is shown along with the narrow component of Sample L. The increasing decay rate of the broad component at early time in Sample L indicates a dipolar coupling, via proton spin diffusion, with the mobile protons in the narrow component. On the other hand, the divergence of the broad and narrow magnetizations at later times indicates that the mobile protons are not distributed evenly throughout the polymer on a molecular scale. Since Sample F is processed from a true solution and Sample L from a higher concentration, phase-separated solution, one expects to see the slower decay signature of the PBT homopolymer at longer times for Sample L. This is not seen partly due to the influence of the mobile proton species which can exist in the PBT phase as well.

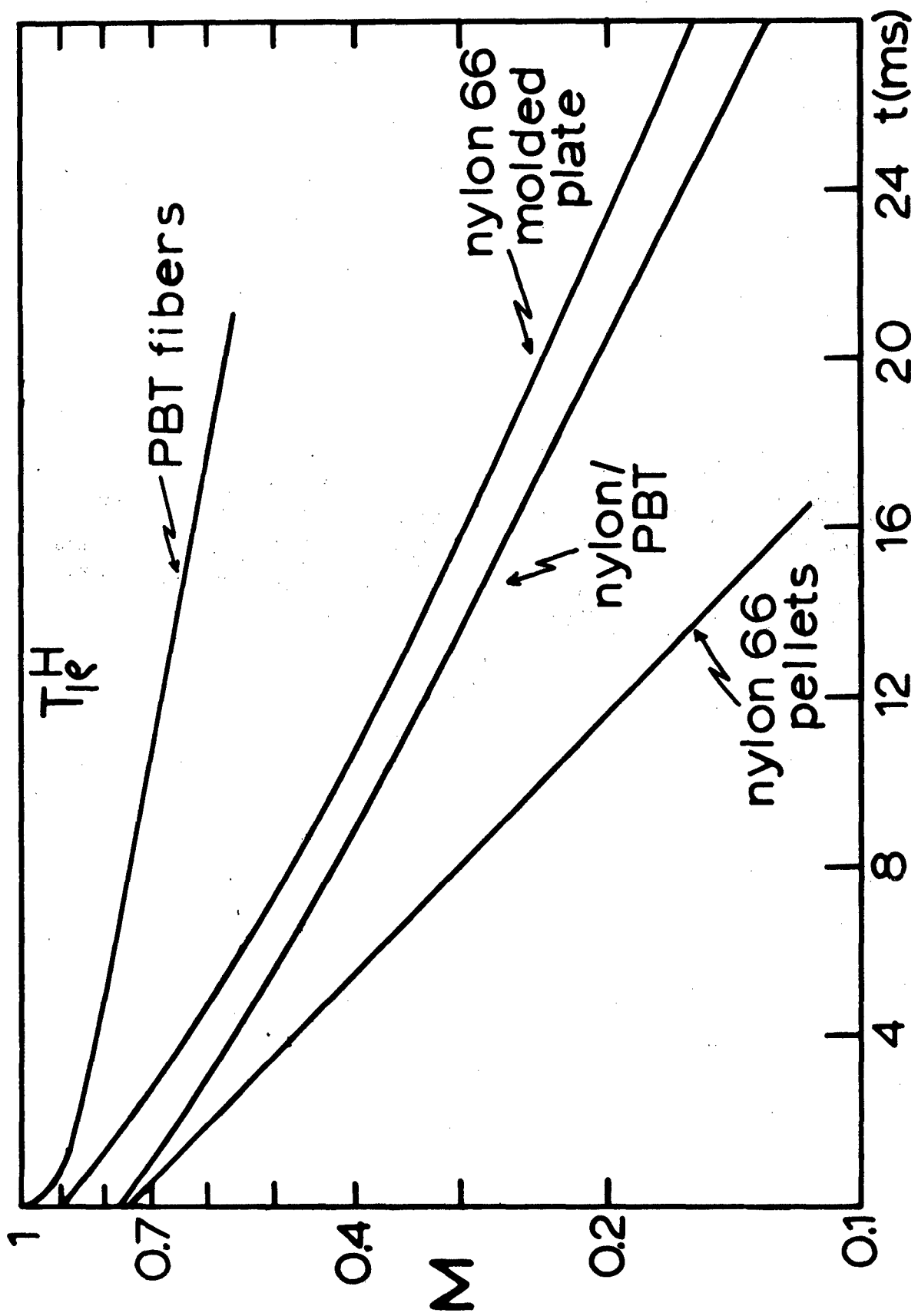


Figure 9

$T_{1\rho}^H$ decay curves for Sample G,M,I and Q (top to bottom respectively). All samples are in evacuated tubes. The fact that the decay of the annealed nylon/PBT sample is not intermediate between the PBT and the nylon molded plate strongly suggests that the nylon and the PBT are intimately enough mixed in the composite so as to lower the chain order in the nylon more towards the lower crystallinity nylon pellets.

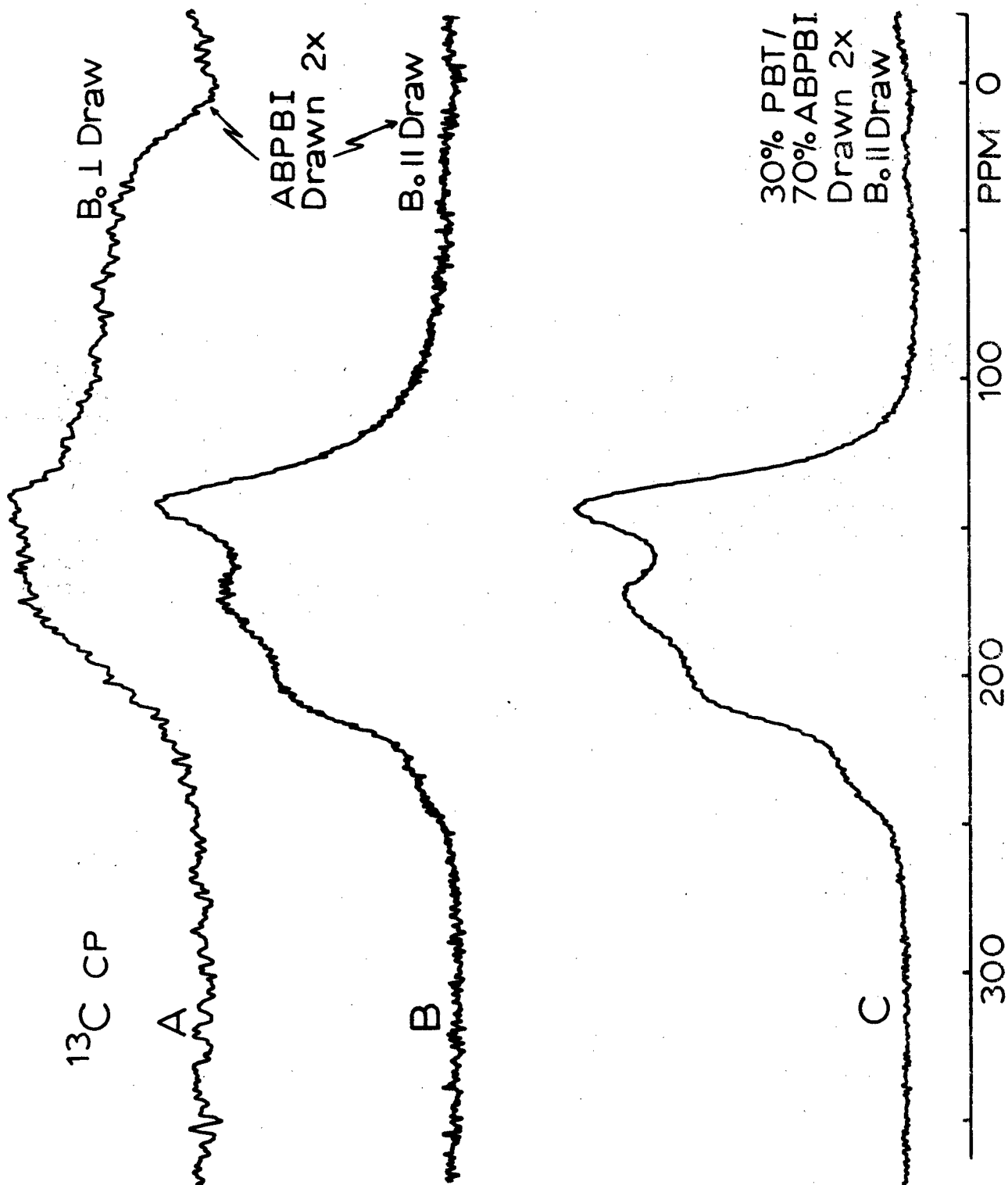


Figure 10

50 MHz ^{13}C CP spectra of macroscopically oriented Samples K (A and B) and J (C). B_0 is perpendicular to the draw axis in Spectrum A and parallel in Spectra B and C. The shoulder at 25 ppm in Spectrum A is associated with the normals to the aromatic rings parallel to B_0 . The near absence of this shoulder in Spectra B and C indicates that the chains have a strong projection along the draw direction. The stronger downfield shoulder in Spectrum C relative to B indicates that the PBT is also oriented in the composite (see Figure 11). Note that the precursor to Sample K before the 2X stretch, was also run. This oriented sample gave the same spectrum as Spectrum B. Therefore the 2X wet drawing did not impart the primary orientation into this sample.

PBT fibers
(AFTECH I)
B₀ II Draw

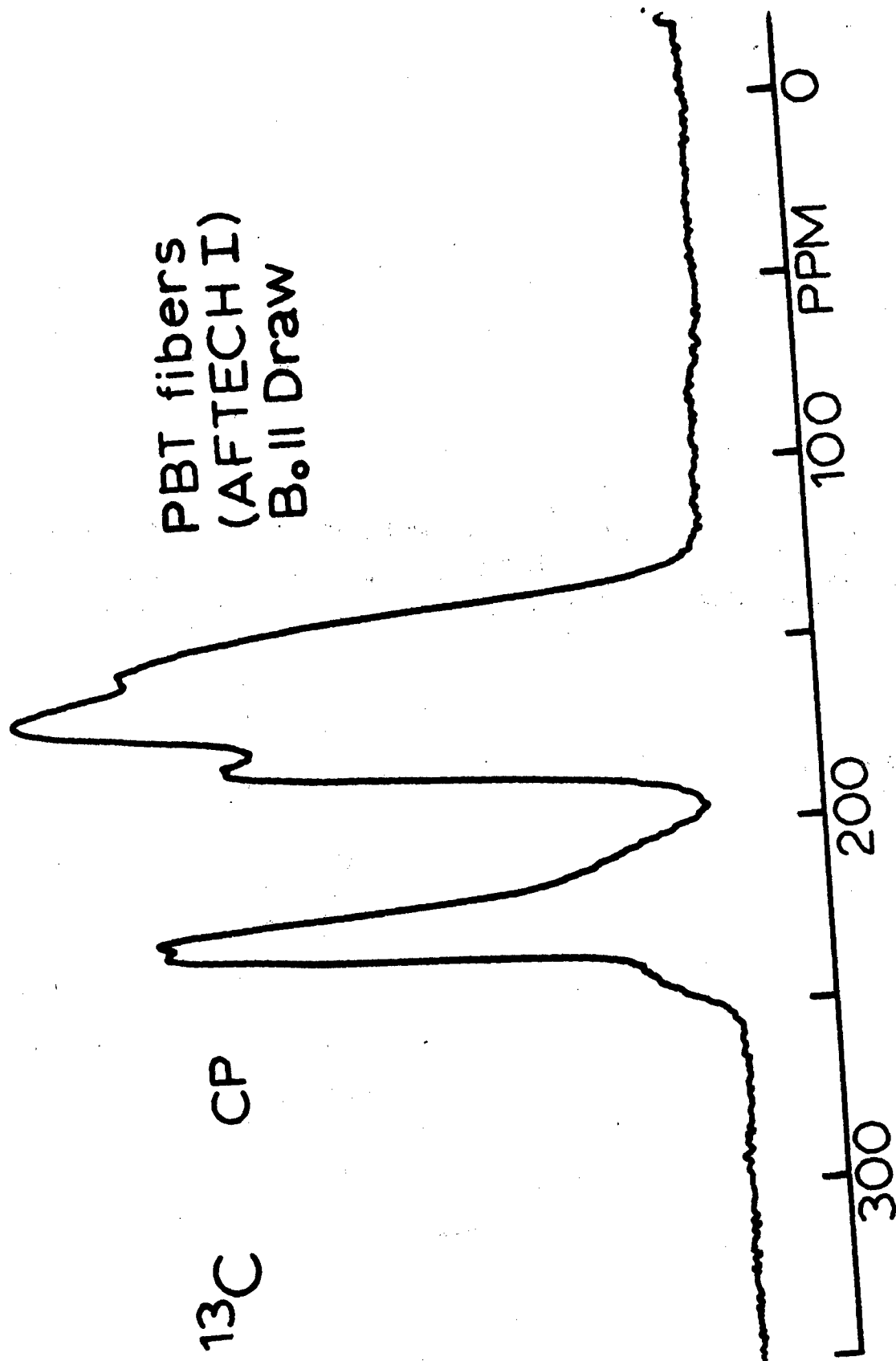


Figure 11

50 MHz ^{13}C CP spectrum of an oriented bundle of PBT fibers (Sample G). The CP time is 0.5 ms and 10,000 scans were taken. The strong PBT resonance at 230 ppm is not nearly as pronounced in the oriented ABPBI spectrum of Figure 10B and may provide a semiquantitative basis for separating PBT and ABPBI signals in highly oriented composite samples.

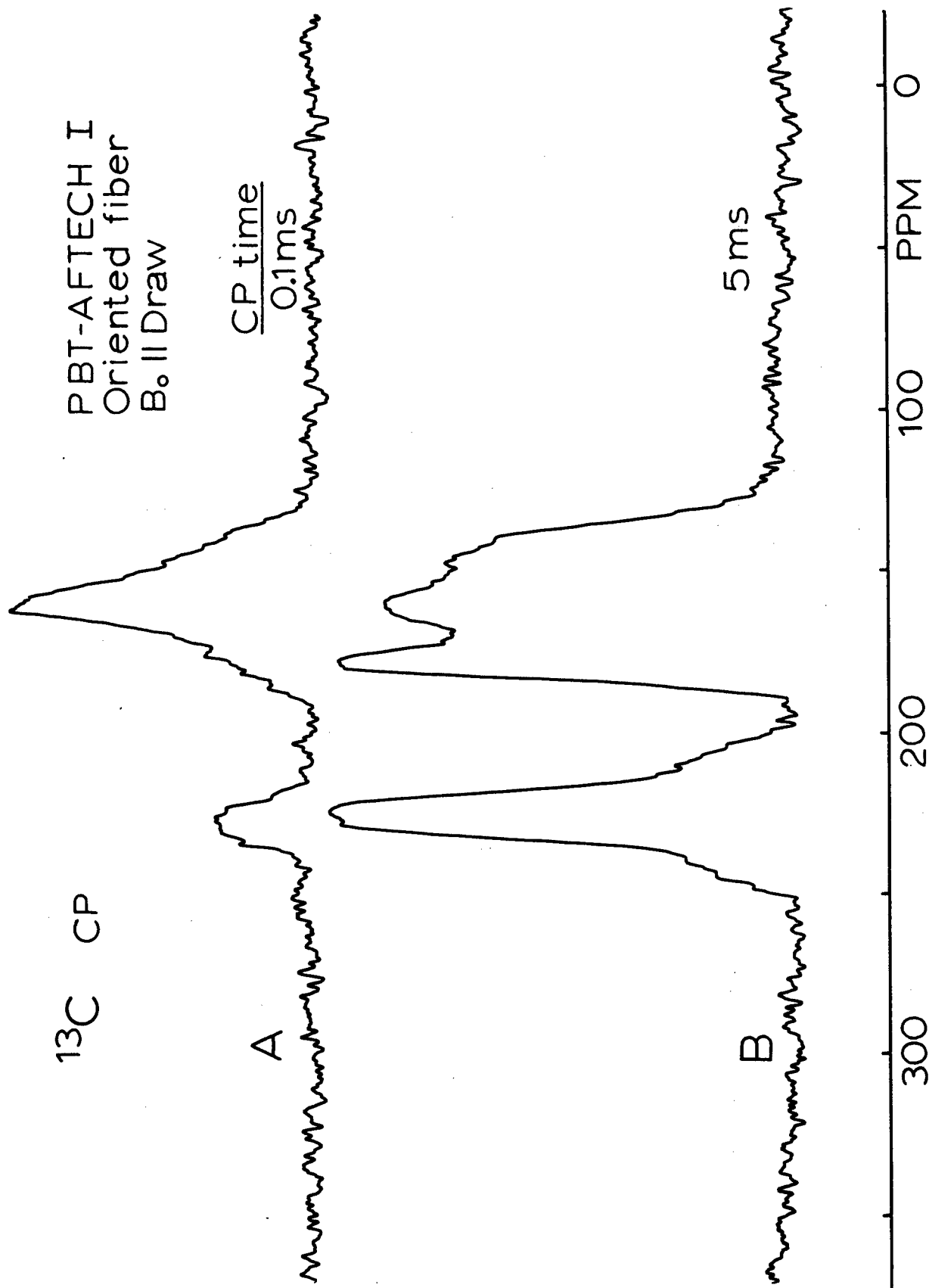


Figure 12

50 MHz ^{13}C CP spectra of an oriented bundle of PBT fibers (Sample G). The dependence of the lineshape on CP time illustrates the differential polarization behavior of protonated and unprotonated carbons. The stronger peak near 160 ppm is very likely the protonated phenylene carbons of PBT.

^{13}C CP
Unoriented films

30% PBT /
70% ABPBI

A

60% PBT /
40% Nylon

B

300 200 100 0
PPM

Figure 13

50 MHz ^{13}C CP spectra of two unoriented composite films, Samples K and I: 30% PBT/70% ABPBI (A) and 60% PBT/40% nylon (B). Both spectra were taken with a 0.5 ms CP time. Note the lack of distinct resonance features in (A) since the chemical shift anisotropy profiles of aromatic carbons are quite similar. In contrast the much narrower shift anisotropy patterns of aliphatic carbons render the aliphatic nylon resonances in (B) quite distinct from the PBT resonances.

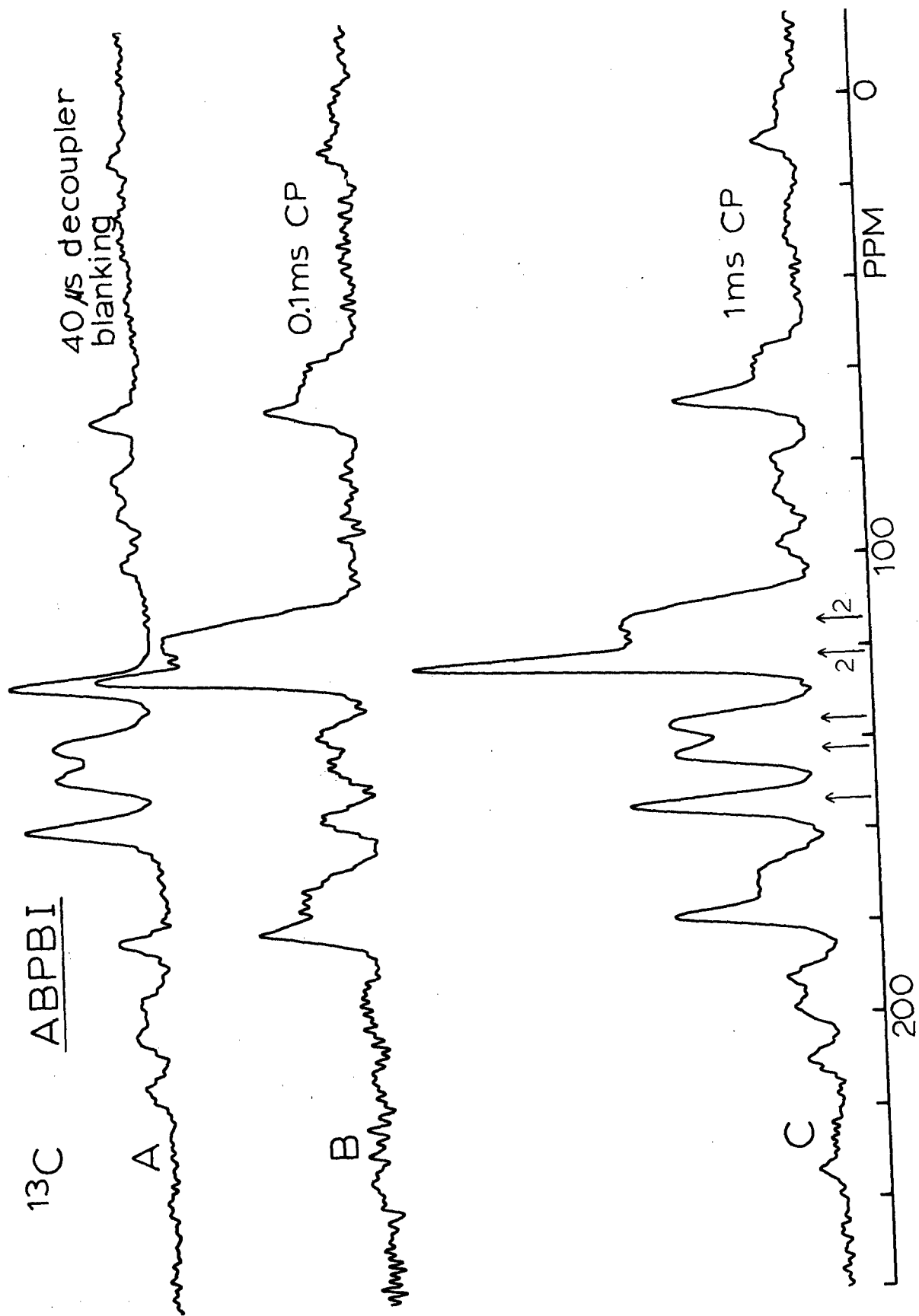


Figure 14

Different 50 MHz ^{13}C CP-MAS spectra of the ABPBI film (Sample K prior to the 2X stretching). In spectrum A, the decoupler was turned off for 40 μs prior to sample observation with decoupling. This preparation causes the protonated carbon resonances to vanish. Spectrum B employs a 0.1 ms CP time so as to enhance the protonated carbon resonances with respect to those that are unprotonated. Spectrum C is taken with a more typical 1ms CP time so that both the protonated and non-protonated resonances have comparable intensities. Arrows point to the positions of centerbands and the arrows with the number '2' indicate that two carbons contribute. The two carbons at highest field plus one of the carbons at 121 ppm are protonated. All other resonances are spinning sidebands of the central resonances. The spinning frequency was 2.75 kHz.

^{13}C CP-MAS
15 MHz

AFTECH I
fibers
(PBT)

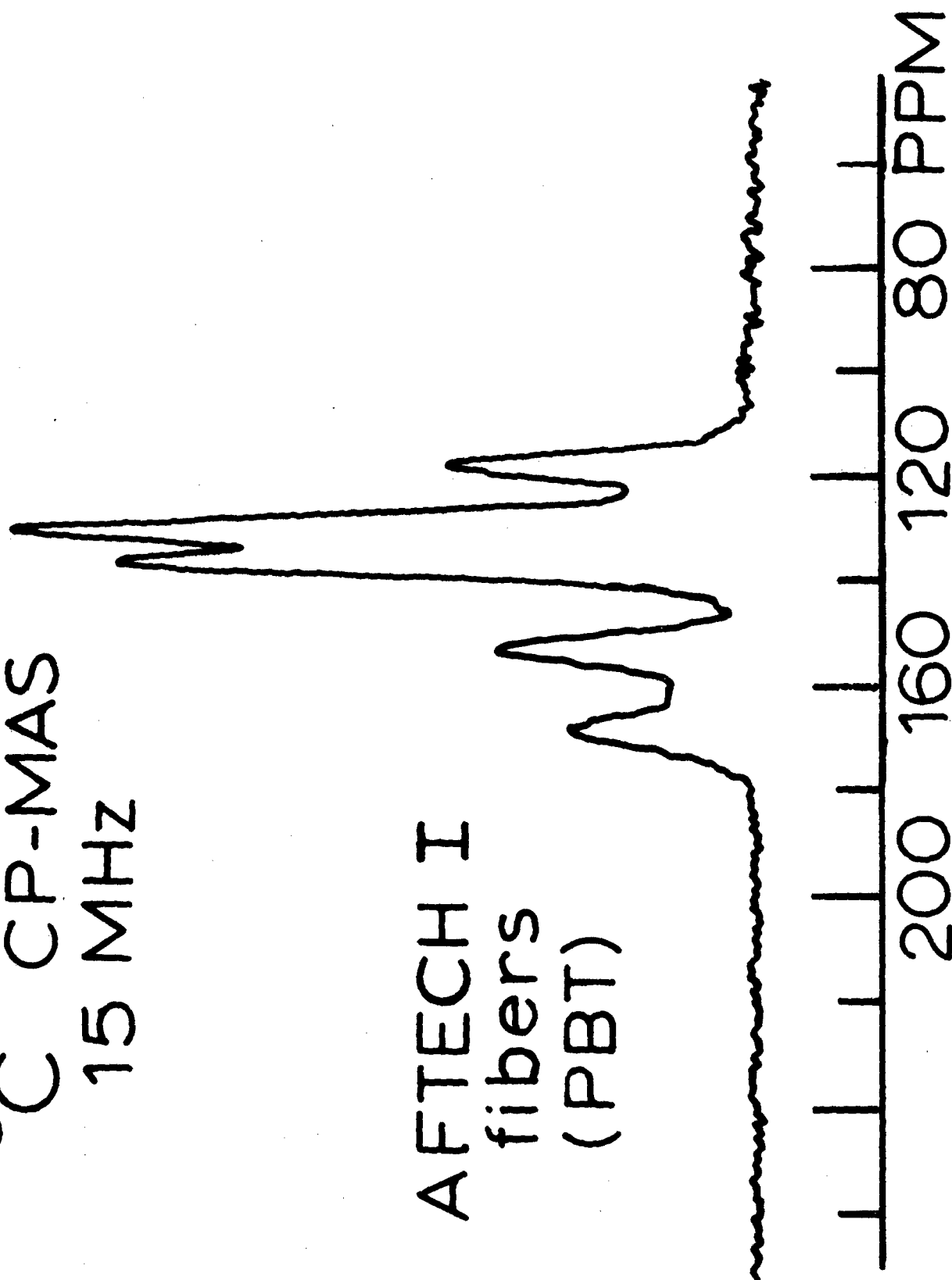


Figure 15

15 MHz CP-MAS spectrum of PBT fibers (Sample G). Note that spinning sidebands are virtually absent at a 2.2 kHz spinning frequency. Five of the seven inequivalent carbons are resolved; the three protonated carbons occupy the two highest field resonances as determined by experiments similar to those in Figure 14.

^{13}C CP-MAS

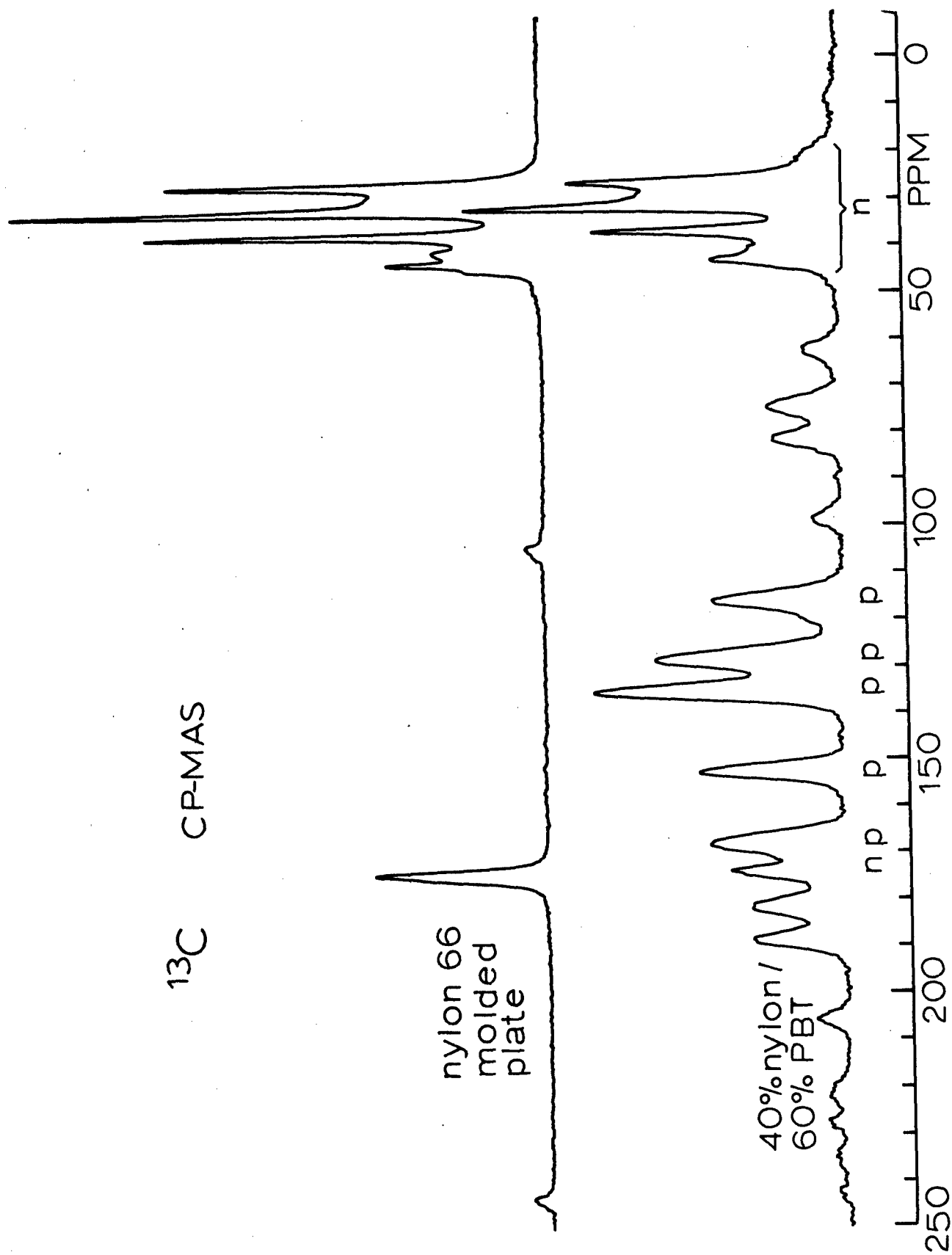


Figure 16

50 MHz ^{13}C CP-MAS spectra of Samples M (upper) and I (lower). In the latter spectrum, the centerband resonances are denoted by n (nylon) and p (PBT). Note the larger proportion of the sharp-line (crystalline) component in the aliphatic nylon region (20-50 ppm) of Sample M compared with Sample I. These spectra show that the composite contains nylon crystalline regions; however, the crystallinity is lower than it would be in a molded plate of the nylon homopolymer.

PBT/ABPBI
30 / 70

1ms CPT

$T_{1\rho}^H$

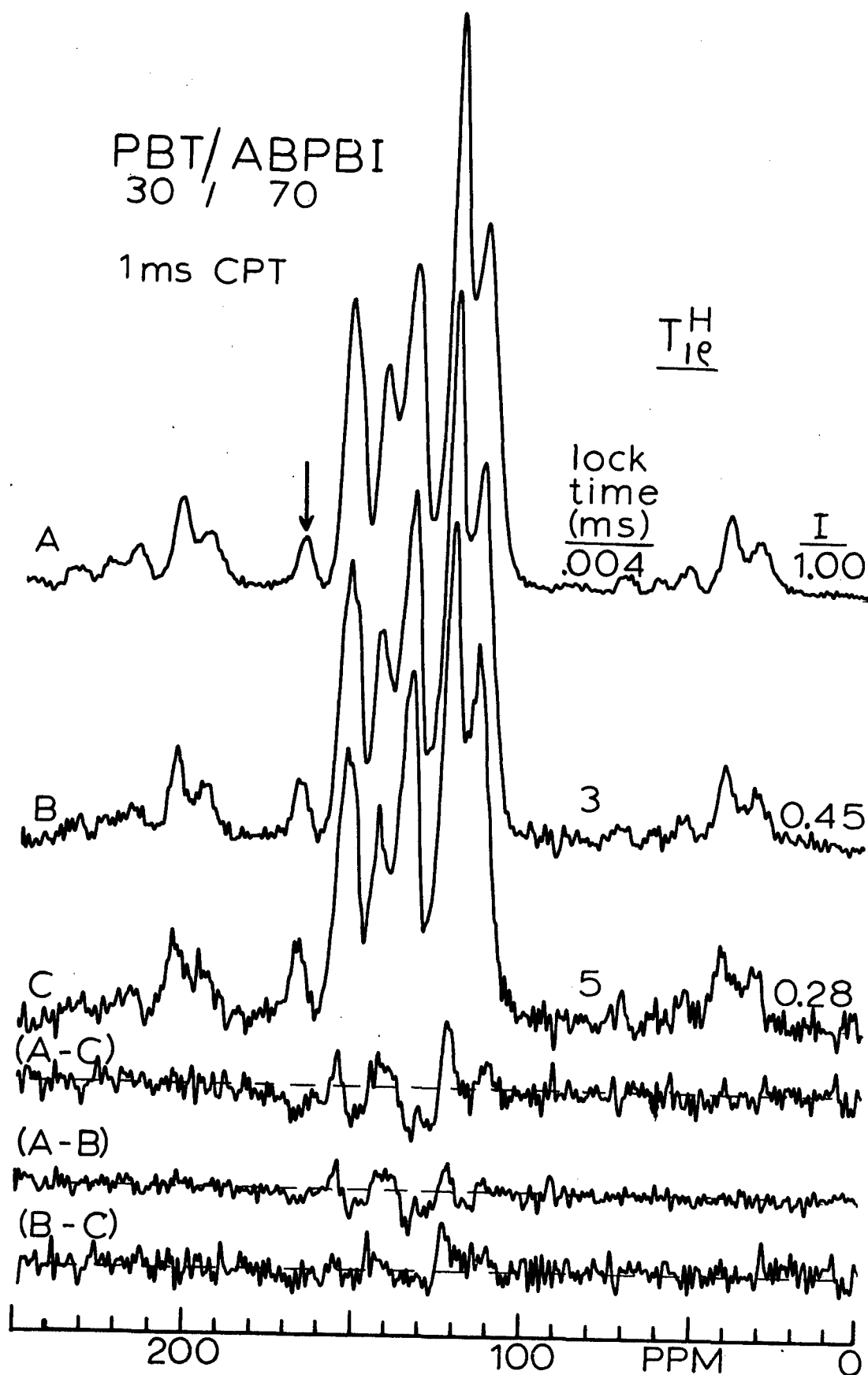


Figure 17

50 MHz ^{13}C CP-MAS spectra and difference spectra of Sample J as a function of proton spin-locking time, prior to a 1 ms CP period. The arrow points to the single (PBT) resonance which is completely resolvable. Even though the total signal is diminishing according to the total integral, I, given on the right, spectra A,B and C are normalized to the same total intensity for lineshape comparison. At longer spin locking times the PBT resonance gains strength over the ABPBI resonance, thereby indicating a slightly longer $T_{1\rho}^H$ for PBT. The inequality of the $T_{1\rho}^H$'s suggests that this sample does not strictly represent a molecular composite.

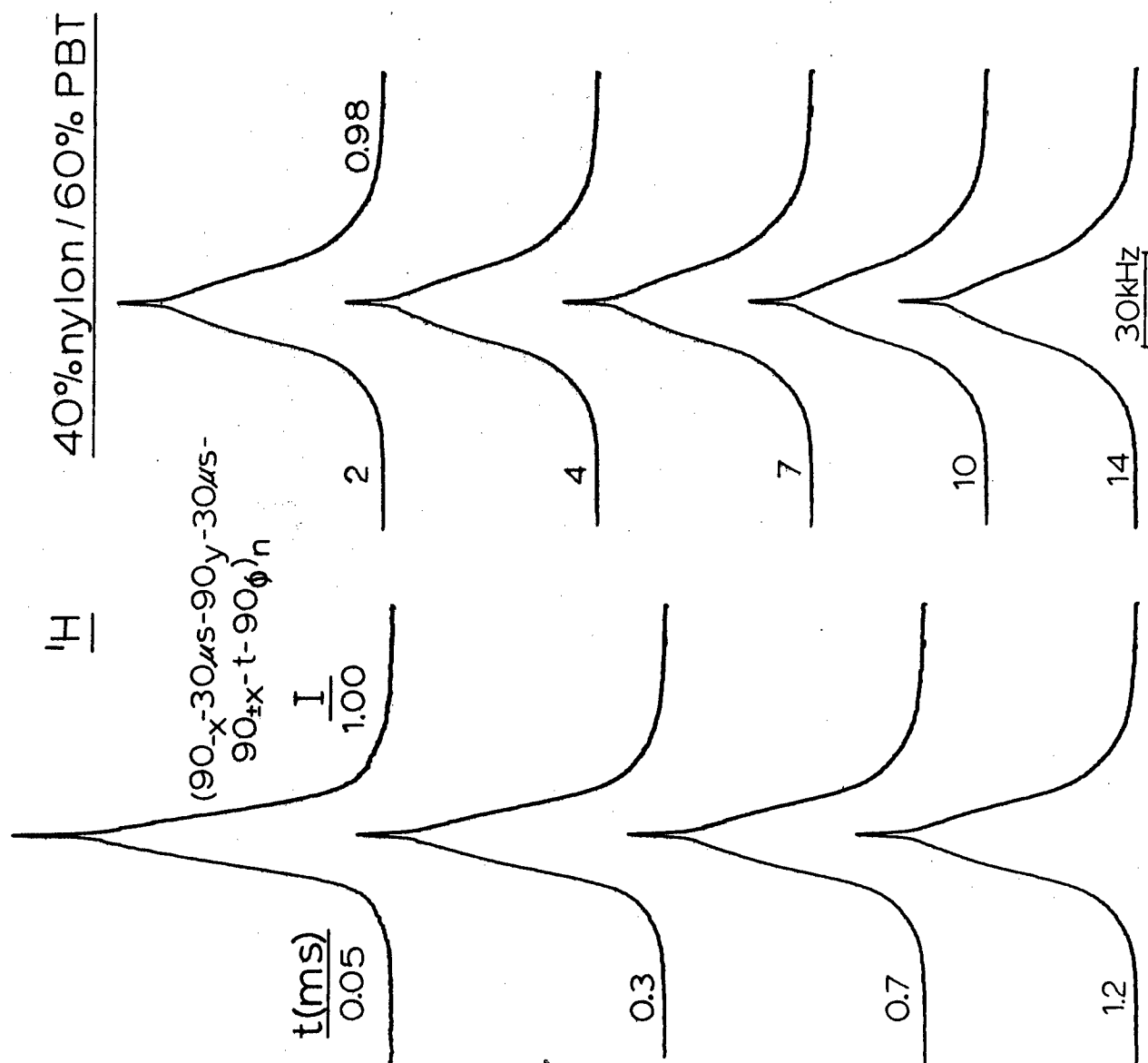


Figure 18

200 MHz proton spectra of Sample I as a function of t in the spin diffusion pulse sequence given. The dipolar echo preparation selectively preserves PBT magnetization because of weaker average dipolar couplings. As spin diffusion progresses (longer t values) the lineshape returns to a shape close to its equilibrium (M_0) shape, as judged by the final difference spectrum. The slight decay of the total magnetization, I , is indicated for some of the t values; this decay gives a measure of the interference from T_1^H processes. The growth of the nylon signal is evidenced by the growth of the broader skirts of the lineshape at longer times.

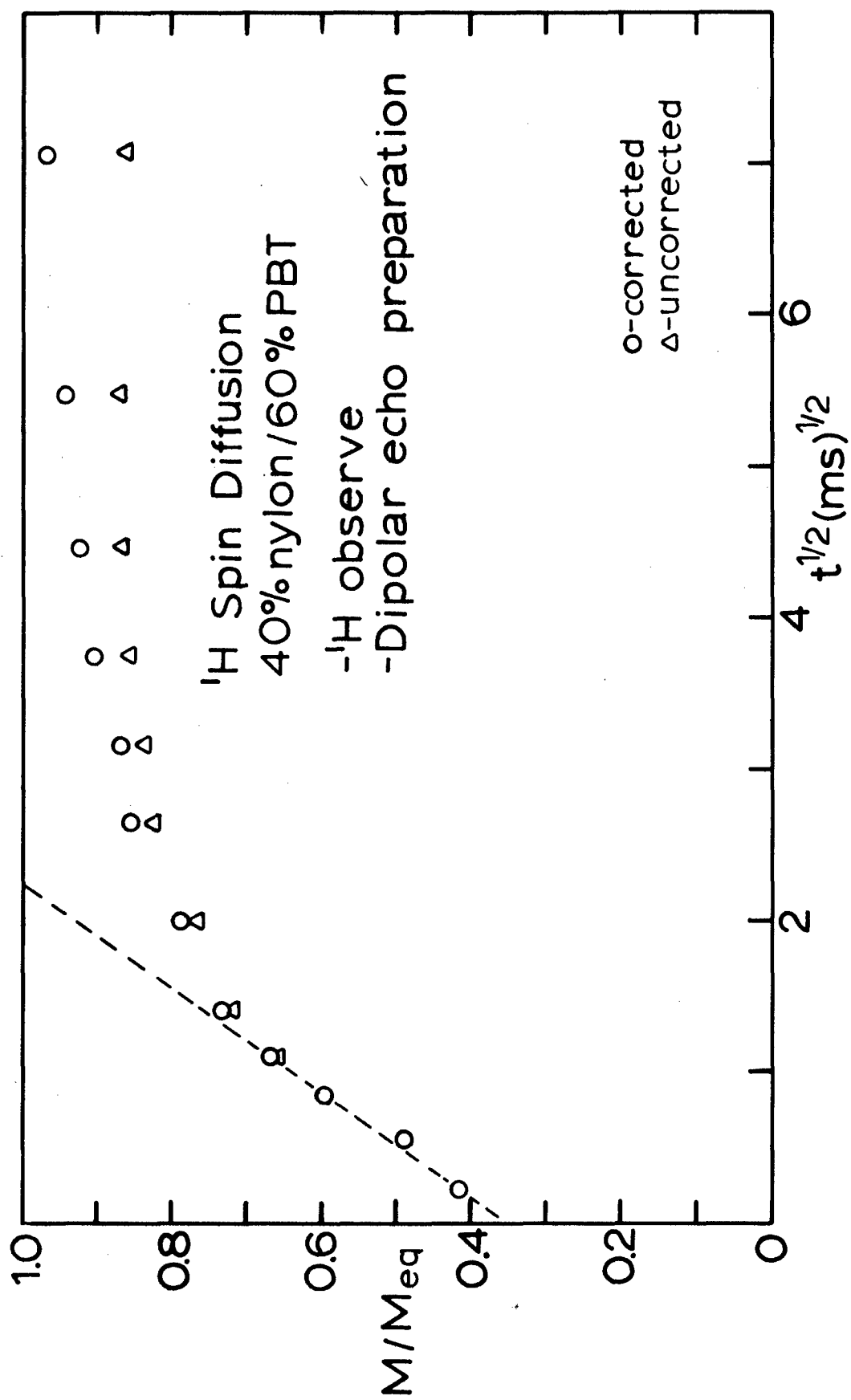


Figure 19

Growth of the nylon component magnetization from the data in Figure 18. Lineshape decomposition was based on a spectral component having the shape of the nylon 66 homopolymer, Sample M. The triangles are the uncorrected data based on the initial total proton magnetization at $t=0.05$ ms. The circles are corrected data derived from the uncorrected data by dividing by the total lineshape integral at that value of t . The dashed line defines the initial slope.

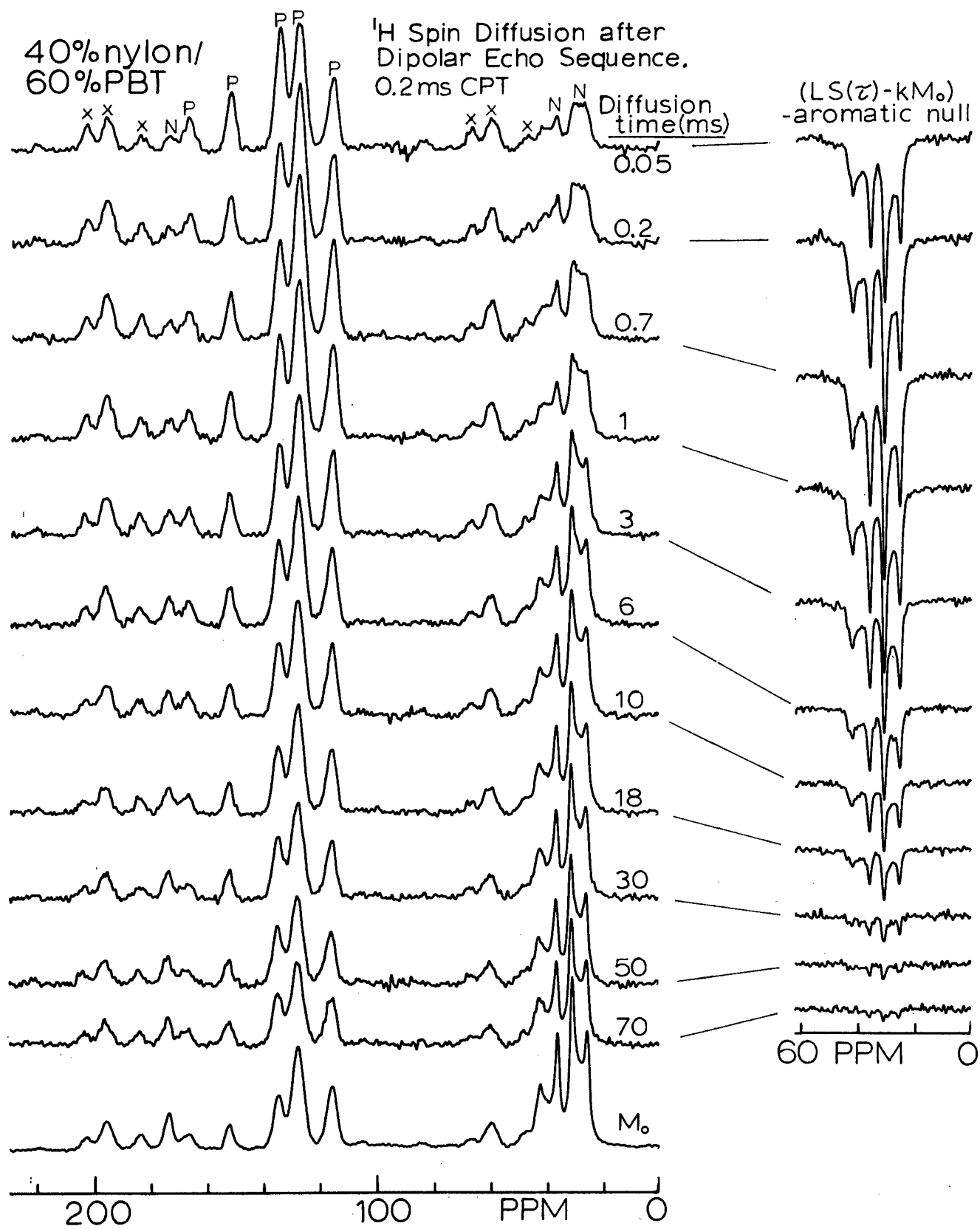


Figure 20

50 MHz ^{13}C CP-MAS spectra as a function of the proton spin diffusion time. The pulse sequence is discussed in the text. The spectra are taken with a relatively short (0.2 ms) CP time following both magnetization gradient preparation and a proton spin diffusion time. Centerband resonances for nylon (N) and PBT (P) are labelled; spinning sidebands are indicated by an 'X'. The PBT spectra are somewhat distorted as a result of the more complete CP of the protonated carbons relative to the unprotonated carbons. Transfer of proton magnetization from the PBT to the nylon protons is reflected in the growth of the nylon and the reduction of the PBT resonances. For a conserved proton magnetization during spin diffusion, nylon ^{13}C signals grow more slowly than PBT ^{13}C signals decay. The equilibrium (M_0) spectrum is also taken with a 0.2ms CP time. In the right hand column difference spectra of the aliphatic nylon region are displayed. These difference spectra result from scaling the M_0 spectrum to match the amplitude of the protonated aromatic resonances of PBT at each value of the diffusion time. Thus, these difference spectra give a qualitative measure of the approach to proton spin equilibrium.

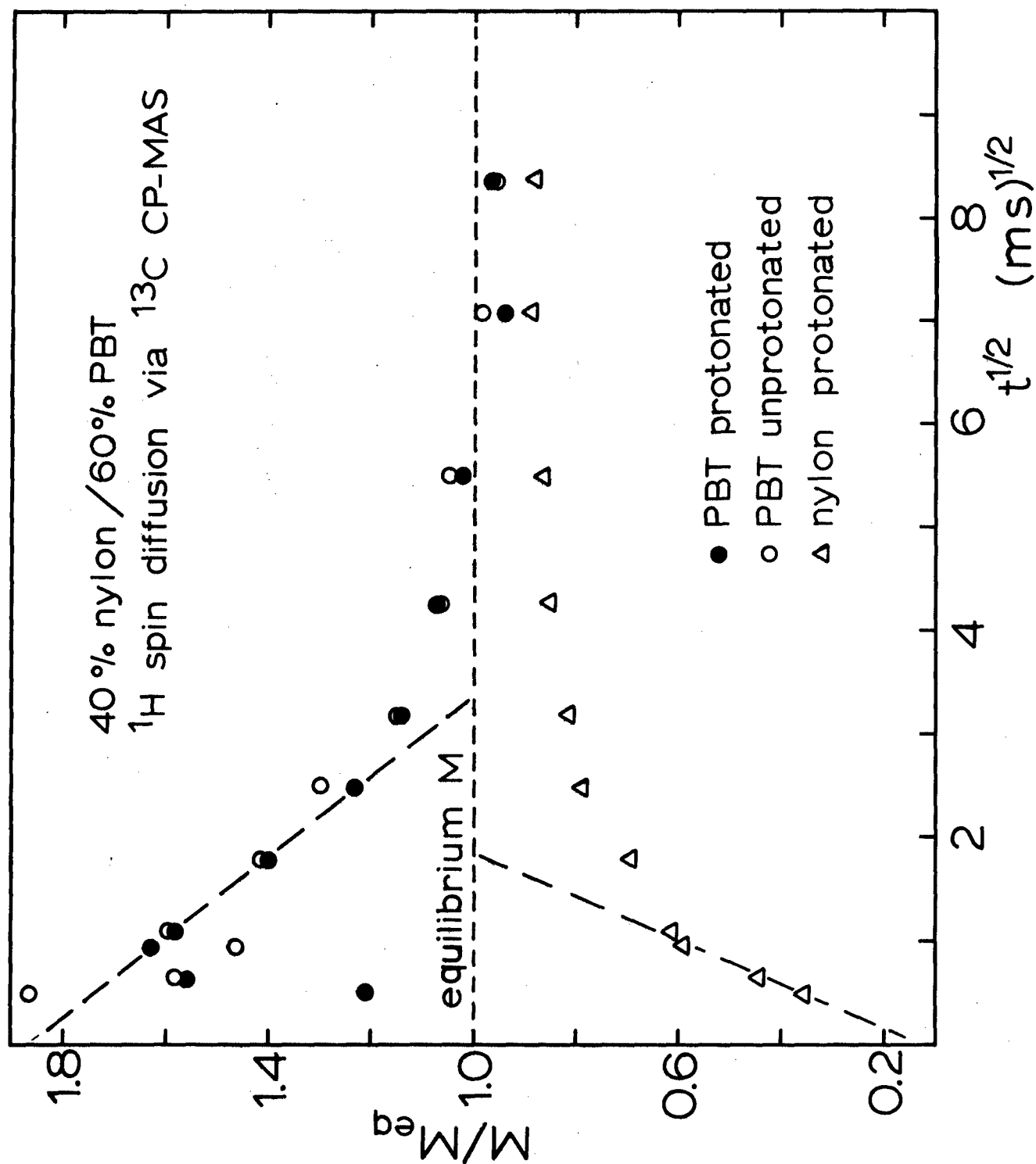


Figure 21

Plots of the relative growth of nylon magnetization and the decay of PBT magnetization as a function of the square root of the diffusion time, t , for the Spectra of Sample I in Figure 20. The correspondence between carbons and the different curves is indicated in the figure. Data have been corrected for T_1^H effects (see Figure 19). Note the anomalous behavior of the protonated PBT intensity at early times. The dashed curves give the linear-shapes at early time. If the CP intensities were true monitors of the proton polarization, then these dashed curves ought to intersect the equilibrium line at the same place. The fact that they do not exposes the experimental biases discussed in the text. The two intersection points should, however, bracket the true intersection point.

¹³C SPIN DIFFUSION
40% nylon / 60% PBT

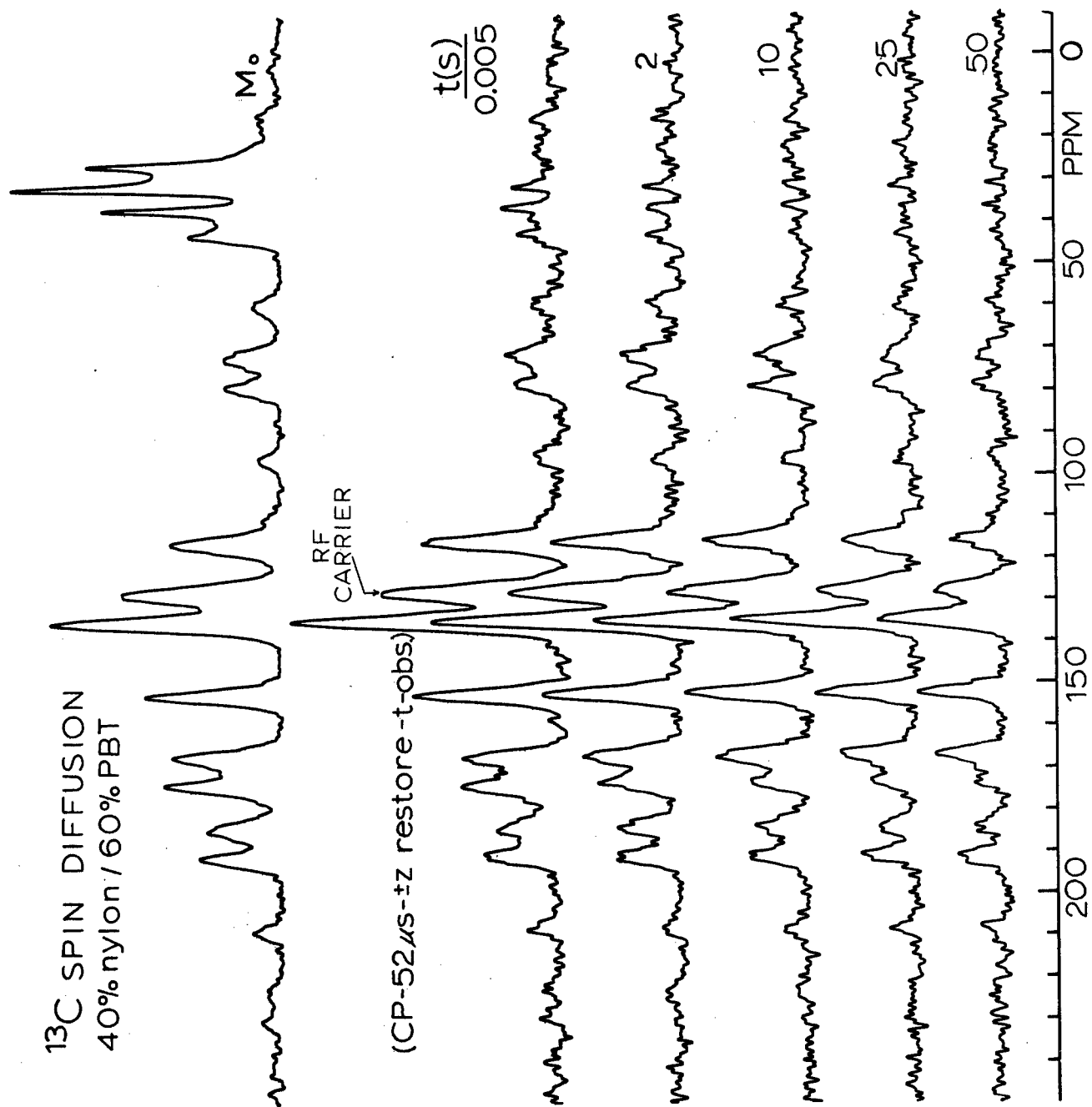


Figure 22

^{13}C CP-MAS spectra resulting from the unsuccessful attempt to observe evidence of intimate mixing in Sample I using the relatively inefficient ^{13}C spin diffusion. The upper spectrum is the normal CP spectrum and is used for reference. The pulse sequence indicated utilizes ^{13}C rf phases orthogonal to the CP pulse for the $\pm z$ restore portion of the pulse sequence. This preserves magnetization along B_0 near the rf carrier. The 0.052 ms interval is chosen to null approximately the aliphatic nylon resonances after the $\pm z$ restore pulses. The proton decoupler is turned off during t as well as the waiting time between experiments. Observation is accomplished with a simple ^{13}C 90° pulse with decoupling. The absence of nylon signal growth in spite of strong PBT signals indicates that ^{13}C Spin diffusion is not observable between the nylon and PBT. That nylon and PBT are therefore phase separated into large domains does not automatically follow (see Figure 23).

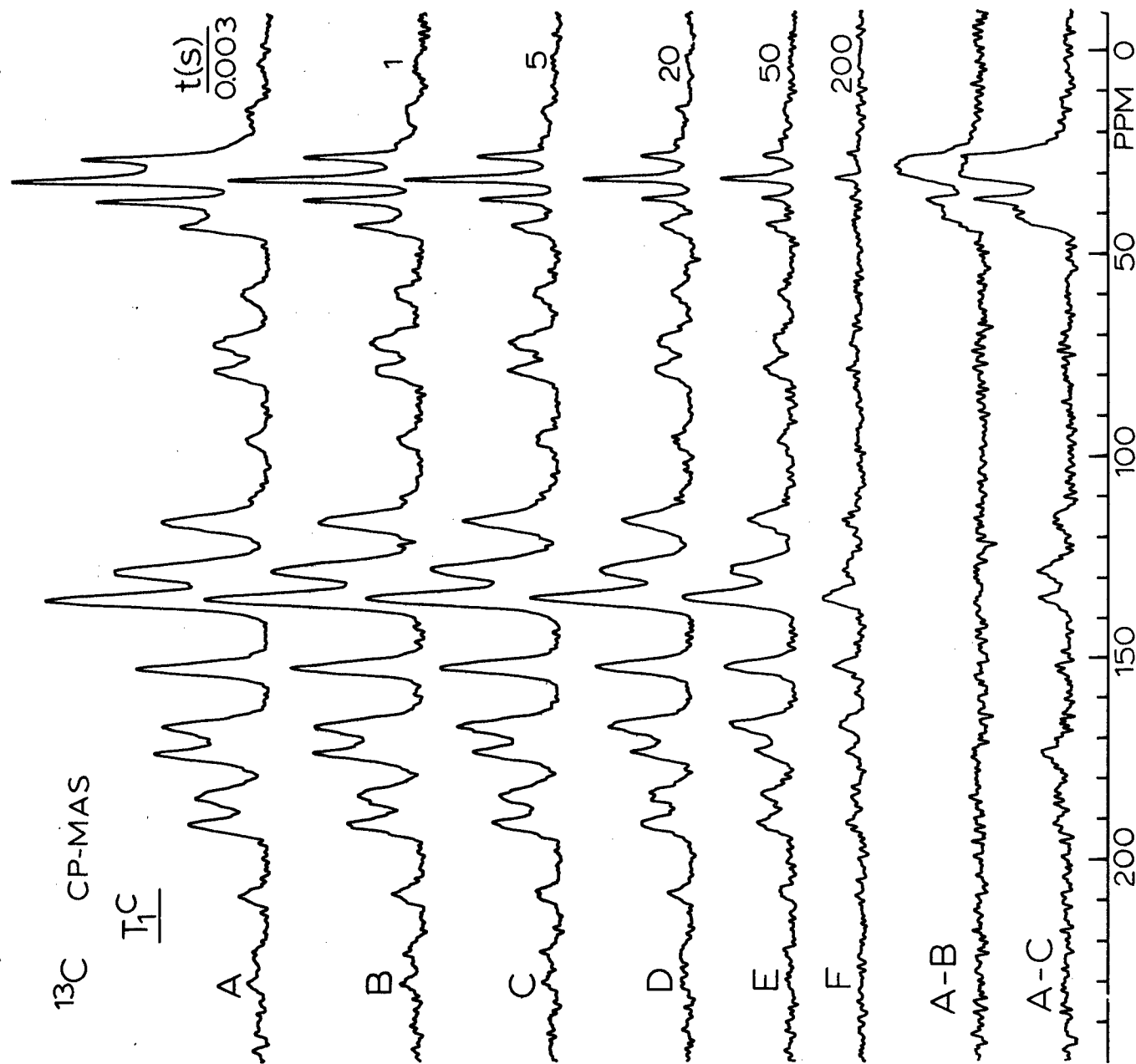
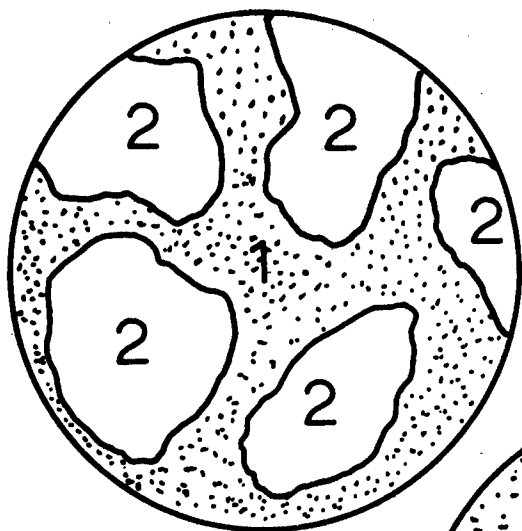
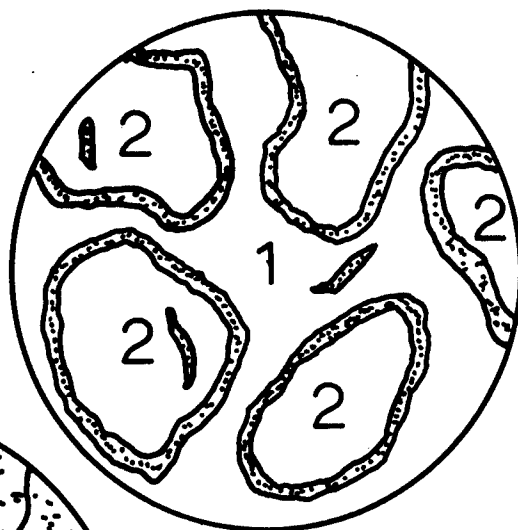


Figure 23

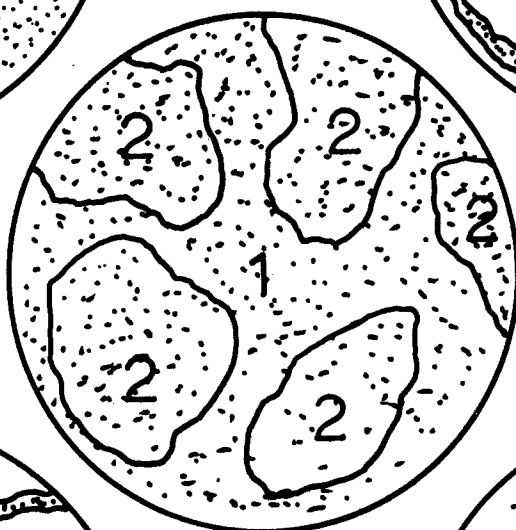
50 MHz ^{13}C spectra and difference spectra of Sample G for various delay times t in a $T_1\rho$ experiment following the method of Torchia et al (reference 29). The broader nylon aliphatic resonances lose most of their intensity in 1s (see the 'A-B' difference spectrum). the crystalline (sharper) nylon and the PBT resonances have $T_1\rho$'s of roughly 60s. The rapid relaxation of the non-crystalline nylon carbons prevents observation of any significant spin diffusion between nylon and PBT carbons in Figure 22.



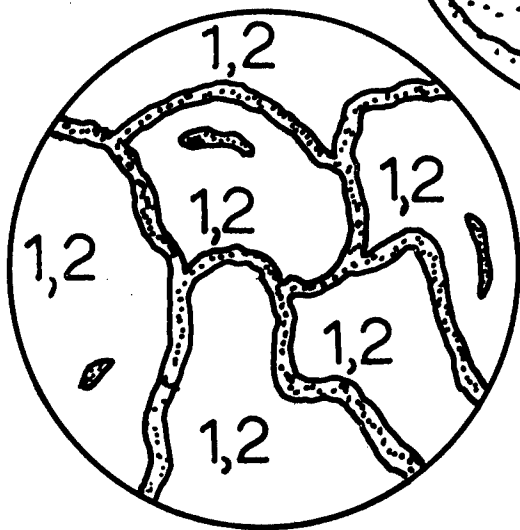
A



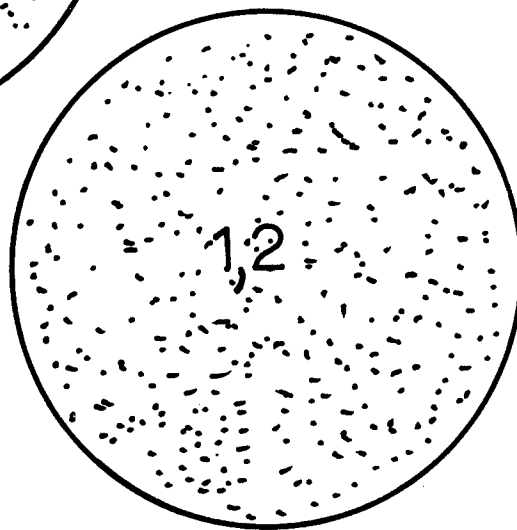
B



C



D



E

Figure 24

Idealized situations for distributing mobile protons, indicated by dots, in a polymer blend of homopolymers 1 and 2. Sketches A,B and C correspond to phase separated blends while D and E correspond to polymers intimately blended on a molecular scale. The sketches represent the following situations: A - mobile protons in polymer 1 only; B and D - mobile protons excluded into void or defect regions; C and E - mobile protons evenly distributed throughout the polymer phase(s).

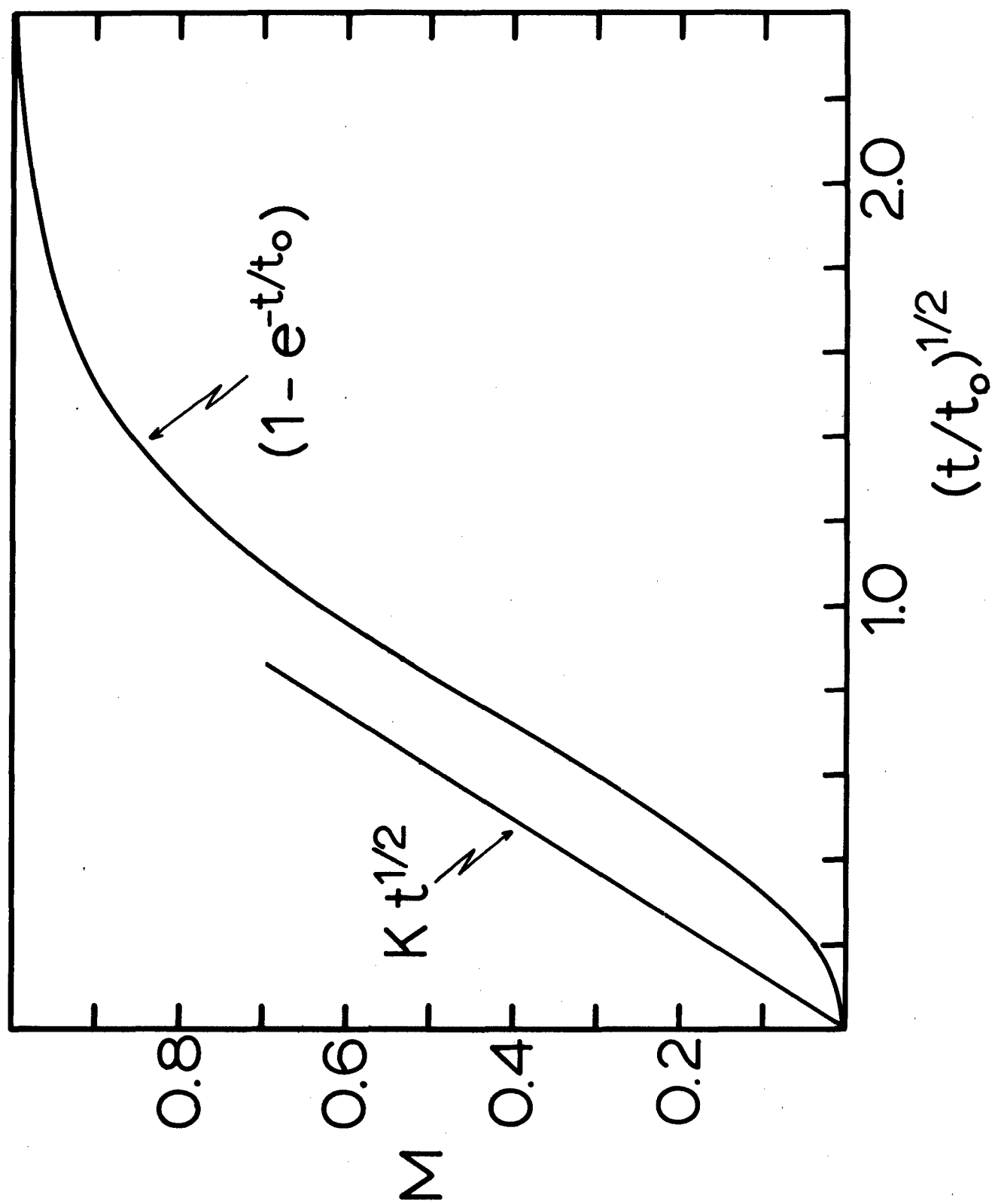


Figure 25

Expected growth rates for initially depleted polymer proton magnetization. It is assumed that at $t=0$ a mobile proton population also exists with finite polarization. Then if spin diffusion between the mobile and polymer protons is allowed to happen, an early growth proportional to the square root of t will characterize those cases like Figure 24 A,B and D whereas exponential growth, given by the second curve, will describe cases like Figure 24C and E. The fact that both curves have a rather large linear region in this plot makes it difficult to differentiate the two mechanisms unless one has very good data at early times.

¹H SPIN DIFFUSION
30%PBT / 70%ABPI (Sample L)

(Hahn echo-zz restore-t-obs)

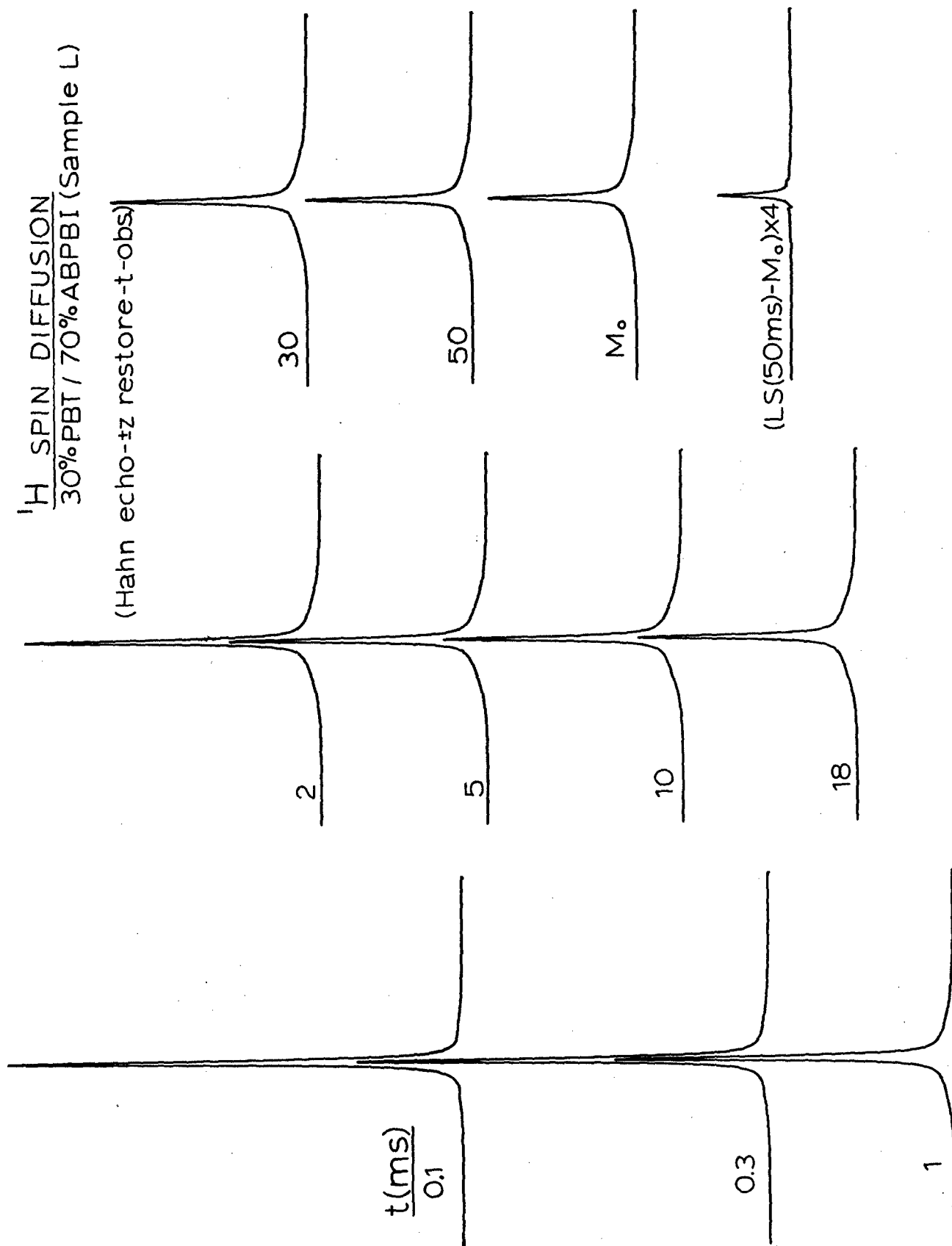


Figure 26

200 MHz proton lineshapes for the PBT/ABPBI composite, Sample L, which was coagulated from an MSA solution above the critical concentration for phase separation. This experiment monitors the proton spin diffusion between the mobile proton species and the broader polymer protons. The Hahn echo initially selecting the narrow component had a 50 μ s separation between pulses. Equilibration is not yet complete at 50 ms since this spectrum still has a detectable excess of the narrow component when compared to the M_0 spectrum and the final difference spectrum. Note the 4X amplification factor in the difference spectrum.

¹H SPIN DIFFUSION
30%PBT/70%ABPBI(Sample L)

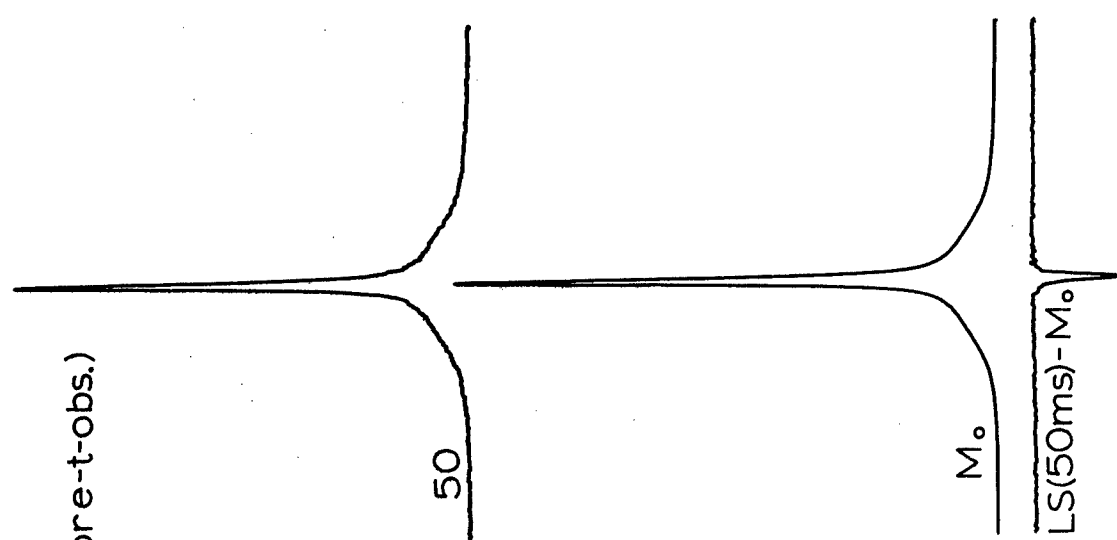
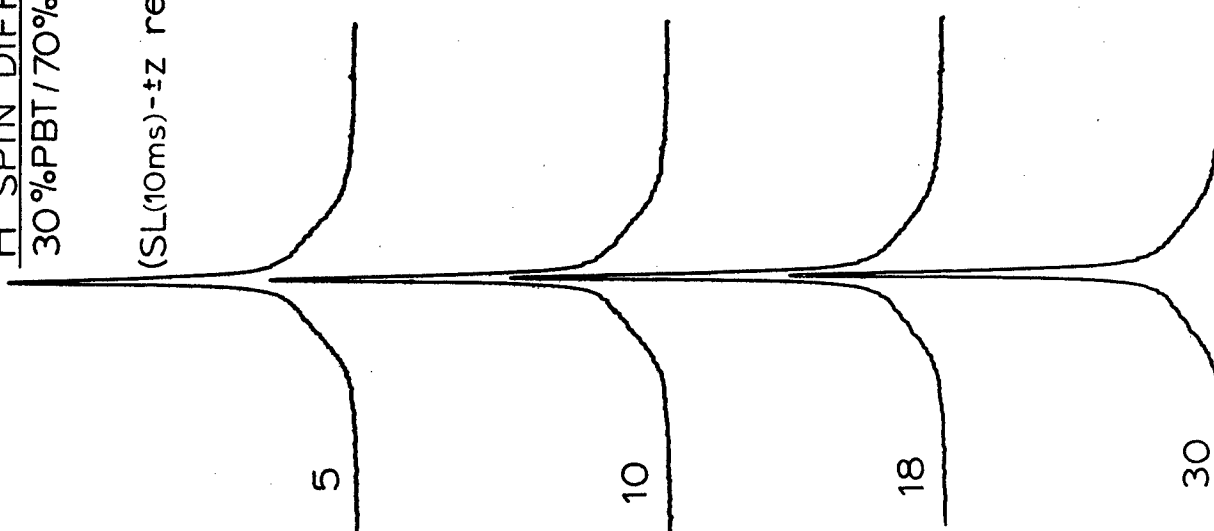
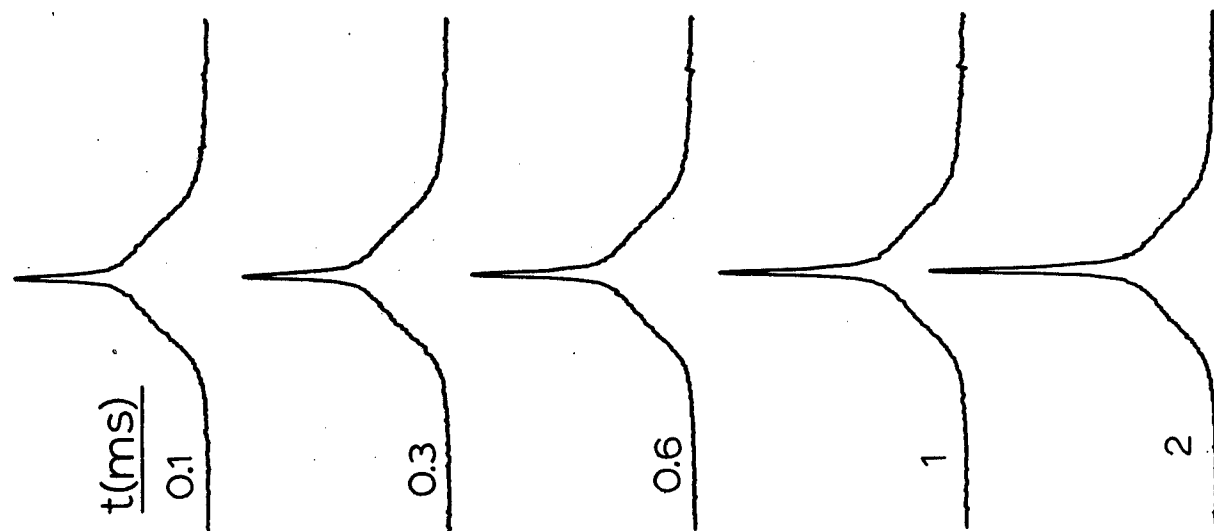


Figure 27

200 HMz proton lineshapes for a monitoring of proton spin diffusion in Sample L from the broader polymer protons to the mobile protons. The generation of the magnetization gradient by a 10 ms spin locking does not generate a sharp gradient as does the Hahn echo in Figure 26. Nevertheless, at 50ms, much of the equilibrium narrow proton of the line has been regenerated, see the final three spectra.

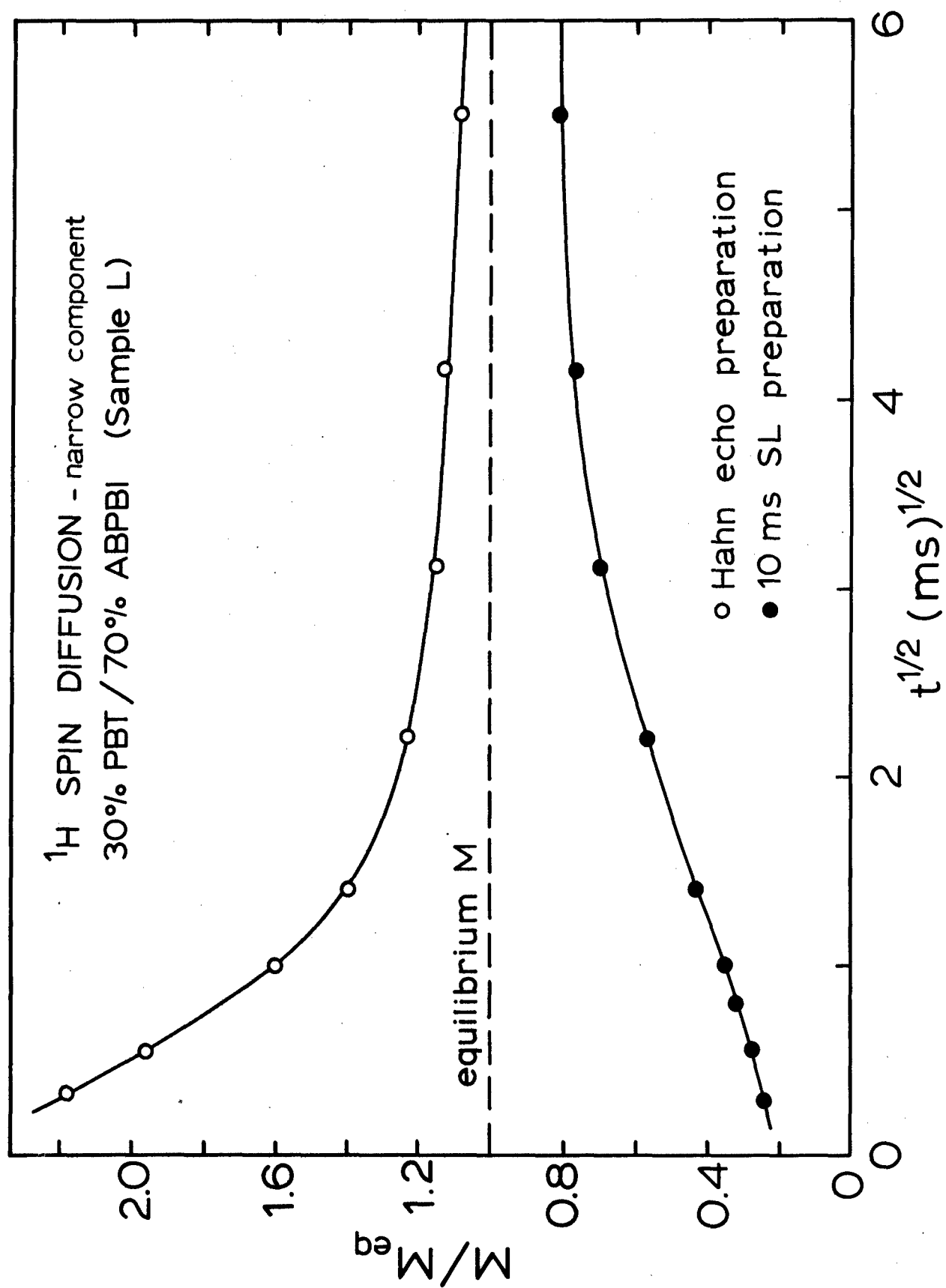


Figure 28

Plots of the behavior of the narrow-line intensity in Sample L according to the data of Figures 26 and 27. Data are corrected for T_1^H effects as described for Figure 19. The steeper slope of the decay of the top curve relative to the growth in the lower curve is partly a result of the fact that the spin lock preparation does not generate sharp magnetization gradients at $t=0$. The disparate differences from equilibrium of the two curves at 50 ms suggests that there may be a small component of magnetization in the spin lock preparation which resides in a larger domain. Certainly the uniform distribution of the mobile species (see Figures 24C and E) can be dismissed on the basis of these curves not being scaled mirror images of one another.

¹H SPIN DIFFUSION
30%PBT/70%ABPBI (Sample F)

(Hahn echo- τ z restore-t-obs.)

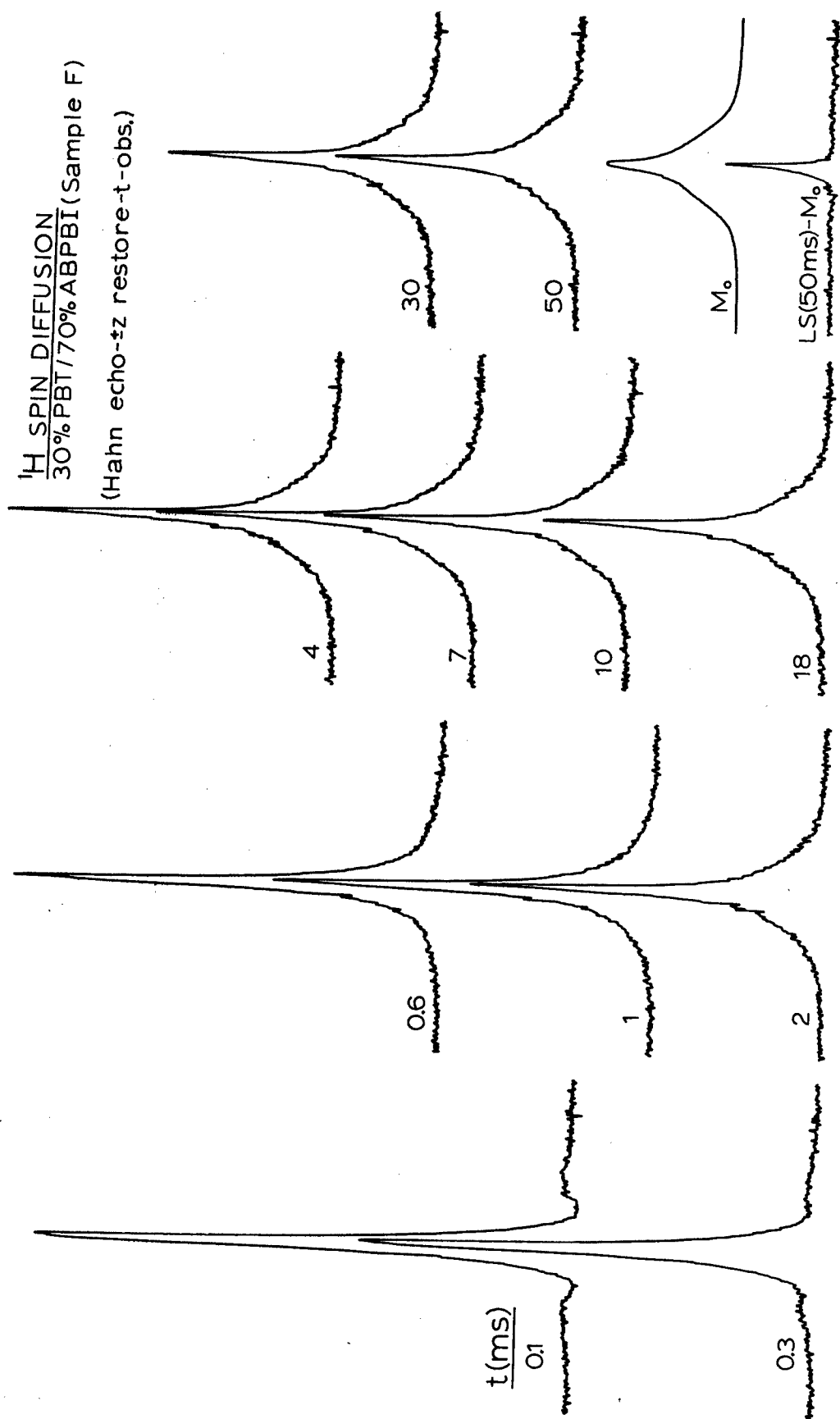


Figure 29

200 MHz proton spectra for the PBT/ABPBI composite, Sample F. The experiment is the same as that used in Figure 26 except the separation between pulses in the Hahn echo was 25 μ s. Note the preferential loss, by spin diffusion, of intensity on the downfield side of the narrow resonance. the upfield side of the narrow line is not well-coupled by spin diffusion to the polymer protons. the asymmetric base of the difference spectrum also indicates that equilibration of the downfield portion of the narrow line with the polymer protons is not complete after 50 ms.

^1H SPIN DIFFUSION

30%PBT/70%ABPBI(Sample F)

(SL(10ms)- \pm z restore-t-obs.)

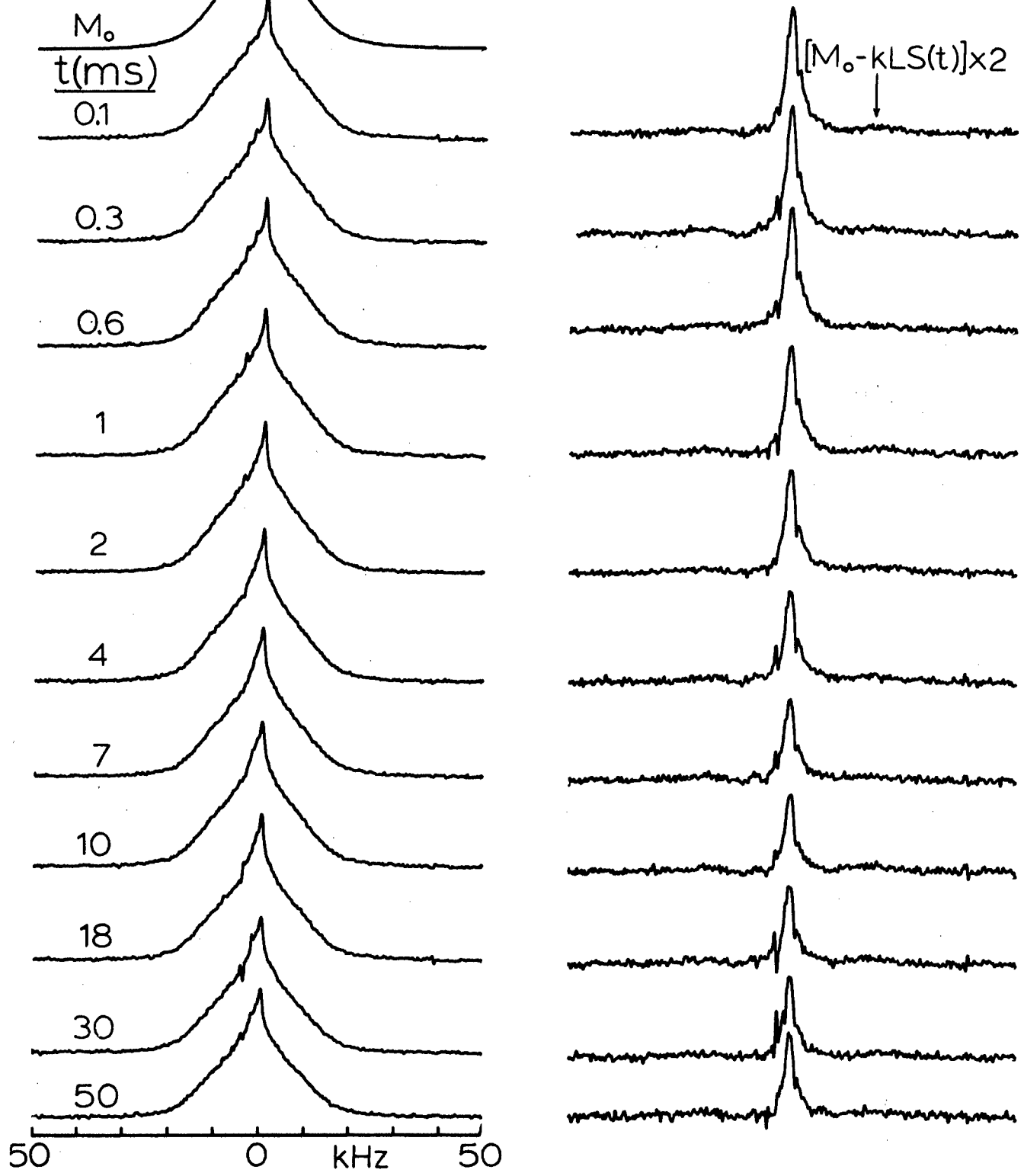


Figure 30

200 MHz proton, spectra for composite Sample F. This spin diffusion experiment is the same as that for Figure 27. There is only modest growth with t of the downfield portion of the narrow component (see the difference spectra on the right). This slow growth suggests that the 10ms preparation has enhanced magnetization from those regions which are relatively depleted of mobile protons. Moreover, the slow rise of this magnetization indicates that Sample F has larger domains, depleted of mobile protons, than does Sample L.

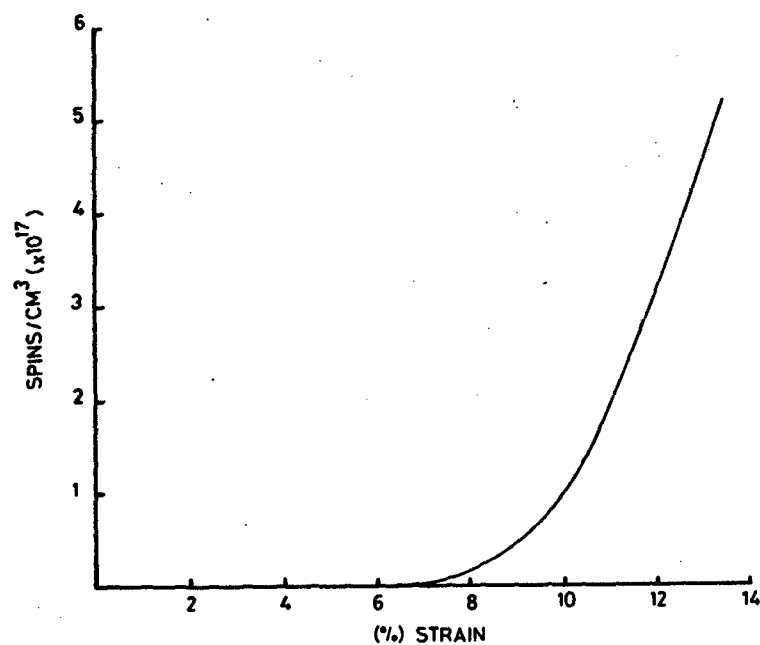


Figure 31

Generation of free radicals in nylon-6 fibers as a function of strain. Reproduced from reference 8.

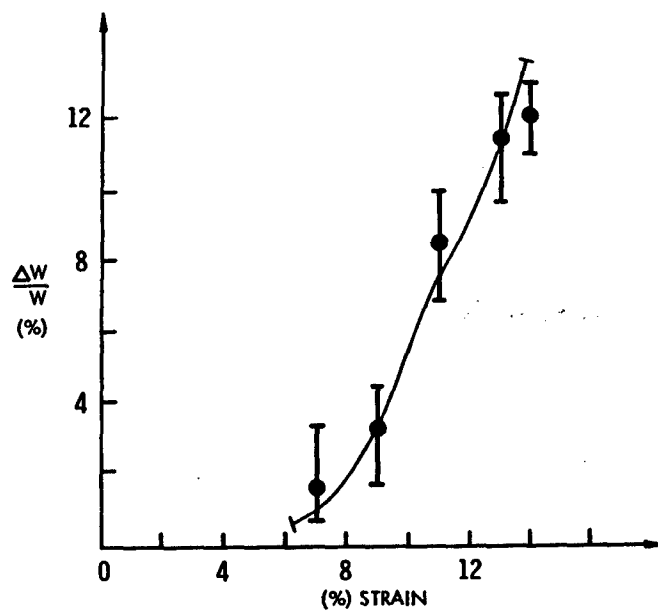
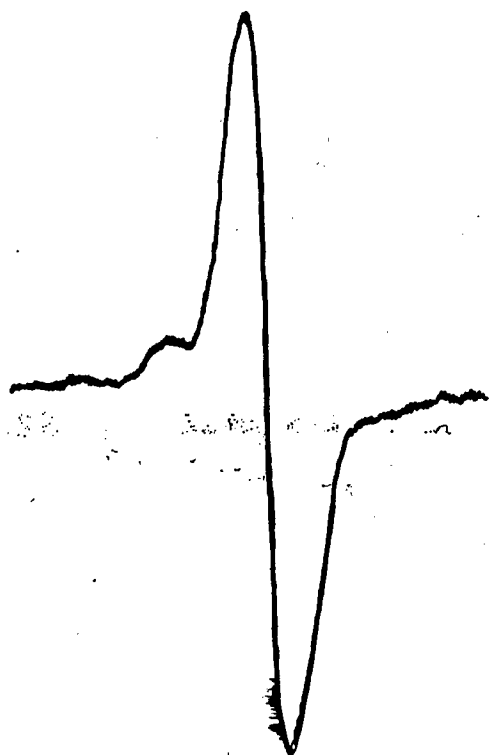


Figure 32

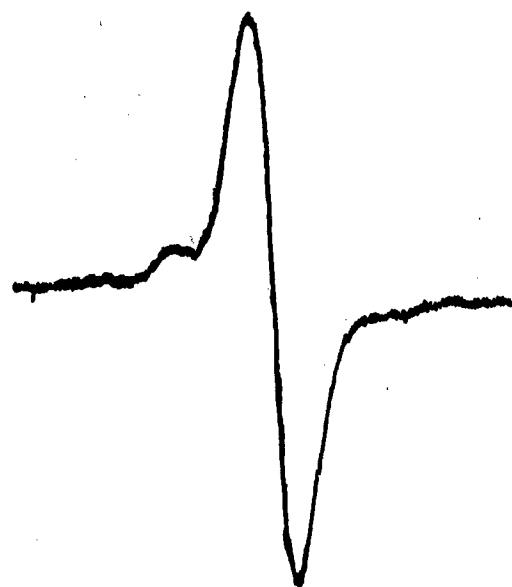
Change in molecular weight versus strain for nylon-6 fibers.
Reproduced from reference 8.

ELECTRON SPIN RESONANCE

AFTECH 1



AS RECEIVED



HEAT TREATED

1 hr @ 150C
1.5 hr @ 180C
16 hr @ 205C

Figure 33a

Electron spin resonance spectrum of AFTECH 1 fibers before and after thermal treatment.

ELECTRON SPIN RESONANCE

AFTECH 1

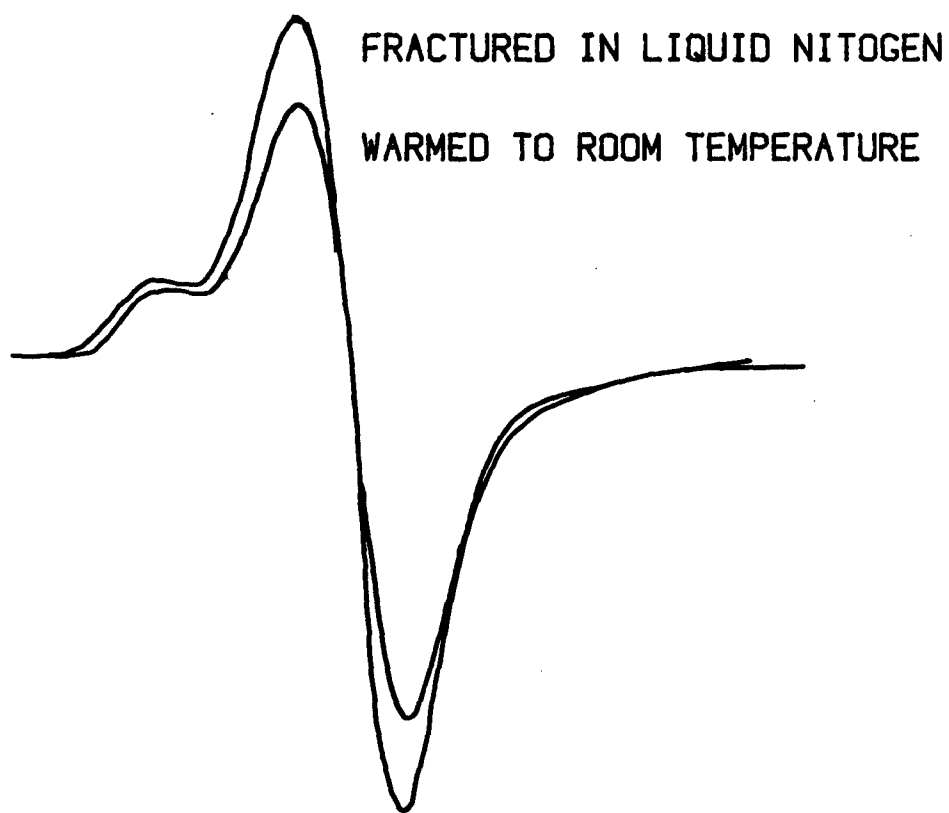
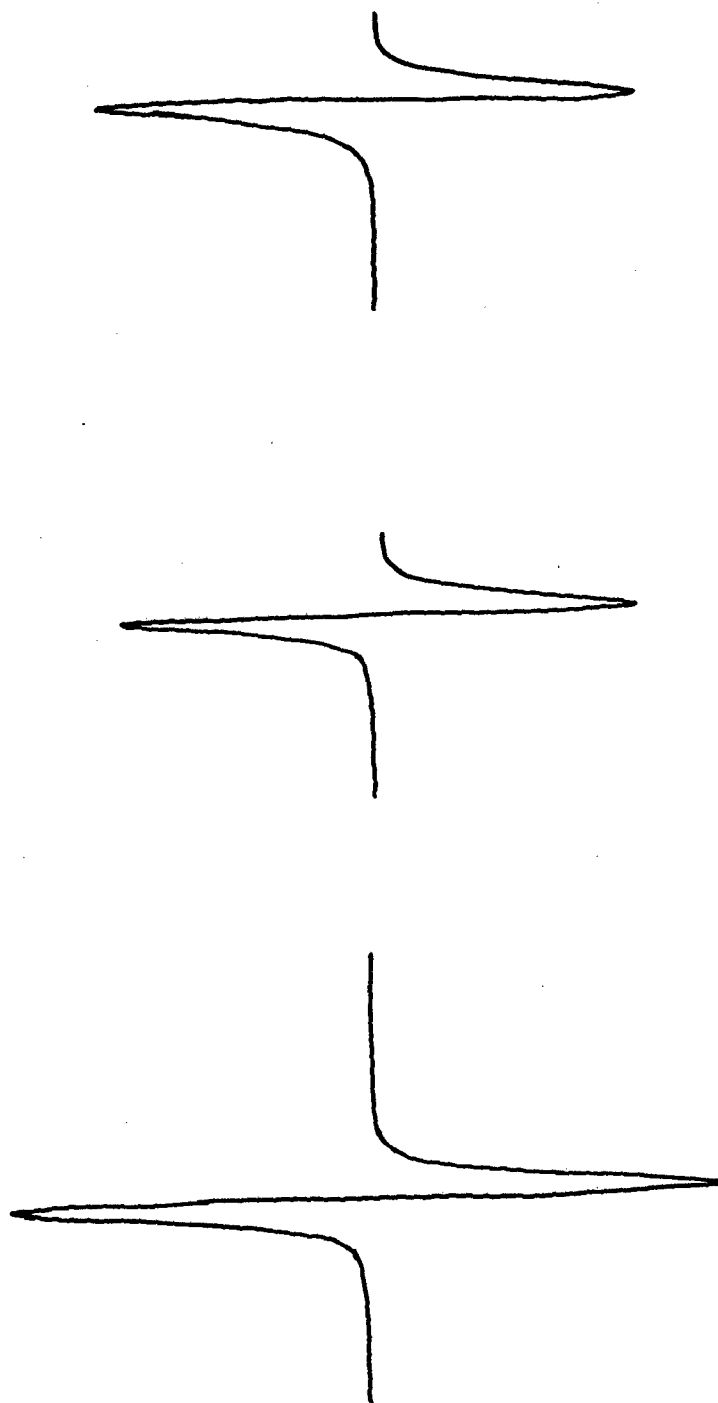


Figure 33b

Electron spin resonance spectra of AFTECH 1 fiber fractured by crushing under liquid nitrogen, and subsequently warmed to room temperature.

ELECTRON SPIN RESONANCE

AFTECH 2



AS RECEIVED

HEAT TREATED
1 hr @ 150C
1.5 hr @ 180C
16 hr @ 205

PULLED TO RUPTURE

Figure 34a

Electron spin resonance spectrum of AFTECH 2 fibers before and after thermal treatment and pulled to rupture subsequent to thermal treatment.

ELECTRON SPIN RESONANCE

AFTECH 2

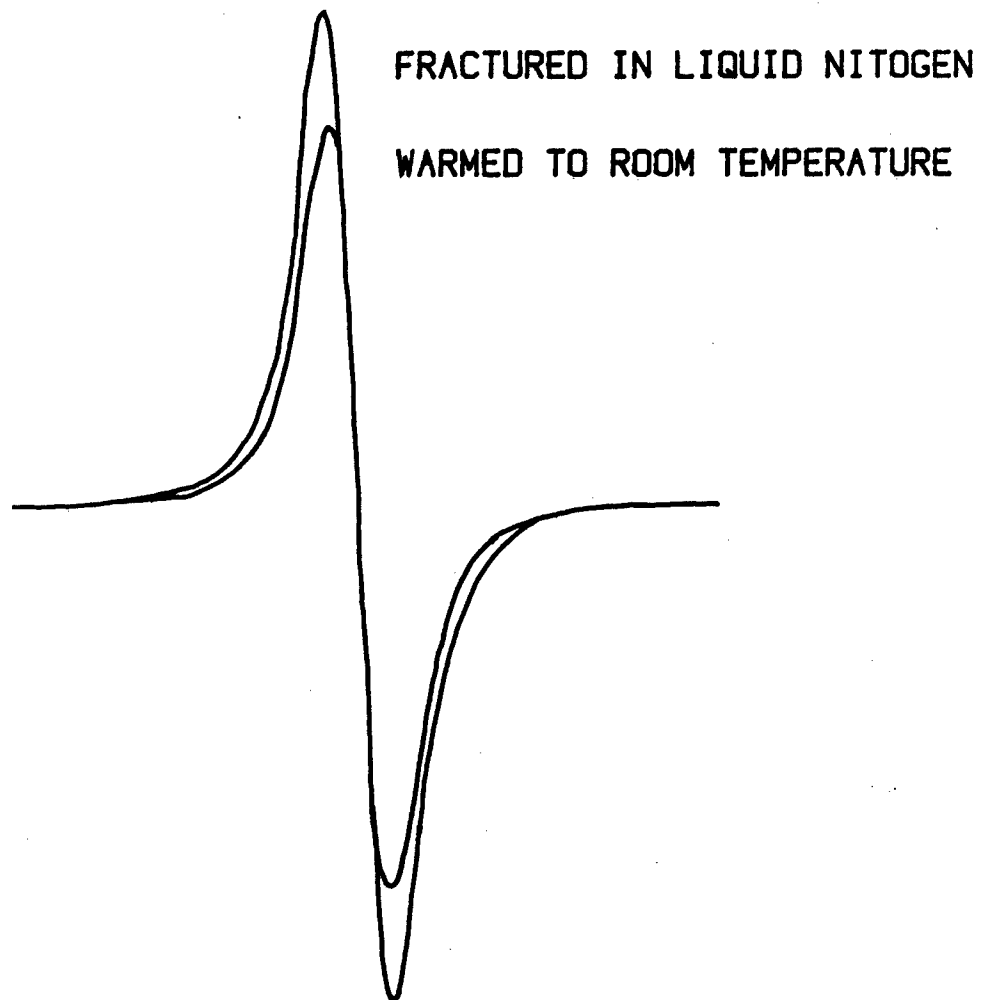


Figure 34b

Electron spin resonance spectra of AFTECH 2 fibers fractured by crushing under liquid nitrogen and subsequently warmed to room temperature.

ELECTRON SPIN RESONANCE

AFTECH 1

EFFECT OF MECHANICAL DEFORMATION

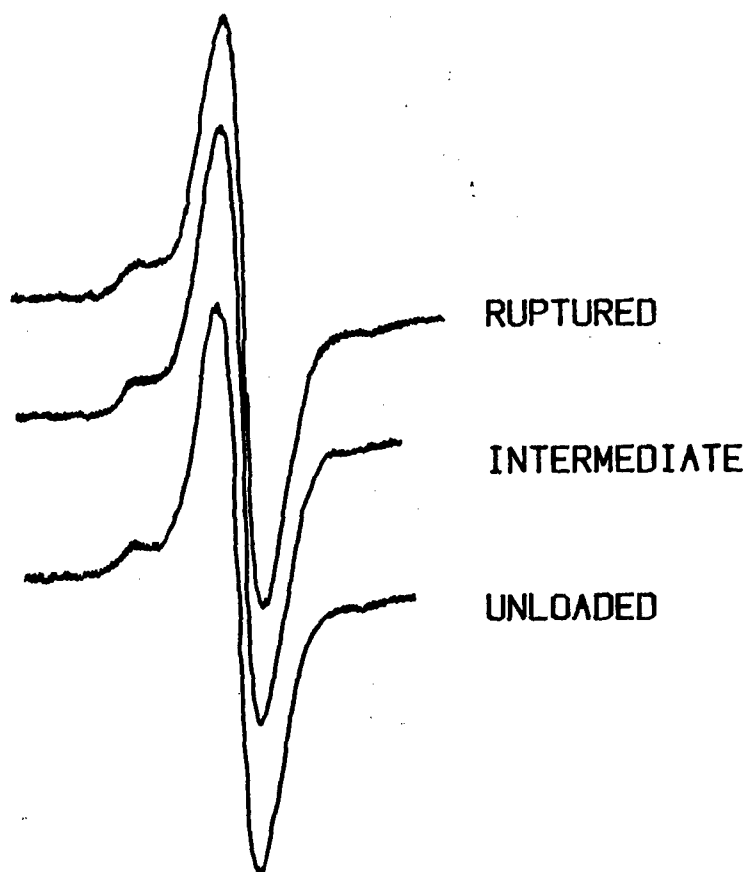


Figure 35

Effect of mechanical deformation on the ESR spectrum of AFTECH 1 fiber that had been thermally treated.

ABPBT

EMI=585nm, EXC=515nm

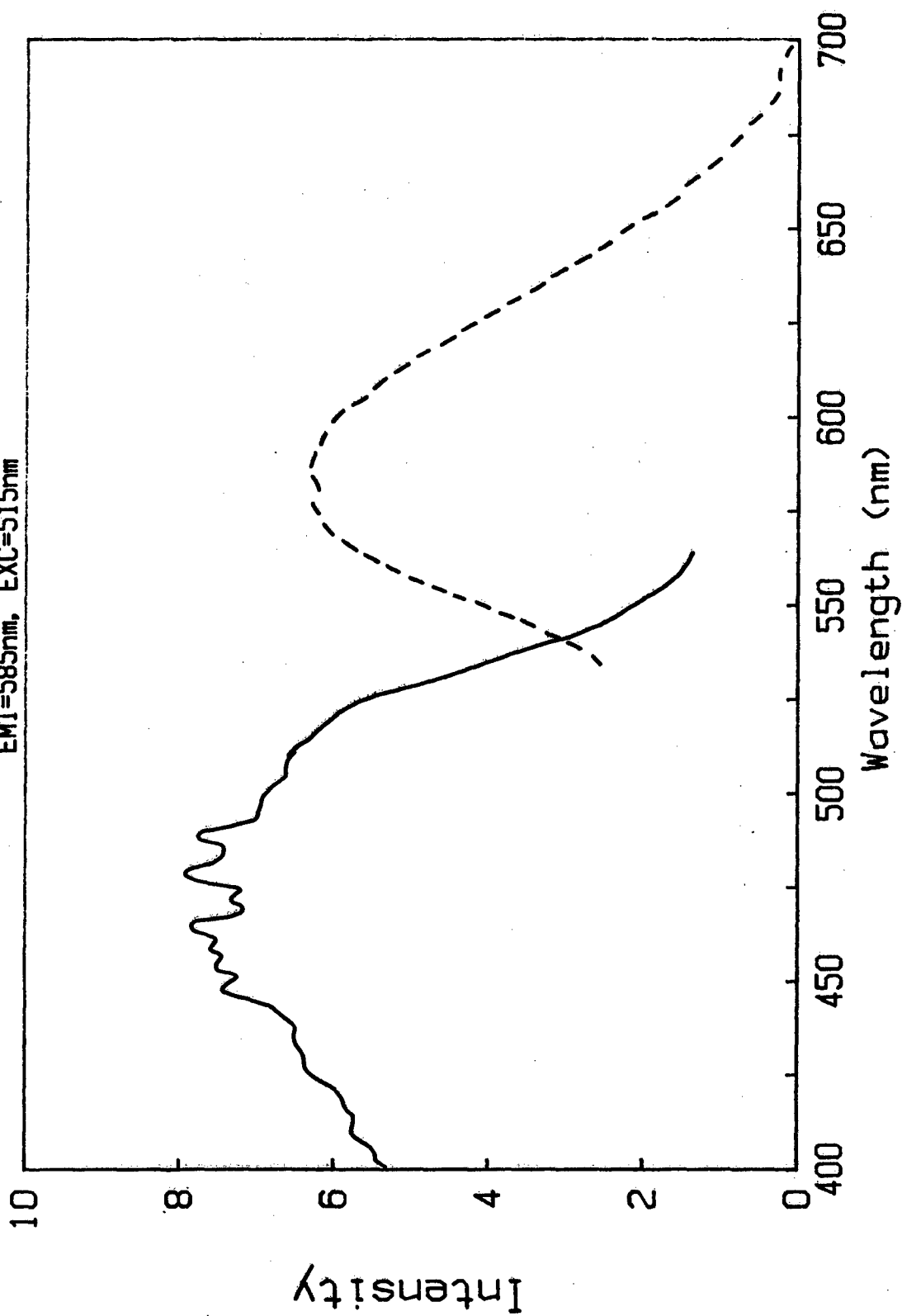


Figure 36

Solid state fluorescence (dashed curve) and excitation (solid curve) spectra of poly (2,5(6) benzothiazole), ABPBT, fibers. The wavelength of the excitation radiation for the fluorescence spectrum was 515 nm and the intensity of the excitation spectrum was monitored at 585 nm.

ABPBT in MSA

EXC=412nm

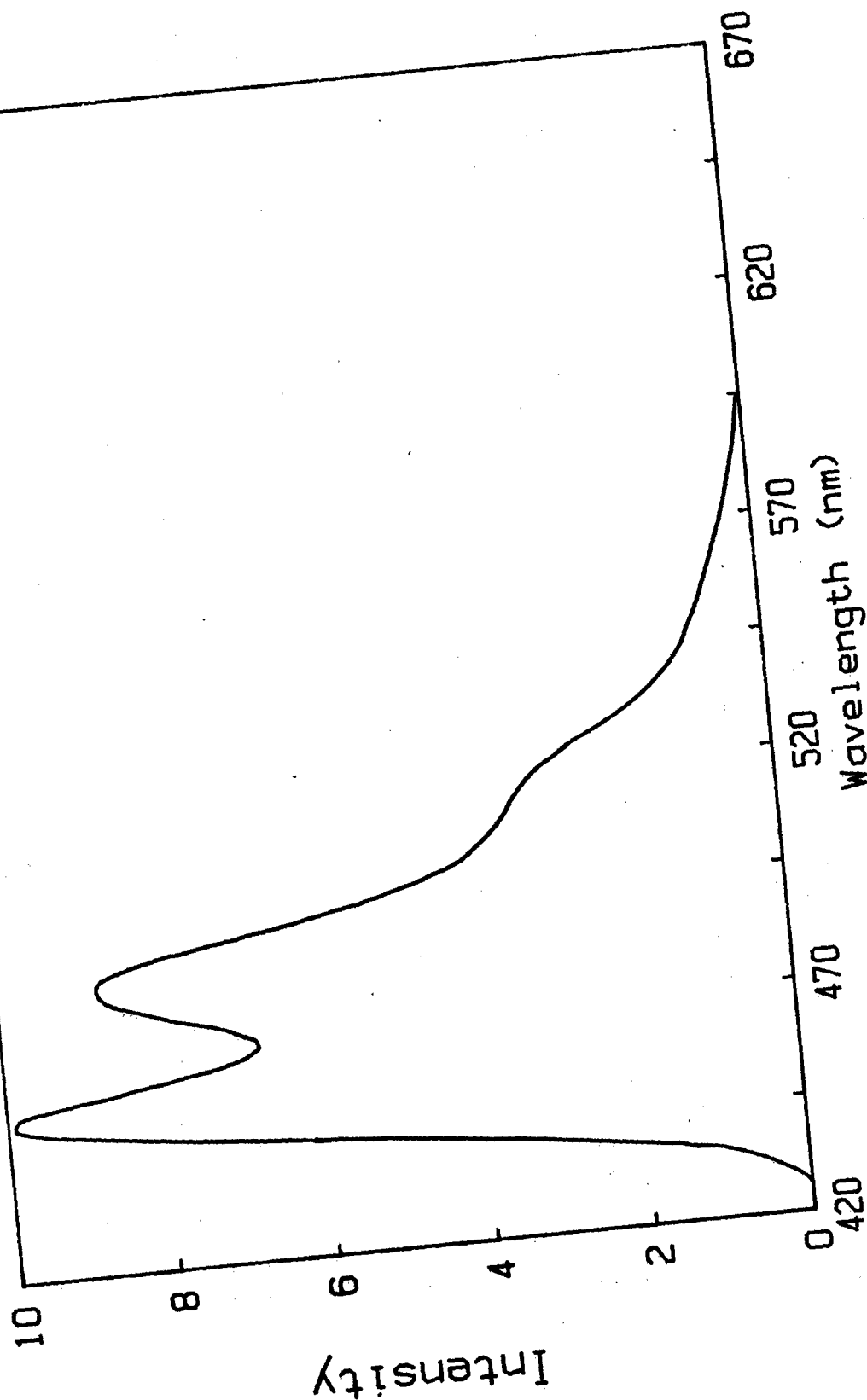


Figure 37
The solution fluorescence spectrum of poly (2,5(6) benzothiazole),
ABPBT, in methane sulfonic acid, excited by 412 nm radiation.

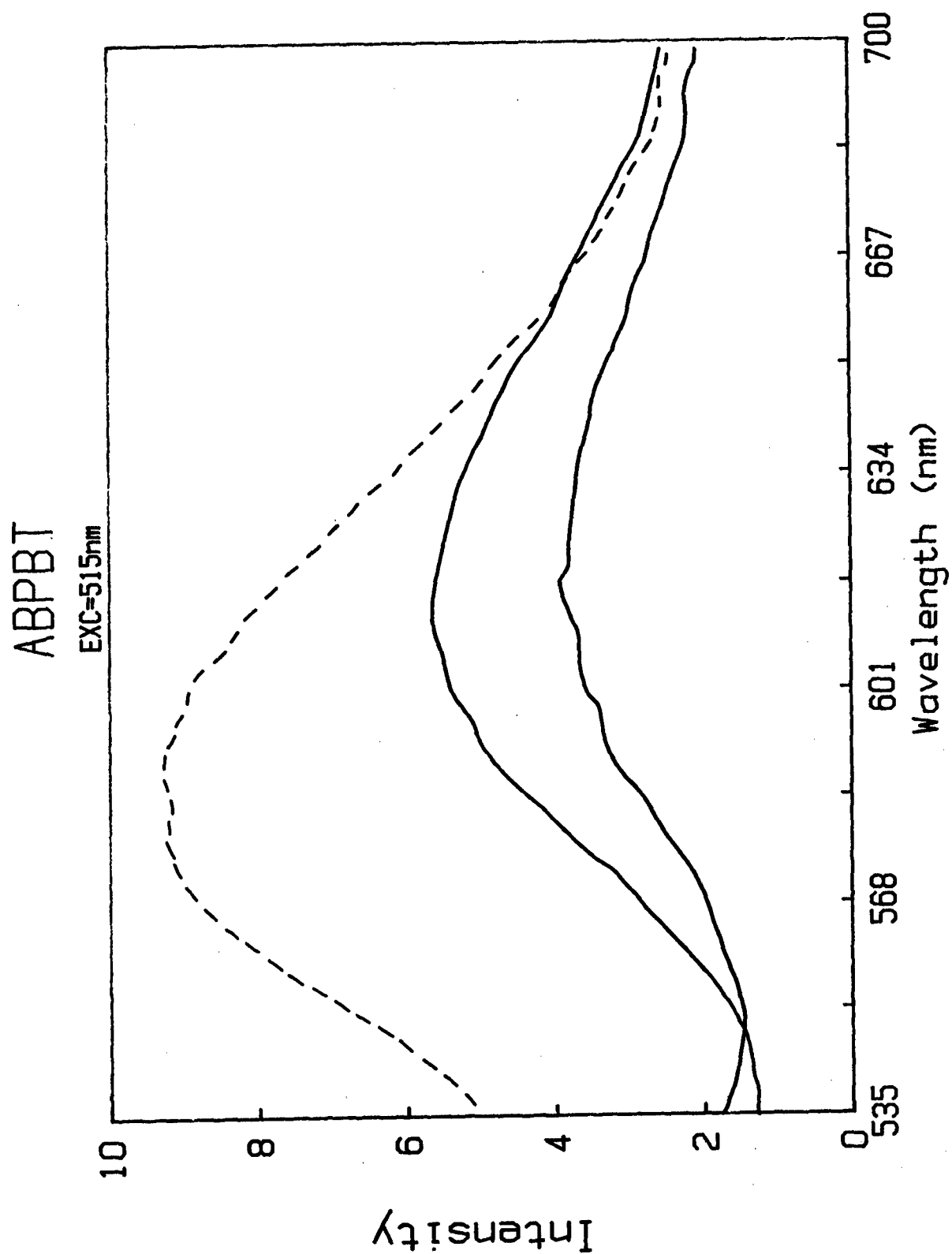


Figure 38

Solid state fluorescence spectra of poly (2,5(6) benzothiazole), ABPBT, fibers, as received (dashed curve), precipitated from MSA and exposed to concentrated HCL solution (middle spectrum) and precipitated from MSA and exposed to HCL vapor for 15 minutes (bottom spectrum).

PBT FILM in MSA
EXC=435nm

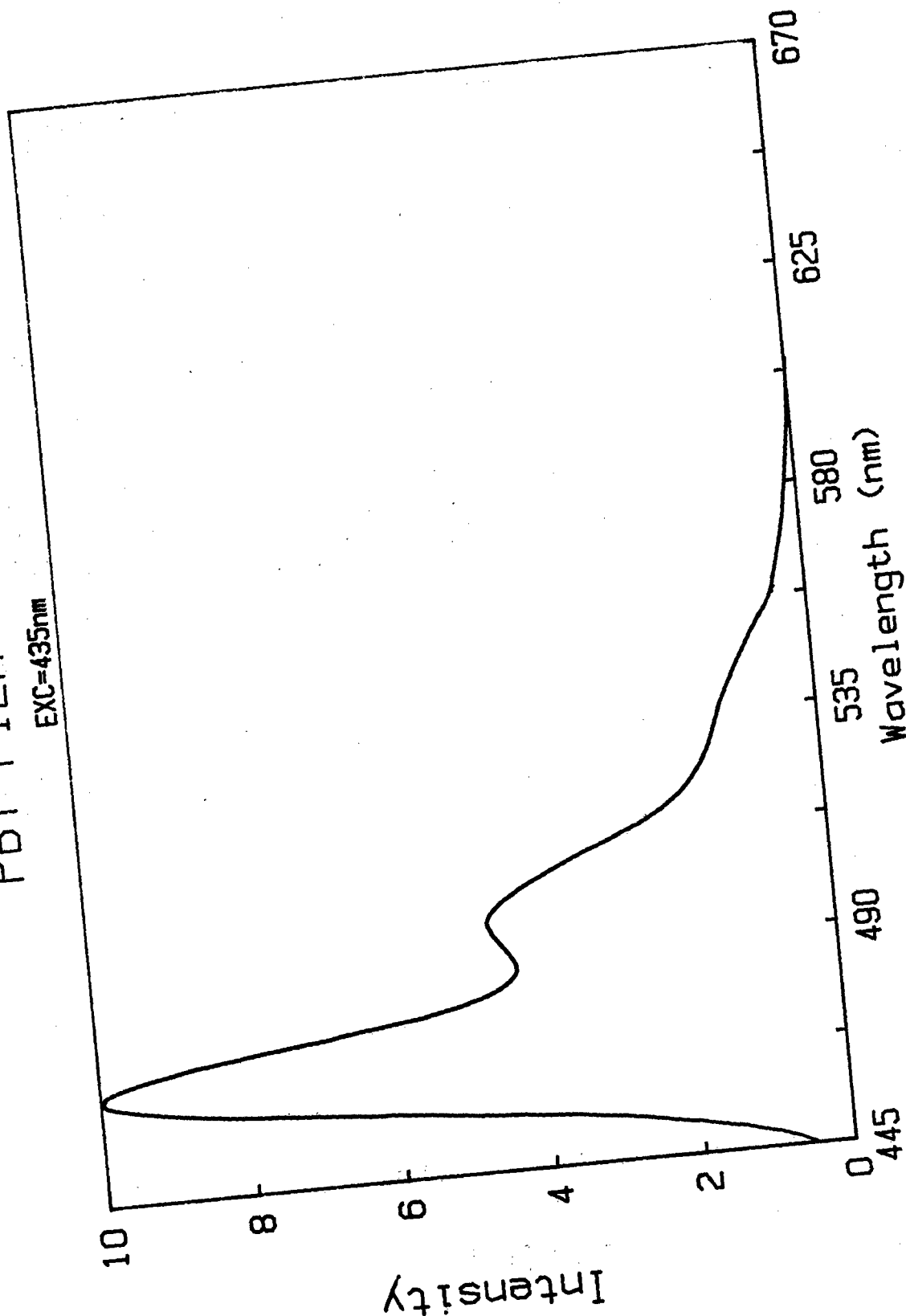


Figure 39
The solution fluorescence spectrum of poly (p-phenylene-bisbenzothiazole), PBT, in methane sulfonic acid recorded with 435nm excitation radiation.

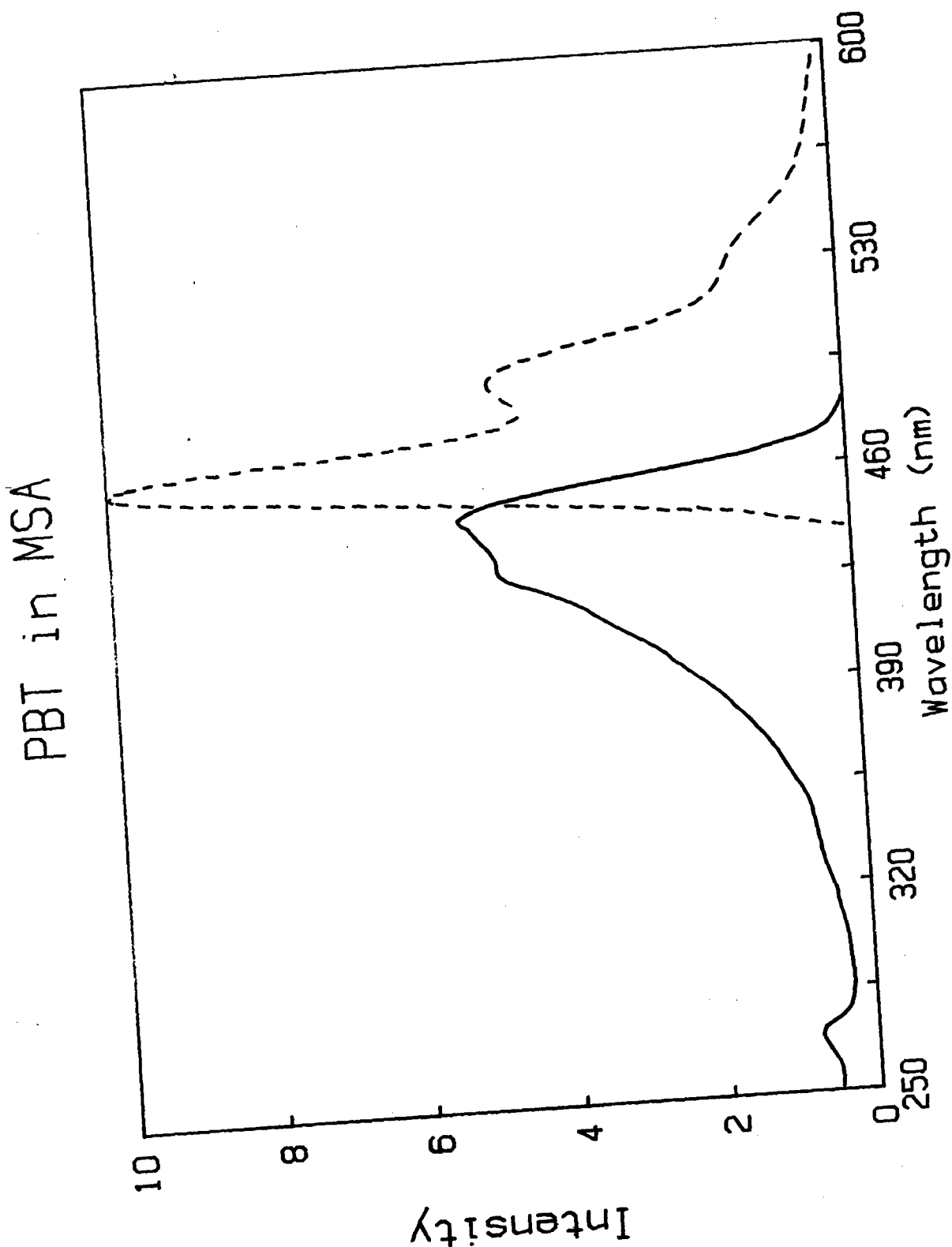


Figure 40

The solution fluorescence (dashed curve) and excitation spectrum (solid curve) of poly (p-phenylene-bisbenzothiazole), PBT, in methane sulfonic acid. The fluorescence spectrum was obtained with 435 nm excitation radiation and the intensity of the excitation spectrum was monitored at 497 nm.

PBT COAG., WATER WASHED

EMI=577nm, EXC=503nm

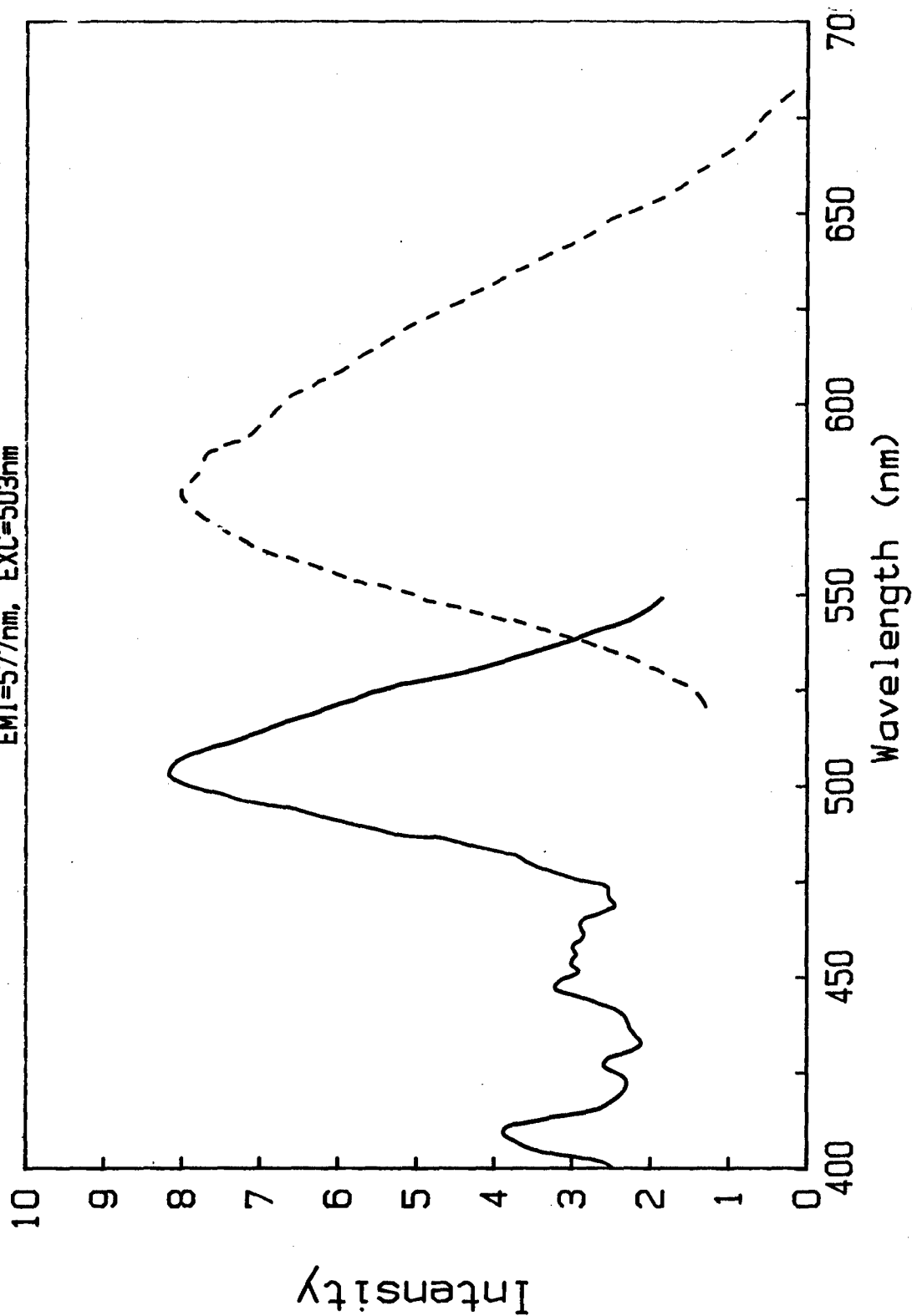


Figure 41

The solid state fluorescence (dashed curve) and excitation (solid curve) spectra of poly (p-phenylene-bisbenzothiazole), PBT, precipitated from MSA. The emission spectrum was obtained with 503 nm excitation radiation, and the intensity of the excitation spectrum was monitored at 577 nm.

PBT/NYLON

EMI=608nm, EXC=521nm

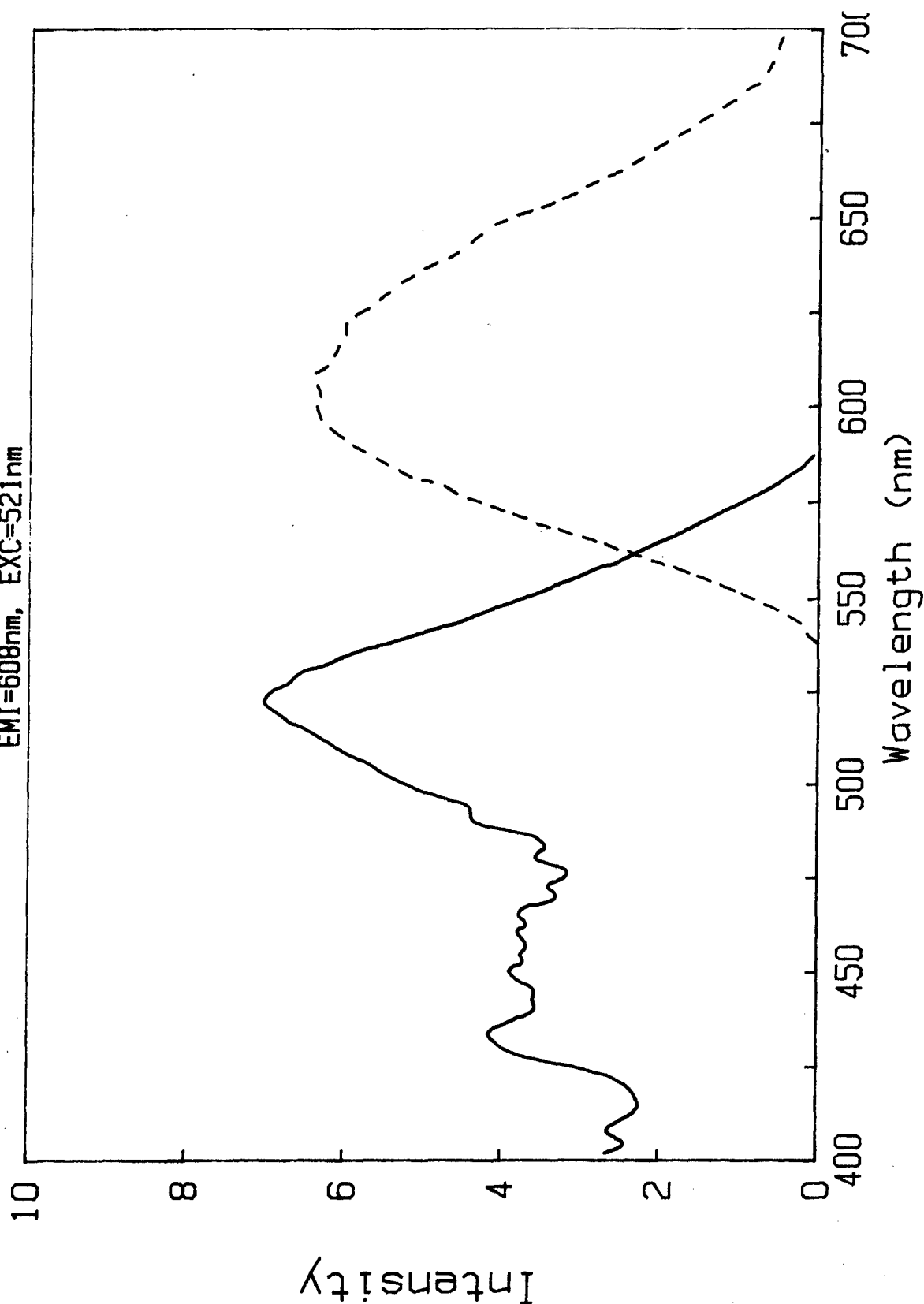
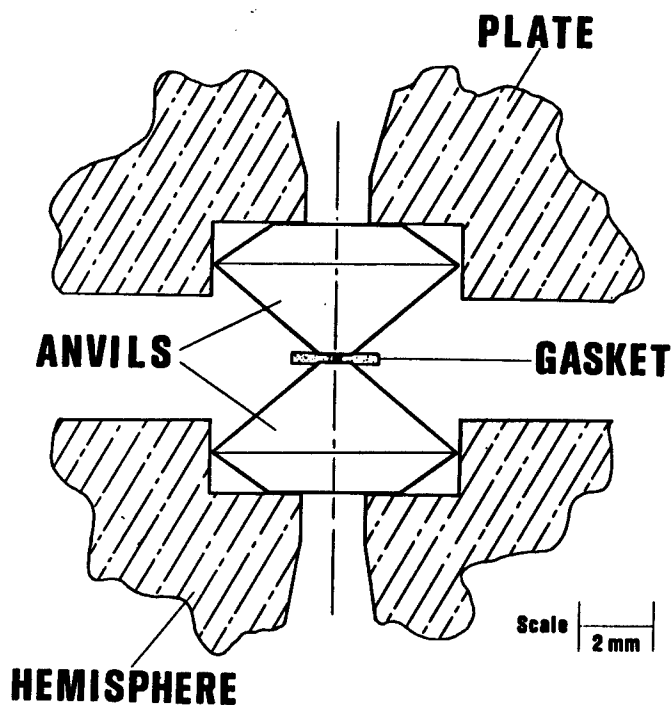
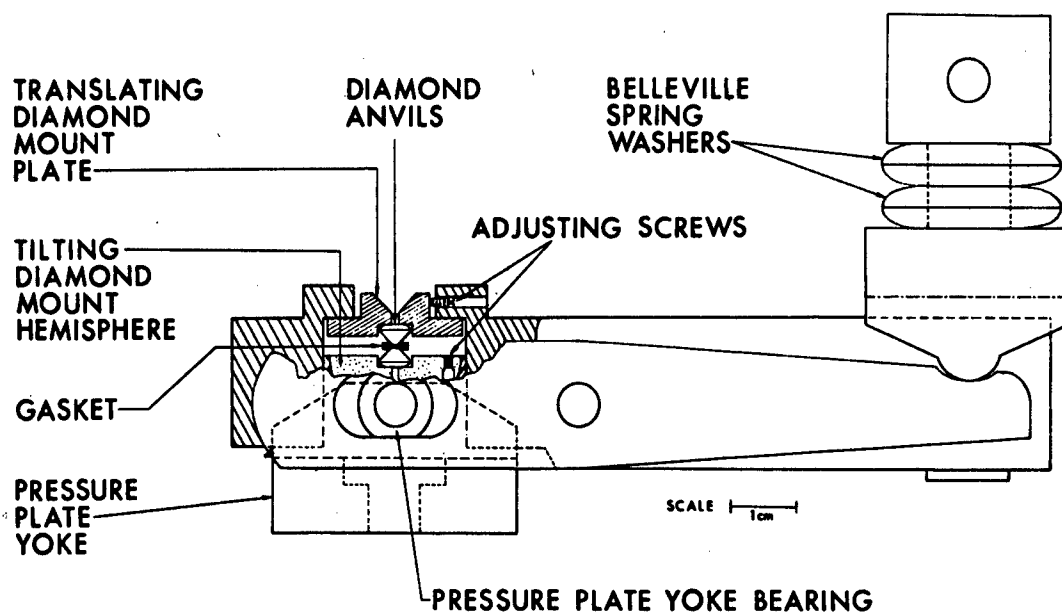


Figure 42

Solid state fluorescence (dashed curve) and excitation (solid curve) spectra of a molecular composite of poly (p-phenylene-bisbenzothiazole), PBT, and nylon. The emission spectrum was obtained with 521 nm excitation and the intensity of the excitation spectrum was monitored at 608 nm.



DIAMOND ANVIL PRESSURE CELL



MOUNTING OF PRESSURE CELL

Figure 43

Diamond anvil pressure cell.

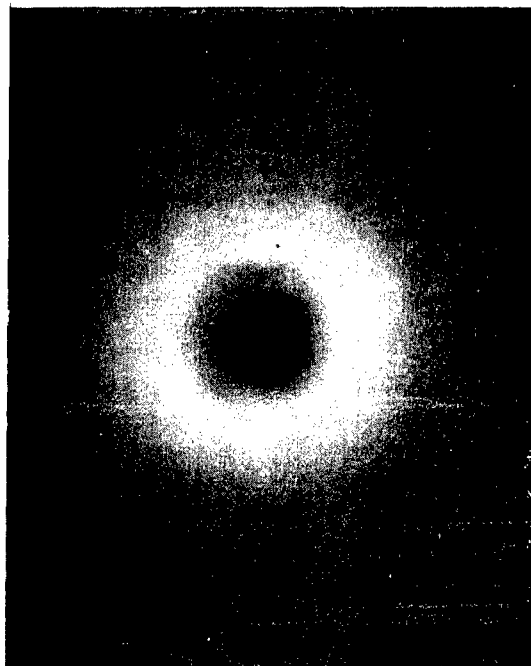


Figure 44

Flat plate x-ray diffraction patterns obtained with dope.

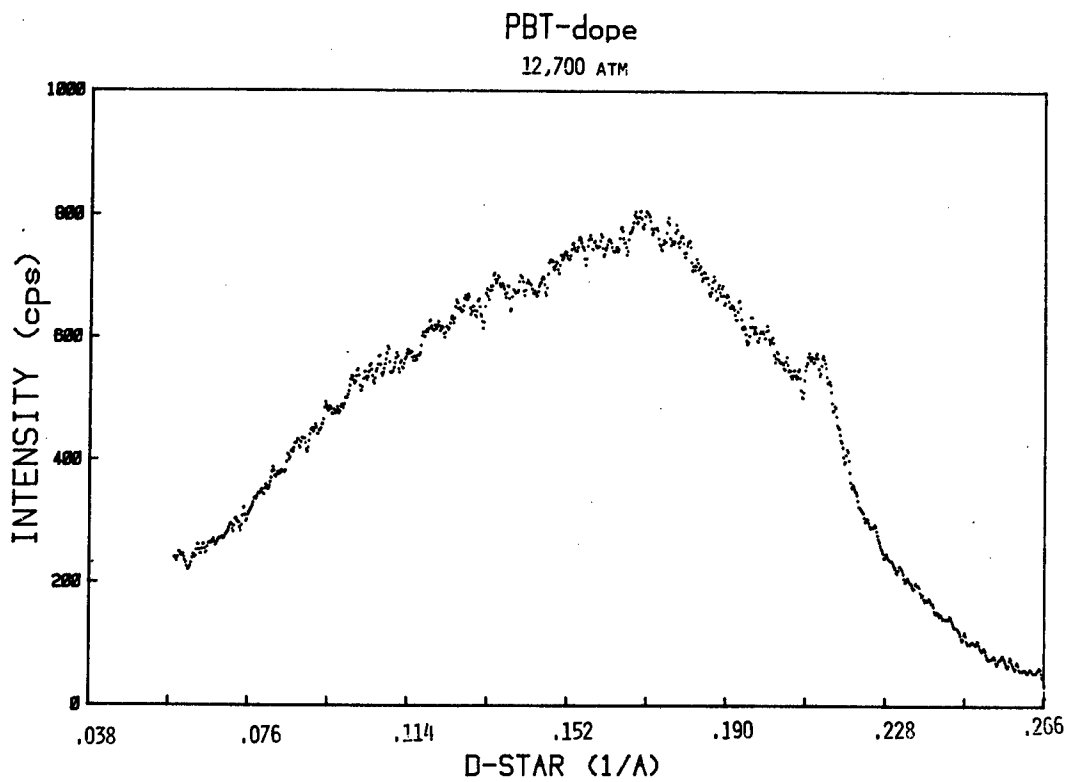


Figure 45

Energy dispersive x-ray diffraction pattern obtained with dope at 12,700 atm.